

Contents

Glossary	xi
Acronyms	xiii
1 Introduction and Literature Review	1
1.1 Cancer Research in the Post-Genomic Era	1
1.1.1 Cancer is a Global Health Issue	2
1.1.1.1 The Genetics and Molecular Biology of Cancers	3
1.1.2 The Genomics Revolution in Cancer Research	3
1.1.2.1 High-Throughput Technologies	4
1.1.2.2 Bioinformatics and Genomic Data	5
1.1.3 Genomics Projects	5
1.1.3.1 The Cancer Genome Project	6
1.1.3.2 The Cancer Genome Atlas Project	6
1.1.4 Genomic Cancer Medicine	8
1.1.4.1 Cancer Genes and Driver Mutations	8
1.1.4.2 Precision Cancer Medicine	9
1.1.4.3 Molecular Diagnostics and Pan-Cancer Medicine	9
1.1.4.4 Targeted Therapeutics and Pharmacogenomics	10
1.1.5 Systems and Network Biology	11
1.2 Synthetic Lethal Cancer Medicine	12
1.2.1 Synthetic Lethal Genetic Interactions	12
1.2.2 Synthetic Lethal Concepts in Genetics	14
1.2.3 Synthetic Lethality in Model Systems	14
1.2.3.1 Synthetic Lethal Pathways and Networks	15
1.2.3.2 Evolution of Synthetic Lethality	15
1.2.4 Synthetic Lethality in Cancer	16
1.2.5 Clinical Impact of Synthetic Lethality in Cancer	18
1.2.6 High-throughput Screening for Synthetic Lethality	19
1.2.6.1 Synthetic Lethal Screens	21
1.2.7 Computational Prediction of Synthetic Lethality	22
1.2.7.1 Bioinformatics Approaches to Genetic Interactions	22
1.2.7.2 Comparative Genomics	24
1.2.7.3 Analysis and Modelling of Protein Data	26
1.2.7.4 Differential Gene Expression	28
1.2.7.5 Data Mining and Machine Learning	29

1.2.7.6	Mutual Exclusivity and Bimodality	31
1.2.7.7	Rationale for Further Development	33
1.3	E-cadherin as a Synthetic Lethal Target	33
1.3.1	The <i>CDH1</i> gene and its Biological Functions	33
1.3.1.1	Cytoskeleton	34
1.3.1.2	Extracellular and Tumour Micro-environment	34
1.3.1.3	Cell-Cell Adhesion and Signalling	34
1.3.2	<i>CDH1</i> as a Tumour (and Invasion) Suppressor	35
1.3.2.1	Breast Cancers and Invasion	35
1.3.3	Hereditary Diffuse Gastric (and Lobular Breast) Cancer	35
1.3.4	Cell Line Models of <i>CDH1</i> Null Mutations	37
1.4	Summary and Research Direction of Thesis	37
1.4.1	Thesis Aims	39
2	Methods and Resources	40
2.1	Bioinformatics Resources for Genomics Research	40
2.1.1	Public Data and Software Packages	40
2.1.1.1	Cancer Genome Atlas Data	41
2.1.1.2	Reactome and Annotation Data	42
2.2	Data Handling	42
2.2.1	Normalisation	42
2.2.2	Sample Triage	42
2.2.3	Metagenes and the Singular Value Decomposition	43
2.2.4	Candidate Triage and Integration with Screen Data	45
2.3	Techniques	45
2.3.1	Statistical Procedures and Tests	46
2.3.2	Gene Set Over-representation Analysis	47
2.3.3	Clustering	47
2.3.4	Heatmap	47
2.3.5	Modelling and Simulations	48
2.3.5.1	Receiver Operating Characteristic Curves	49
2.3.6	Resampling Analysis	49
2.4	Pathway Structure Methods	50
2.4.1	Network and Graph Analysis	50
2.4.2	Sourcing Graph Structure Data	51
2.4.3	Constructing Pathway Subgraphs	51
2.4.4	Network Analysis Metrics	52
2.5	Implementation	53
2.5.1	Computational Resources and Linux Utilities	53
2.5.2	R Language and Packages	54
2.5.3	High Performance and Parallel Computing	57
3	Methods Developed During Thesis	59
3.1	A Synthetic Lethal Detection Methodology	59
3.2	Synthetic Lethal Simulation and Modelling	61
3.2.1	A Model of Synthetic Lethality in Expression Data	62

3.2.2	Simulation Procedure	66
3.3	Detecting Simulated Synthetic Lethal Partners	69
3.3.1	Binomial Simulation of Synthetic Lethality	69
3.3.2	Multivariate Normal Simulation of Synthetic Lethality	71
3.3.2.1	Multivariate Normal Simulation with Correlated Genes	73
3.3.2.2	Specificity with Query-Correlated Pathways	81
3.4	Graph Structure Methods	83
3.4.1	Upstream and Downstream Gene Detection	83
3.4.1.1	Permutation Analysis for Statistical Significance	84
3.4.2	Simulating Gene Expression from Graph Structures	85
3.5	Customised Functions and Packages Developed	89
3.5.1	Synthetic Lethal Interaction Prediction Tool	89
3.5.2	Data Visualisation	90
3.5.3	Extensions to the iGraph Package	91
3.5.3.1	Sampling Simulated Data from Graph Structures	91
3.5.3.2	Plotting Directed Graph Structures	91
3.5.3.3	Computing Information Centrality	93
3.5.3.4	Testing Pathway Structure with Permutation Testing	93
3.5.3.5	Metapackage to Install iGraph Functions	94
4	Synthetic Lethal Analysis of Gene Expression Data	96
4.1	Synthetic Lethal Genes in Breast Cancer	97
4.1.1	Synthetic Lethal Pathways in Breast Cancer	98
4.1.2	Expression Profiles of Synthetic Lethal Partners	100
4.1.2.1	Subgroup Pathway Analysis	103
4.2	Comparing Synthetic Lethal Gene Candidates	105
4.2.1	Primary siRNA Screen Candidates	105
4.2.2	Comparison with Correlation	105
4.2.3	Comparison with Primary Screen Viability	108
4.2.4	Comparison with Secondary siRNA Screen Validation	110
4.2.5	Comparison to Primary Screen at Pathway Level	111
4.2.5.1	Resampling Genes for Pathway Enrichment	113
4.2.6	Integrating Synthetic Lethal Pathways and Screens	118
4.3	Synthetic Lethal Pathway Metagenes	119
4.4	Replication in Stomach Cancer	121
4.5	Discussion	122
4.5.1	Strengths of the SLIPT Methodology	122
4.5.2	Synthetic Lethal Pathways for E-cadherin	123
4.5.3	Replication and Validation	125
4.5.3.1	Integration with siRNA Screening	125
4.5.3.2	Replication across Tissues	126
4.6	Summary	126

5 Synthetic Lethal Pathway Structure	128
5.1 Synthetic Lethal Genes in Reactome Pathways	128
5.1.1 The PI3K/AKT Pathway	129
5.1.2 The Extracellular Matrix	131
5.1.3 G Protein Coupled Receptors	134
5.1.4 Gene Regulation and Translation	134
5.2 Network Analysis of Synthetic Lethal Genes	136
5.2.1 Gene Connectivity and Vertex Degree	137
5.2.2 Gene Importance and Centrality	138
5.2.2.1 Information Centrality	138
5.2.2.2 PageRank Centrality	140
5.3 Relationships between Synthetic Lethal Genes	141
5.3.1 Detecting Upstream or Downstream Synthetic Lethality	142
5.3.2 Resampling for Synthetic Lethal Pathway Structure	144
5.4 Discussion	146
5.5 Summary	148
6 Simulation and Modelling of Synthetic Lethal Pathways	150
6.1 Synthetic Lethal Detection Methods	151
6.1.1 Performance of SLIPT and χ^2 across Quantiles	152
6.1.1.1 Correlated Query Genes affects Specificity	155
6.1.2 Alternative Synthetic Lethal Detection Strategies	157
6.1.2.1 Correlation for Synthetic Lethal Detection	158
6.1.2.2 Testing for Bimodality with BiSEp	159
6.2 Simulations with Graph Structures	160
6.2.1 Performance over Graph Structures	161
6.2.1.1 Simple Graph Structures	161
6.2.1.2 Constructed Graph Structures	164
6.2.2 Performance with Inhibitions	166
6.2.3 Synthetic Lethality across Graph Structures	172
6.2.4 Performance within a Large Simulated Datasets	175
6.3 Simulations in More Complex Graph Structures	180
6.3.1 Simulations over Pathway-based Graphs	181
6.3.2 Pathway Structures in a Large Simulated Datasets	184
6.4 Discussion	187
6.4.1 Simulation Procedure	187
6.4.2 Comparing Methods with Simulated Data	188
6.4.3 Design and Performance of SLIPT	189
6.4.4 Simulations from Graph Structures	191
6.5 Summary	192
7 Discussion	193
7.1 Synthetic Lethality and <i>CDH1</i> Biology	193
7.1.1 Established Functions of <i>CDH1</i>	194
7.1.2 The Molecular Role of <i>CDH1</i> in Cancer	194
7.2 Significance	195

7.2.1	Synthetic Lethality in the Genomic Era	195
7.2.2	Clinical Interventions based on Synthetic Lethality	197
7.3	Future Directions	198
7.4	Conclusions	200
	Bibliography	202
A	Sample Quality	226
A.1	Sample Correlation	226
A.2	Replicate Samples in TCGA Breast Cancer Data	229
B	Software Used for Thesis	233
C	Mutation Analysis in Breast Cancer	242
C.1	Synthetic Lethal Genes and Pathways	242
C.2	Synthetic Lethal Expression Profiles	243
C.3	Comparison to Primary Screen	246
C.3.1	Resampling Analysis	248
C.4	Compare SLIPT genes	250
D	Metagene Analysis	252
D.1	Pathway Signature Expression	252
D.2	Synthetic Lethal Reactome Metagenes	256
E	Intrinsic Subtyping	257
F	Stomach Expression Analysis	259
F.1	Synthetic Lethal Genes and Pathways	259
F.2	Comparison to Primary Screen	263
F.2.1	Resampling Analysis	265
F.3	Metagene Analysis	267
G	Synthetic Lethal Genes in Pathways	268
H	Network Analysis for Mutation SLIPT	275
I	Pathway Structure for Mutation SLIPT	278
J	Performance of SLIPT and χ^2	280
J.1	Correlated Query Genes affects Specificity	286
K	Simulations on Graph Structures	292
K.0.1	Simulations from Inhibiting Graph Structures	293
K.1	Simulation across Graph Structures	296
K.2	Simulations from Complex Graph Structures	300
K.2.1	Simulations from Complex Inhibiting Graphs	303
K.3	Simulations from Pathway Graph Structures	309

List of Figures

1.1	Synthetic genetic interactions	13
1.2	Synthetic lethality in cancer	17
2.1	Read count density	44
2.2	Read count sample mean	44
3.1	Framework for synthetic lethal prediction	60
3.2	Synthetic lethal prediction adapted for mutation	61
3.3	A model of synthetic lethal gene expression	63
3.4	Modelling synthetic lethal gene expression	64
3.5	Synthetic lethality with multiple genes	65
3.6	Simulating gene function	67
3.7	Simulating synthetic lethal gene function	67
3.8	Simulating synthetic lethal gene expression	68
3.9	Performance of binomial simulations	70
3.10	Comparison of statistical performance	70
3.11	Performance of multivariate normal simulations	72
3.12	Simulating expression with correlated gene blocks	74
3.13	Simulating expression with correlated gene blocks	75
3.14	Synthetic lethal prediction across simulations	77
3.15	Performance with correlations	78
3.16	Comparison of statistical performance with correlation structure	79
3.17	Performance with query correlations	80
3.18	Statistical evaluation of directional criteria	81
3.19	Performance of directional criteria	82
3.20	Simulated graph structures	86
3.21	Simulating expression from a graph structure	87
3.22	Simulating expression from graph structure with inhibitions	88
3.23	Demonstration of violin plots with custom features	92
3.24	Demonstration of annotated heatmap	92
3.25	Simulating graph structures	93
4.1	Synthetic lethal expression profiles of analysed samples	101
4.2	Comparison of SLIPT with siRNA	106
4.3	Comparison of SLIPT and siRNA genes with correlation	106
4.4	Comparison of SLIPT and siRNA genes with correlation	108
4.5	Comparison of SLIPT and siRNA genes with screen viability	109

4.6	Comparison of SLIPT genes with siRNA screen viability	109
4.7	Resampled intersection of SLIPT and siRNA candidate genes	114
5.1	Synthetic lethality in the PI3K cascade	130
5.2	Synthetic lethality in Elastic Fibre Formation	132
5.3	Synthetic lethality in Fibrin Clot Formation	133
5.4	Synthetic lethality in the GPCRs	135
5.5	Synthetic lethality and vertex degree	137
5.6	Synthetic lethality and centrality	139
5.7	Synthetic lethality and PageRank	141
5.8	Structure of synthetic lethality resampling	143
6.1	Performance of χ^2 and SLIPT across quantiles	153
6.2	Performance of χ^2 and SLIPT across quantiles with more genes	154
6.3	Performance of χ^2 and SLIPT across quantiles with query correlation .	155
6.4	Performance of χ^2 and SLIPT across quantiles with query correlation and more genes	156
6.5	Performance of negative correlation and SLIPT	159
6.6	Simple graph structures	162
6.7	Performance of simulations on a simple graph	163
6.8	Performance of simulations is similar in simple graphs	164
6.9	Performance of simulations on a pathway	165
6.10	Performance of simulations on a simple graph with inhibition	167
6.11	Performance is higher on a simple inhibiting graph	169
6.12	Performance of simulations on a constructed graph with inhibition . .	170
6.13	Performance is affected by inhibition in graphs	171
6.14	Detection of synthetic lethality within a graph structure	173
6.15	Performance of simulations including a simple graph	177
6.16	Performance on a simple graph improves with more genes	178
6.17	Performance on an inhibiting graph improves with more genes	179
6.18	Performance of simulations on the PI3K cascade	183
6.19	Performance of simulations including the PI3K cascade	185
6.20	Performance on pathways improves with more genes	186
A.1	Correlation profiles of removed samples	227
A.2	Correlation analysis and sample removal	228
A.3	Replicate excluded samples	229
A.4	Replicate samples with all remaining	230
A.5	Replicate samples with some excluded	231
C.1	Synthetic lethal expression profiles of analysed samples	244
C.2	Comparison of mtSLIPT to short interfering RNA (siRNA)	246
C.3	Compare mtSLIPT and siRNA genes with correlation	250
C.4	Compare mtSLIPT and siRNA genes with correlation	250
C.5	Compare mtSLIPT and siRNA genes with siRNA viability	251
D.1	Pathway metagene expression profiles	254

D.2	Expression profiles for estrogen receptor related genes	255
F.1	Synthetic lethal expression profiles of stomach samples	261
F.2	Comparison of SLIPT in stomach to siRNA	263
G.1	Synthetic lethality in the PI3K/AKT pathway	268
G.2	Synthetic lethality in the PI3K/AKT pathway in cancer	269
G.3	Synthetic lethality in the Extracellular Matrix	270
G.4	Synthetic lethality in the GPCR Downstream	271
G.5	Synthetic lethality in the Translation Elongation	272
G.6	Synthetic lethality in the Nonsense-mediated Decay	273
G.7	Synthetic lethality in the 3' UTR	274
H.1	Synthetic lethality and vertex degree	275
H.2	Synthetic lethality and centrality	276
H.3	Synthetic lethality and PageRank	276
I.1	Structure of synthetic lethality resampling	278
J.1	Performance of χ^2 and SLIPT across quantiles	280
J.2	Performance of χ^2 and SLIPT across quantiles	282
J.3	Performance of χ^2 and SLIPT across quantiles with more genes	284
J.4	Performance of χ^2 and SLIPT across quantiles with query correlation	286
J.5	Performance of χ^2 and SLIPT across quantiles with query correlation	288
J.6	Performance of χ^2 and SLIPT across quantiles with query correlation and more genes	290
K.1	Performance of simulations on a simple graph	292
K.2	Performance of simulations on an inhibiting graph	293
K.3	Performance of simulations on a constructed graph with inhibition	294
K.4	Performance of simulations on a constructed graph with inhibition	295
K.5	Detection of synthetic lethality within a graph structure	296
K.6	Detection of synthetic lethality within an inhibiting graph	298
K.7	Detection of synthetic lethality within an inhibiting graph	299
K.8	Performance of simulations on a branching graph	300
K.9	Performance of simulations on a complex graph	301
K.10	Performance of simulations on a large graph	302
K.11	Performance of simulations on a branching graph with inhibition	303
K.12	Performance of simulations on a branching graph with inhibition	304
K.13	Performance of simulations on a complex graph with inhibition	305
K.14	Performance of simulations on a complex graph with inhibition	306
K.15	Performance of simulations on a large constructed graph with inhibition	307
K.16	Performance of simulations on a large constructed graph with inhibition	308
K.17	Performance of simulations on the $G_{\alpha i}$ signalling pathway	309
K.18	Performance of simulations including the $G_{\alpha i}$ signalling pathway	310

List of Tables

1.1	Methods for predicting genetic interactions	23
1.2	Methods for predicting synthetic lethality in cancer	23
1.3	Methods used by Wu <i>et al.</i> (2014)	25
2.1	Excluded samples by batch and clinical characteristics.	43
2.2	Computers used during thesis	53
2.3	Linux utilities and applications used during thesis	54
2.4	R installations used during thesis	55
2.5	R Packages used during thesis	55
2.6	R packages developed during thesis	57
4.1	Candidate synthetic lethal gene partners of <i>CDH1</i> from SLIPT	98
4.2	Pathways for <i>CDH1</i> partners from SLIPT	99
4.3	Pathways for clusters of <i>CDH1</i> partners from SLIPT	104
4.4	ANOVA for synthetic lethality and correlation with <i>CDH1</i>	107
4.5	Comparison of Synthetic Lethal Interaction Prediction Tool (SLIPT) genes against secondary siRNA screen	111
4.6	Pathways for <i>CDH1</i> partners from SLIPT and siRNA	112
4.7	Pathways for <i>CDH1</i> partners from SLIPT	115
4.8	Pathways for <i>CDH1</i> partners from SLIPT and siRNA primary screen .	116
4.9	Examples of candidate metagenes synthetic lethal for <i>CDH1</i> from SLIPT	120
5.1	ANOVA for synthetic lethality and vertex degree	138
5.2	ANOVA for synthetic lethality and information centrality	139
5.3	ANOVA for synthetic lethality and PageRank centrality	140
5.4	Resampling for pathway structure of synthetic lethal detection methods	145
B.1	Complete list of R packages used during this thesis	233
C.1	Candidate synthetic lethal gene partners of <i>CDH1</i> from mtSLIPT . . .	242
C.2	Pathways for <i>CDH1</i> partners from mtSLIPT	243
C.3	Pathways for clusters of <i>CDH1</i> partners from mtSLIPT	245
C.4	Pathways for <i>CDH1</i> partners from mtSLIPT and siRNA	247
C.5	Pathways for <i>CDH1</i> partners from mtSLIPT	248
C.6	Pathways for <i>CDH1</i> partners from mtSLIPT and siRNA primary screen	249
D.1	Candidate synthetic lethal metagenes against <i>CDH1</i> from mtSLIPT . .	256

E.1	Comparison of intrinsic subtypes	257
F.1	Synthetic lethal gene partners of <i>CDH1</i> from SLIPT in stomach cancer	259
F.2	Pathways for <i>CDH1</i> partners from SLIPT in stomach cancer	260
F.3	Pathways for clusters of <i>CDH1</i> partners in stomach SLIPT	262
F.4	Pathways for <i>CDH1</i> partners from SLIPT and siRNA	264
F.5	Pathways for <i>CDH1</i> partners from SLIPT in stomach cancer	265
F.6	Pathways for <i>CDH1</i> partners from SLIPT in stomach and siRNA	266
F.7	Synthetic lethal metagenes against <i>CDH1</i> in stomach cancer	267
H.1	ANOVA for synthetic lethality and vertex degree	277
H.2	ANOVA for synthetic lethality and information centrality	277
H.3	ANOVA for synthetic lethality and PageRank centrality	277
I.1	Resampling for pathway structure of synthetic lethal detection methods	279

Glossary

allele	A gene variant with a specific sequence and phenotype.
bioinformatics	Statistical or computational approaches to biological data or research tools.
centrality	A network metric which identifies important <i>vertices</i> .
edge or link	A relationship connecting a pair of elements of a graph structure or network, may be weighted or directional.
essential	A gene which is required to be functional or expressed for a cell or organism to be viable, grow or develop.
gene expression	A measure of the relative expression of each gene from the mRNA extracted from (pooled) cells.
genome	All of the DNA sequence in the genome.
genomic	The use of data from all genes in the genome.
graph or network	A mathematical structure modelling or depicting the relationships between elements.
information centrality	A network <i>centrality</i> metric which uses the impact of removing a <i>vertex or node</i> on connections in the network.
metagene	A consistent signal of expression for a collection of genes such as a biological pathway, derived from singular value decomposition.
methylation	A measure of the epigenetic regulation of DNA at <i>CpG dinucleotide (CpG)</i> sites.
microarray	A high-throughput technique to measure presence or abundance of nucleic acid sequences from binding to probes.

mutant	A variant or dysfunctional phenotype arising from a mutation in a gene.
mutation	A change in DNA sequence that disrupts gene function.
PageRank centrality	A network centrality metric which uses eigenvectors with a scaling factor (Brin and Page, 1998).
pathway	A series of biomolecules that produces a particular product or biological function.
RNA-Seq	The generation of transcriptome data from sequencing RNA.
shortest path	A path with the fewest possible edges which connects two particular vertices .
somatic mutation	A mutation that occurs in somatic cells, during a patient's lifespan.
synthetic lethal	Genetic interactions where inactivation of multiple genes is inviable (or deleterious) which are viable if inactivated separately.
vertex or node	An element of a graph structure or network.
wild-type	A natural phenotype of a trait or the normally functional allele which encodes it.

Acronyms

ANOVA	Analysis of Variance.
AUROC	Area Under the Receiver Operating Characteristic (curve).
Bash	Bourne Again Shell.
BioPAX	Biological Pathway Exchange.
CpG	5'-C-phosphate-G-3'.
CPM	Counts Per Million mapped reads.
CPU	Central Processing Unit.
CRAN	comprehensive R archive network.
DNA	Deoxyribonucleic Acid.
ER	Estrogen Receptor.
FDR	False Discovery Rate.
HPC	High Performance Computing.
ICGC	International Cancer Genome Consortium.
mtSLIPT	Synthetic Lethal Interaction Prediction Tool (against mutation).
NeSI	New Zealand eScience Infrastructure.
PAM50	Prediction Analysis of Microarray 50.
RNA	Ribonucleic Acid.
ROC	Reciever Operating Characteristic (curve).
RSEM	RNA-Seq by Expectation Maximization (normalisation).
siRNA	Short Interfering RNA.

SLIPT	Synthetic Lethal Interaction Prediction Tool.
Slurm	Simple Linux Utility for Resource Management.
SOCKS	Socket Secure.
TCGA	The Cancer Genome Atlas (genomics project).

Chapter 2

Methods and Resources

In this Chapter, I will outline the various existing resources and methods that were used throughout this project. This includes public data repositories, stable and development releases of software packages (primarily using the R programming environment), and custom implementation of [bioinformatic](#) methods and statistical concepts with Shell or R scripts developed for this purpose. The methods and packages that have been developed specifically for this project will be covered in Chapter 3 with supporting data and demonstration of their use .

2.1 Bioinformatics Resources for Genomics Research

2.1.1 Public Data and Software Packages

Various [bioinformatics](#) resources, such as databases and methods, have become integral parts of genetics and [genomics](#) research. Reference [genomes](#), genotyped variants, [gene expression](#), and epigenetics profiles are among the most commonly used resources. [Gene expression](#) data, in particular, is widely available from [microarray](#) and [RNA-Seq](#) projects, driven by data sharing, data mining, and the wider initiatives for publicly available data for enabling the scientific community to further utilise the data generated beyond a single research group or consortium ([Rung and Brazma, 2013](#)) These datasets are a valuable resource to examine the changes in [gene expression](#) occurring in cancers and the variation between samples. The potential for integrating findings from publicly available [genomic](#) data with experimental investigations has expanded with [RNA-Seq](#) datasets, including large-scale cancer [genomics](#) projects ([Zhang *et al.*, 2011](#)). This thesis presents such an investigation, enabled by the release of these datasets and tools developed to handle them.

It is now common practice for **bioinformatics** researchers to release open-source code or provide software packages to enable replication of the findings or further applications of the methods (Stajich and Lapp, 2006). This is part of a wider movement in software and data analysis, including the development of Linux and the R programming environment (R Core Team, 2016). In addition to the R packages hosted on **comprehensive R archive network** (CRAN) (CRAN, 2017), many packages specifically developed for applications in **bioinformatics** are hosted on the Bioconductor repositories (Gentleman *et al.*, 2004), and numerous packages in various stages of development are hosted on GitHub (<https://github.com/>). Packages from each of these resources have been used throughout this project and are cited wherever possible. Several R packages have been developed during this thesis project and publicly released on GitHub or will be released in conjunction with a publication.

2.1.1.1 Cancer Genome Atlas Data

Molecular profile data for normal and tumour samples were downloaded from publicly available sources, using the **The Cancer Genome Atlas** (TCGA) (TCGA, 2017) and the **International Cancer Genome Consortium** (ICGC) web portals (Zhang *et al.*, 2011). These include **gene expression** (RNA-Seq), **somatic mutations**, and clinical data. The versions were downloaded on the 6th of August 2015 (Release 19) and the 2nd of May 2016 (Release 20) for breast and stomach cancer respectively via the **ICGC** data portal (<https://dcc.icgc.org/>).

The TCGA project (Koboldt *et al.*, 2012) used widely adopted tools: “Bowtie” for alignment (Langmead *et al.*, 2009), “mapsplice” to detect splice sites (Wang *et al.*, 2010), and the RNA-Seq by Expectation Maximization (RSEM) approach to quantify reads as a measure of gene expression (Li *et al.*, 2010). These are widely acceptable tools for processing RNA-Seq data which were used to produce the raw counts of mapped reads (tier 1) and normalised **expression** data (tier 3) publicly downloaded from **ICGC** and **TCGA** respectively.

Raw count and **RSEM** normalised **TCGA expression** data from Illumina **RNA-Seq** protocols were downloaded for 1177 breast samples (113 normal, 1057 primary tumour, and 7 metastases) for 20,501 genes. **TCGA** breast **somatic mutation** data for 981 samples (976 primary tumours and 5 metastases) across 25,836 genes were downloaded. These included 969 samples (964 primary tumours and 5 metastases) with corresponding **RNA-Seq expression** data and 19,166 genes mapped from Ensembl identifiers to gene symbols. Of these genes, 16,156 had corresponding **gene expression** information. Unless otherwise stated, the raw counts were used for further processing

rather than the **RSEM** normalised data (provided by **TCGA** tier 3). **Somatic mutations** was reported if there were non-synonymous substitutions, frameshifts, or truncations (by premature stop codons) detected which would likely disrupt the **wild-type** gene function.

Raw count **TCGA** expression data (**TCGA** tier 1) from Illumina **RNA-Seq** was downloaded for 450 stomach samples (35 normal, 415 primary tumour) for 20,501 genes. **TCGA** stomach **mutation** data was also used for 289 samples across 25807 genes, corresponding to 19436 genes with **expression** data.

2.1.1.2 Reactome and Annotation Data

Pathway analysis was performed for human **pathway** annotation from the Reactome database (version 52) with **pathway** gene sets derived from the **reactome.db** R package. Entrez identifiers were mapped to gene symbols or aliases to match to **TCGA** expression and **mutation** data using the **org.Hs.eg.db** R package. Gene **expression** for breast cancer from Gatza and colleagues were also used (Gatza *et al.*, 2011; Gatza *et al.*, 2014). The gene symbols for each pathway were matched to the **expression** data and to construct a matrix of category membership using the **safe** R package (Barry, 2016).

2.2 Data Handling

2.2.1 Normalisation

Apart from the Prediction Analysis of Microarray 50 (**PAM50**) subtyping procedure (Parker *et al.*, 2009), which required **RSEM** normalised data (J.S. Parker personal communication), the analysis of the **RNA-Seq** data presented here was based on raw read count data. After some samples were removed for consistency (based on a Euclidean distance correlation matrix as described in Section 2.2.2), raw read counts were log-scaled and the final dataset was normalised as **Counts per Million mapped reads (CPM)**, weighted by variance modelling, using the **voom** function (Law *et al.*, 2014) in the **limma** R package (Ritchie *et al.*, 2015). This procedure adjusts the data to account for differences in read count by sequencing depth between samples and length between genes.

2.2.2 Sample Triage

The **TCGA** breast **RNA-Seq** data were assessed for batch effects using a correlation matrix of the log-transformed raw counts for which a heatmap (Euclidean distance, complete linkage) is shown in Figure A.2. While no major batch effects were de-

tectable between the samples, 9 samples were excluded due to poor correlation with the remaining samples, as detailed in Table 2.1. These samples showed unusual density plots compared to the rest of the dataset, and exhibited low mean read count in Figures 2.1 and 2.2. A heatmap showing key clinical properties of these excluded samples and their correlation with the remainder of the samples is shown in Figure A.1, and a full correlation heatmap (Figure A.2) shows these samples as relatively poorly correlated outliers in the bottom rows and left columns. In addition to the clustering analysis (in Appendix A.1), replicate tumour samples were also examined for sample quality in Appendix A.2. After removal of these samples, the TCGA dataset used for analysis consisted of the remaining 1168 samples (from 1040 patients): 1049 tumour samples, 112 normal tissue for matched samples, and 7 metastases.

Table 2.1: Excluded samples by batch and clinical characteristics.

Tissue Source	Type	Batch	Plate	Patient	Samples	p53	Subtype	Treatment (History)	Clinical Subtypes (Stage)
A7 Christiana	Tumour	47	A227	A0DB	1 of 3	NA	Luminal A	Mastectomy (no)	Estrogen receptor (ER) ⁺ Ductal (2)
A7 Christiana	Tumour	96	A220	A13D	1 of 3	Wildtype	Luminal A	Mastectomy (no)	ER ⁺ Ductal (2)
A7 Christiana	Tumour	96	A227	A13E	1 of 3	NA	Basal	Lumpectomy (no)	ER ⁻ Ductal (2)
A7 Christiana	Tumour	142	A277	A26E	1 of 3	NA	Basal	Lumpectomy (no)	ER ⁺ Ductal (2)
A7 Christiana	Tumour	47	A277	A0DC	1 of 2	NA	Luminal A	Mastectomy (yes)	ER ⁺ Lobular (3)
A7 Christiana	Tumour	142	A220	A26I	1 of 2	Mutant	Basal	Lumpectomy (yes)	ER ⁻ Ductal (2)
AC Intl Genomics	Tumour	177	A18M	A2QH	2 of 2	Mutant	Basal	Radical Mastectomy (no)	ER ⁻ Metaplastic (2)
AC Intl Genomics	Tumour	177	A220	A2QH	2 of 2	Mutant	Basal	Radical Mastectomy (no)	ER ⁻ Metaplastic (2)
GI ABS IUPUI	Normal	177	A16F	A2C8	1 of 1	NA	Luminal A	Radical Mastectomy and Neoadjuvant (no)	ER ⁺ Ductal (2)

Similarly, a correlation matrix of log-transformed raw counts was used to evaluate sample quality for TCGA stomach RNA-Seq. A tumour sample (patient 4294) was removed due to similar quality concerns leaving a final dataset for 449 samples (from 417 patients): 414 tumour samples and 35 normal tissue samples.

2.2.3 Metagenes and the Singular Value Decomposition

A “metagene” offers a one-dimensional summary of pathway (expression) activation or inactivation by dimension reduction of a matrix, avoiding negatively correlated genes averaging out the signal of a mean-based centroid (Huang *et al.*, 2003). Constructing pathway metagenes used gene sets for Reactome and the Gatzka signatures (Gatzka *et al.*, 2011, 2014) as specified above (in Section 2.1.1.2). The singular-value decomposition was performed ($X = U^T DV$, where X is the data matrix of the gene set, with genes \times samples) and the leading eigenvector (first column of V) corresponding to the largest singular value was used as a metagene for the pathway gene set. To ensure consistent directionality of metagene signals, the median of the gene set in each sample was calculated and correlated against the metagene with the (arbitrary) metagene sign adjusted as needed to conform with the majority of the gene set (i.e., positive

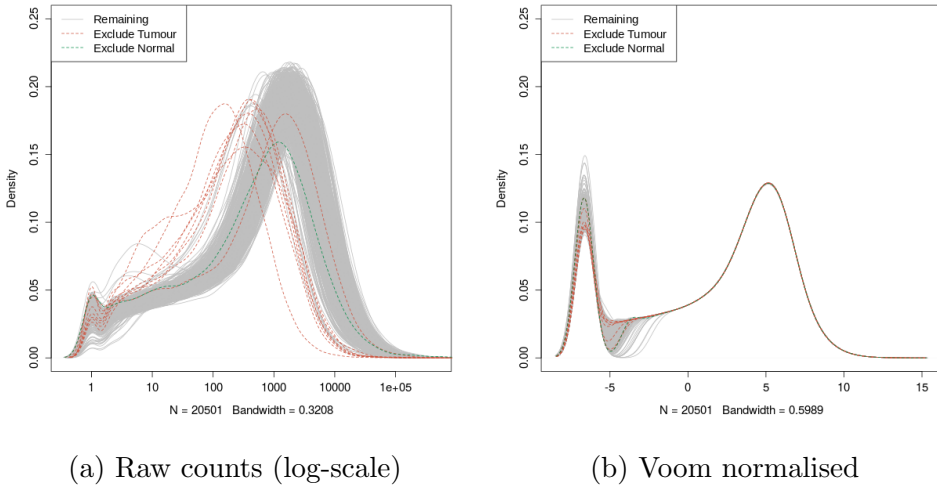


Figure 2.1: **Read count density.** Sample density plots of raw counts on log-scale and voom normalised showing samples removed due to quality concerns.

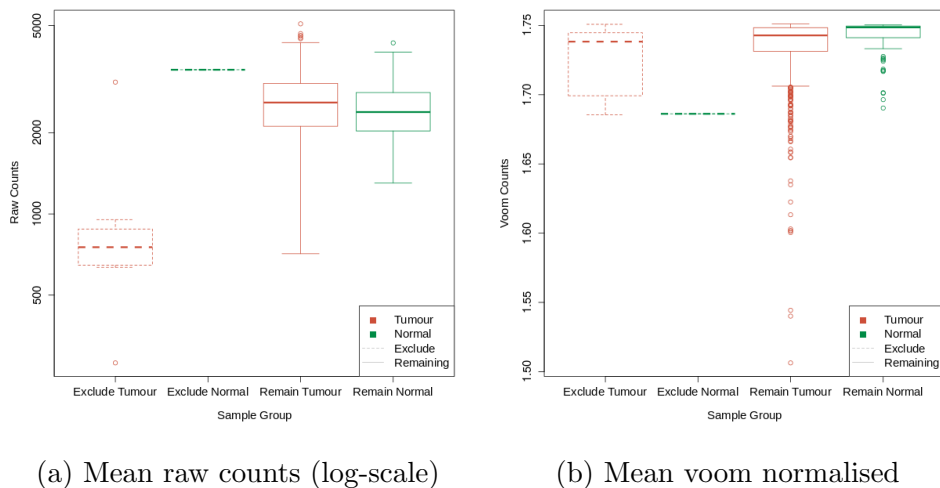


Figure 2.2: **Read count sample mean.** Boxplots of sample means for raw counts on log-scale and voom normalised show removed tumour samples with low mean read count.

correlation between [metagene](#) and the median-based centroid). To ensure that genes and [pathways](#) were weighted equally, [metagenes](#) were derived from a z-transformed (mean 0, standard deviation 1) dataset of [gene expression](#) and samples were scaled (by fractional ranking) for each [metagene](#) so that they were comparable on a [0, 1] scale.

2.2.4 Candidate Triage and Integration with Screen Data

Candidate triage in combination with the experimental data was intended to integrate findings of the [SLIPT](#) analysis with an ongoing experiment project ([Chen et al., 2014](#); [Telford et al., 2015](#)). The first procedure to compare the [SLIPT](#) gene candidates for *CDH1* with an [siRNA](#) experimental screen ([Telford et al., 2015](#)) was a direct comparison of the overlapping candidates, presented in a Venn diagram and tested with the χ^2 test. Since these candidates modestly overlapped at the gene level (even when excluding genes not contained in both datasets), further gene set over-representation analysis was performed for pathways specific to each detection approach and the intersection of the two.

The [pathway](#) composition of the intersection was further verified by a permutation resampling analysis (as described in Section 2.3.6): the same number of genes detected by [SLIPT](#) were sampled randomly from the universe of genes tested by both approaches. These samplings were performed over 1 million iterations and the [pathway](#) over-representation was compared for each of the 1652 reactome [pathways](#). These over-representation scores (χ^2) were compared the observed over-representation in the intersection of the [SLIPT](#) candidates, with the proportion of resamplings with higher χ^2 values used for empirical p-values of [pathway](#) composition. The χ^2 test was used as an appropriation of Fisher's exact test on a hypergeometric distribution for resampling to computationally scale [pathway](#) over-representation tests across iterations. Pathways for which no resamplings were occurred as high as the observed were reported as $p < 10^{-6}$. These empirical p-values were adjusted for multiple comparisons ([False discovery rate \(FDR\)](#)). Intersection size was not assumed to be constant across resamplings, so similarly with the proportion of resamplings with higher or lower intersection size were used to evaluate significance of enrichment or depletion respectively (of [siRNA](#) candidate among [SLIPT](#) candidate genes).

2.3 Techniques

Various statistical, computational, and [bioinformatics](#) techniques were performed throughout this thesis. This Section describes these techniques and gives the parameters used

unless otherwise specified. Where relevant, the R package implementation which provided the technique will be acknowledged.

2.3.1 Statistical Procedures and Tests

As described in Sections 2.3.4 and 2.2.3, the z-transform has been used to generate z-scores in various analyses in this thesis. Each row of the dataset (x_i) is transformed into a scores (z_i) using the mean (\bar{x}_i) and standard deviation (s_i) of the data such that:

$$z_i = \frac{x_{ij} - \bar{x}_i}{s_i}$$

This generates data where each row (gene) has a mean of 0 and standard deviation of 1. Where plotted as a heatmap, any data more than 3 standard deviations above or below the mean was plotted as 3 or -3 respectively.

Where specified, the Fisher's exact test, χ^2 test, and correlation were used to measure associations between variables, as implemented in the **stats** R package (R Core Team, 2016). Unless otherwise specified, Pearson correlation was used for correlation analyses (r) and coefficient of determination (R^2). Where these comparisons are discussed in more detail, Fisher's exact test and χ^2 tests are supported by a table or Venn diagram, rendered with the **limma** R package (Ritchie *et al.*, 2015). In some analyses, correlation is further supported by a scatter plot and a line of best fit derived by least squares linear regression.

The **t.test** function (R Core Team, 2016) has also been used to implement the t-test to compare pairs of data. Where relevant, an analysis of variance (ANOVA) has been performed to report significance of multivariate predictors of outcomes, or least squares linear regression performed for the adjusted coefficient of determination (R^2) and F-statistic p-value to evaluate the fit of the predictor variables. For some analyses these are supported by boxplot or violin plot visualisation (Adler, 2005), rendered in R (R Core Team, 2016).

Multiple comparisons were accounted for with the Benjamini-Hochberg procedure to control the FDR unless otherwise specified (Benjamini and Hochberg, 1995). This procedure adjusts p-values to achieve an average of the proportion of false-positives among significant tests below a threshold, α . The more stringent Holm-Bonferroni (Holm) procedure (Holm, 1979) was also applied in some cases to adjust for multiple comparisons and control the family-wise error rate which adjusts p-values so that the probability that any one of the tests is a false-positive (type-1 error) below a threshold, α .

2.3.2 Gene Set Over-representation Analysis

Gene set enrichment over-representation analysis was performed to test whether there was an enrichment of a gene set (e.g., a biological pathway) among a group of input genes. Such input genes may be predicted synthetic lethal candidates or a subset defined by clustering (in Section 2.3.3) or comparison with experimental candidates (in Section 2.2.4). Initially, these tests were performed using the GeneSetDB web tool (Araki *et al.*, 2012) hosted by the University of Auckland on the Reactome pathways (Croft *et al.*, 2014). Since the GeneSetDB tool used an older version of Reactome (version 40), it was difficult to directly compare with the results of other analysis (in Sections 2.2.4 and 2.3.6) performed on version 52 (as described in Section 2.1.1.2). Thus an implementation of the hypergeometric test in R (R Core Team, 2016) was used to test for over-representation against Reactome (version 52) pathways. Pathways containing less than 10 genes or more than 500 (as performed in GeneSetDB by Araki *et al.*, 2012) were excluded before adjusting for multiple comparisons.

2.3.3 Clustering

The clustering analysis used unsupervised hierarchical clustering with complete linkage (distance calculated from the furthest possible pairing). For correlation matrices or multivariate normal parameters (e.g., Σ), the distance metric used was Euclidean distance. For empirical or simulated gene and pathway expression data correlation distance was used, calculated by $distance = 1 - cor(t(x))$ where cor is Pearson correlation and $t(x)$ is the transpose of the expression matrix.

2.3.4 Heatmap

Standardised z-scores of the data were used to plot heatmaps on an appropriate scale. Raw (log-scale) read counts or voom normalised counts per gene (as specified) were plotted as normalised z-scores on a $[-3, +3]$ blue-red scale. Similarly, correlations were plotted on a $[-1, +1]$ blue-red scale. Heatmap dendograms were generated using the linkage method and distance specified for the clustering performed in Section 2.3.3. The gplots R package (Warnes *et al.*, 2015) was used to generate many of the heatmaps throughout this thesis, along with a customised heatmap function (released as `heatmap.2x`, detailed in Table 2.6 and Section 3.5.2). Where clearly specified, data have been split into subsets with clustering performed separately on each subset with these plotted alongside each other.

2.3.5 Modelling and Simulations

Statistical modelling and simulations were used to test various **synthetic lethal** detection procedures on simulated data. This involved constructing a statistical model of how **synthetic lethality** would appear in (continuous normally distributed) **gene expression** data. Where presented (in Section 3.2.1), the assumptions of the model are stated clearly. The model allows sampling from a multivariate normal distribution (using the `mvtnorm` R package (Genz and Bretz, 2009; Genz *et al.*, 2016)) to generate simulated data with known underlying **synthetic lethal** partners (detailed in Section 3.2.2). We can test whether statistical procedures, including those developed in this thesis (presented in Section 3.1), are capable of detecting **synthetic lethal** partners within the simulated data. This multivariate normal simulation procedure also enables the inclusion of correlation structure which is either given as correlated blocks of genes or derived from **pathway** structures (as detailed in Section 3.4.2).

When this multivariate normal distribution is sampled once and the procedure to add known **synthetic lethal** partners is performed, it generates a simulated dataset. Performing this simulation procedure and testing with a **synthetic lethal** detection procedure iteratively, these simulations can be used to assess the statistical performance of the detection procedure. The number of iterations (`Reps`) will be given for each simulation result. Typically, these are performed 1000 or 10,000 times depending on computational feasibility of doing so on larger datasets.

Several measures of statistical performance were used to assess the simulations. The following measures used the final classification of the detection procedure, statistical significance for χ^2 , significance and directional criteria met for **SLIPT** (in Section 3.1), and an arbitrary threshold: < -0.2 and $> +0.2$ for negative correlation and correlation respectively. Sensitivity (or “true positive rate”) was measured as the proportion of known **synthetic lethal** partners predicted to be **synthetic lethal**. Specificity (or “true negative rate”) was measured as the proportion of known non-synthetic lethal partners predicted not to be **synthetic lethal**. The “false positive rate” was measured here as the proportion of known non-synthetic lethal partners out of all putative partners predicted by the detection procedure. Statistical “accuracy” is the proportion of true predictions for a detection procedure, which is both the correctly predicted known **synthetic lethal** partners and correctly negative known non-synthetic lethal partners.

2.3.5.1 Receiver Operating Characteristic Curves

A more general procedure to measure the statistical performance of a simulation is the receiver operating characteristic (ROC) curve which does not assume a threshold for classification of synthetic lethality but demonstrates the achievable range of sensitivity and specificity for a model (Akobeng, 2007; Fawcett, 2006; Zweig and Campbell, 1993). These curves (implemented with the `ROCR` R package (Sing *et al.*, 2005)) plot the true positive rate (sensitivity) against the false positive rate (1-specificity) as the prediction threshold is varied. An ideal detection method will have a true positive rate of 1 and a false positive rate of 0, hence the Area Under the ROC curve (AUC or area under receiver operating characteristic (AUROC)) is a measure of statistical performance for a detection procedure accounting for this trade-off. AUROC values typically range from 0.5 (the value expected by random chance) to 1 for an optimal detection method, however it is possible for an AUROC below 0.5 for a poor detection method that performs worse than random chance. In cancer biology, it has been suggested that an AUROC of approximately 0.8 is a predictive biomarker suitable for publication (Hajian-Tilaki, 2013) but predictors with lower AUROC values may still be informative depending on the context. In this thesis, the AUROC values varied widely across simulation parameters and were primarily used for comparisons across these parameters, although they can also be used to refine thresholds for optimal classification.

2.3.6 Resampling Analysis

Resampling analyses (e.g., “permutation” analysis) are used to statistically test the significance of an observation without assuming the underlying distribution of expected test statistics (Collingridge, 2013). Instead these are derived from randomly shuffling test statistics or randomly sampling predicted candidates. For the purposes of this thesis, this involved randomly sampling genes from those tested to be analysed as putative synthetic lethal candidates. This was performed both for testing the significance of pathway composition in the intersection with experimental gene candidates (Section 2.2.4) and for assessing the significance of pathway structure among synthetic lethal candidates (Section 3.4.1.1).

These were analysed to compare the observed synthetic lethal genes against values derived from randomly sampling the same number of genes as were observed to be synthetic lethal from among the genes tested. Sampling iteratively across many resampling procedures, these resampling-based values form a null distribution that could be

expected if the null hypothesis were true. Thus the proportion of resampling-based values across these iterations that are greater than or equal to that observed, forms an empirically derived p-value to test significance.

Resampling was performed for comparison (in Section 2.2.4) with fixed experimental screen candidates (Telford *et al.*, 2015) both resampling the number of genes overlapping with the screen candidates and test statistics for *pathway* enrichment. Resampling analysis was also applied to *shortest paths* and network metrics (in Section 3.4.1.1) to test significance of directional relationships between *synthetic lethal* candidate genes within *pathway* structures.

The number of iterations determines the accuracy of these p-values. For *pathway* composition (in Section 2.2.4), a million iterations were performed using high performance computing (as detailed in Section 2.5.3) to provide sufficient accuracy after adjusting for multiple comparisons across *pathways*. For the purposes of network analysis (in Section 3.4.1.1), a thousand iterations were sufficient to reject the null hypothesis for the majority of *pathways* tested before adjusting for multiple comparisons, and thus further iterations were not performed.

2.4 Pathway Structure Methods

2.4.1 Network and Graph Analysis

Networks are important in considering the structure of relationships in molecular biology, including gene regulation, kinase cellular signalling, and metabolic *pathways* (Barabási and Oltvai, 2004). Network theory is an interdisciplinary field which combines the approaches of computer science with the metrics and fundamental principles of graph theory, an area of pure mathematics dealing with relationships between sets of discrete elements. The vast amounts of molecular and cellular data from high-throughput technologies have enabled the application of network-based and *genomes-wide bioinformatics* analysis to examine the complexity of a cell at the molecular level and understand aberrations in cancer. This thesis uses various metrics and analysis procedures developed in Graph and Network theory to analyse *graph* structure of biological *pathways*. Where feasible, these have been implemented using the *igraph* R package with such procedures described below (Csardi and Nepusz, 2006). Custom R functions were used to perform more complex analysis and visualisation of iGraph data (as described in Section 3.5.3).

Graph theory is a branch of pure mathematics which deals with the properties of sets of discrete objects (referred to as a ‘node’ or ‘vertex’) with some pairs are joined (by a ‘link’ or an ‘edge’). While a seemingly reductionist abstraction to mathematically study relationships, graph theory has applications in a wide range of fields, including the life sciences. Network theory is the sub-discipline of graph theory that deals with networks, which has become popular due to the vast potential for applications of networks (van Steen, 2010).

Applications vary depending on the situation modelled, particularly in how the edges between vertices are defined, whether they are directed or weighted, and whether multiple redundant edges between a pair of vertices (referred to as ‘parallel edges’) or edges connecting a vertex to itself (referred to as ‘loops’) are permitted in the model. Networks are defined such that the edges represent a relationship between the vertices and may be directed, weighted, or contain parallel edges or loops depending on the application (van Steen, 2010). Unless otherwise stated, graph structures and networks in this thesis will be unweighted and have no parallel edges or loops. Where a directional relationship is known or modelled, it will be represented with a directed edge in a directed graph.

2.4.2 Sourcing Graph Structure Data

Pathway Commons interaction data was sourced using the Biological PAthway eXchange (BioPAX) with the paxtools-4.3.0 Java application on October 6th 2015 (Cerami *et al.*, 2011; Demir *et al.*, 2013). This utility was used to import ‘sif’ format interaction data into R (R Core Team, 2016) and extract the human Reactome (version 52) dataset of interactions was imported (Croft *et al.*, 2014), matching those used for pathway enrichment analysis. These interactions were used to construct an adjacency matrix for the Reactome network and subnetworks corresponding to each relevant biological pathway.

2.4.3 Constructing Pathway Subgraphs

Subgraphs for each relevant pathway were constructed by matching the nodes in the complete Reactome network to the pathway gene sets (as derived in Section 2.1.1.2). A subgraph with adjacent nodes was constructed by adding nodes which have an edge with a gene in the pathway gene set. The pathways these adjacent nodes belong to were added to form a “meta-pathway” to account for the possibility for nodes within the pathway being linked by the surrounding graph structure.

2.4.4 Network Analysis Metrics

The existing network analysis measures applied in this thesis (as described below) used an implementation in the `igraph` R package to compute vertex degree, shortest paths, and centrality (Csardi and Nepusz, 2006). Additionally, custom features were developed for analysis of iGraph objects in R and released as `igraph.extensions` (as described in Section 3.5.3).

Vertex degree is the number of `edges` a `node` has and is a fundamental measure of the importance and connectivity of a network (van Steen, 2010). More connected `nodes`, such as network hubs, will have a higher `vertex` degree relative to other `nodes`. For the purposes of this thesis, `vertex` degree ignored `edge` direction with loops (edges with itself) and double `edges` to the same `node` excluded.

A fundamental concept in network analysis is a “`shortest path`”, that is the shortest route via `edges` between any two particular `nodes` in a network. These are computed by Dijkstra’s algorithm (Dijkstra, 1959) in the `igraph` R package (Csardi and Nepusz, 2006). Where applicable paths will only use directed `edges` in a particular direction. Shortests paths are a useful measure of how close `nodes` are in a network. This is used to compute `information centrality`, and for further analysis of `pathway` structure (as described in Section 3.4.1).

Network `centrality` is an alternative measure of the importance or influence of a `node` to the `graph` structure (Borgatti, 2005). Various strategies are used to derive centrality, typically based on how connected the `node` is or the impact of `node` removal on the connectivity of the network. One of the most notable is the “`PageRank`” algorithm, a refinement of eigenvector `centrality` based on the eigenvectors of the adjacency matrix (Brin and Page, 1998). This is implemented in the `igraph` R package (Csardi and Nepusz, 2006).

Another network `centrality` measure that has been previously applied to biological protein interaction networks (Kranthi *et al.*, 2013) is the “`information centrality`”. The `information centrality` of a `node` is the relative impact on efficiency (transmission of information via `shortest paths`) of the network when the `node` is removed. Te `centrality` (C) (Kranthi *et al.*, 2013) for `node` n in graph G is defined as:

$$C_n = \frac{E(G) - E(G')}{E(G)}$$

where G' is the subgraph with the `node` removed and E is the efficiency (Latora and Marchiori, 2001), derived from `shortest paths` (d_{ij} between `nodes` i and j).

$$E(G) = \frac{2}{N(N-1)} \sum_{i < j \in G} \frac{1}{d_{ij}}$$

The efficiency of the network can be derived from `shortest paths` implemented in the `igraph` R package and the iterative network `centrality` computation of each `node` has been released as an R package (`info.central`) and included in the `igraph.extensions` package.

2.5 Implementation

2.5.1 Computational Resources and Linux Utilities

Several computers were used to process and store data during this thesis (as summarised in Table 2.2), running different versions of Linux operating systems, including a personal laptop computer, laboratory desktop machine, departmental server, and the New Zealand eScience Infrastructure Intel Pan high-performance computing cluster (a supercomputer based at the University of Auckland). Each of these systems support a 64-bit architecture. Current workflows on local machines use Elementary OS (based on the Ubuntu versions given in Table 2.2) and the ZSH shell. However, Ubuntu OS and the Bourne Again SHell (Bash) were used at the inception of this project and Bash continues to be used for running scripts. Various Linux applications and command-line utilities were used on these machines (as summarised in Table 2.3). As such, the workflows developed in this project should be backwards-compatible with Ubuntu Linux (and other derivatives). The majority of novel methodology and implementations were performed in R which is a cross-platform language, packages developed in R will be available for users of Linux, Mac, and Windows machines.

Table 2.2: Computers used during thesis

	Viao Laptop	Lab Machine	Biochem Server	NeSI Pan Cluster
Operating System (OS)	Elementary OS Freya 0.3.2	Elementary OS Loki 0.4	Red Hat Enterprise Maipo 7.2	Cent OS Final 6.4
	Ubuntu LTS Trusty 14.04	Ubuntu LTS Xenial 16.04		
Upstream OS	3.19.0-65-generic	4.4.0-36-generic	3.10.0-327.36.2.el7.x86_64	2.6.32-504.16.2.el6.x86_64
	Shell: Bash 4.3.11(1)	4.3.46(1)	4.2.46(1)	4.2.1(1)
Linux Kernel	Shell: zsh 5.0.2	5.1.1	5.0.2	5.2

Table 2.3: Linux utilities and applications used during thesis

		Viao Laptop	Lab Machine	Biochem Server	NeSI Pan Cluster
	OS	Elementary OS Freya 0.3.2	Elementary OS Loki 0.4	Red Hat Enterprise Maipo 7.2	Cent OS Final 6.4
	Linux Kernel	3.19.0-65-generic	4.4.0-36-generic	3.10.0-327.36.2.el7.x86_64	2.6.32-504.16.2.el6.x86_64
Scripting	Shell Bash	4.3.11(1)	4.3.46(1)	4.2.46(1)	4.2.1(1)
	Shell zsh	5.0.2	5.1.1	5.0.2	5.2
Programming	Python	2.7.6	2.7.12	2.7.5	
	Java	1.8.0_101	9-ea	1.8.0_101	
	C++	4.8.4	5.4.0	4.8.5	4.4.7
Text Editor	nano	2.2.6	2.5.3	2.3.1	2.0.9
	kile (L ^A T _E X)	2.1.3	2.1.3		
Version Control	git	1.9.1	2.11.0	1.7.1	1.8.3.1
Shell Utilities	sed	4.4.2	4.4.2	4.4.2	4.4.1
	grep	2.16-1	2.25-1	2.20	2.6.3
	nohup	8.21	8.25	8.22	8.4
Typesetting	T _E X	3.1415926	3.14159265		
	TeXLive (L ^A T _E X)	2013	2015		
	PDFT _E X	2.5-1	2.6		
	pandoc	1.12.2.1	1.16.0.2		
Remote Computing	Slurm scheduler				16.05.6
	OpenSSH	7.2p2	7.2p2	6.6.1	5.3p1
	OpenSSL	1.0.2g	1.0.2g	1.0.01e-fips	1.0.01e-fips
	rsync	3.1.0p31	3.1.1p31	3.0.9p30	
	Globus Online Transfer			3.1	3.1
	Cisco AnyConnect VPN		3.1.05170		
Image Processing	Inkscape	0.48.4	0.91		
	GIMP	2.8.10	2.8.16		
	ImageMagick	6.7.7.10-6			

2.5.2 R Language and Packages

The R programming language has been used for the majority of this thesis. Current R installations across the machines used are given in Table 2.4. Local machines currently run the latest version of the R (at the time of writing) and remote machines run the versions and modules as managed by the system administrator.

Various scripts and packages in this thesis were developed or run in previous versions of RStudio and R but these run without error in the current version of R (and the older versions on remote machines). The R packages which were used throughout this thesis (as detailed in Table 2.5 with versions specified) were installed from the [comprehensive R archive network \(CRAN\)](#) ([CRAN, 2017](#)), Bioconductor ([Gentleman *et al.*, 2004](#), version 3.4; BiocInstaller 1.24.0), or GitHub (<https://github.com/>). These packages were not updated when they would change the functionality of scripts or functions in packages, in particular imported data from annotation packages (used to define gene sets) have been saved as local files to continue using stable versions of these [pathway](#) data (across machines).

This is a summary of the key packages which (in addition to their dependencies) have been used throughout this project. Where a package implementation has been central to the methods applied, they are described in more detail in the relevant Section. A full table of packages used in this thesis can be found in Appendix B (Table B.1). The R packages developed during this thesis are given in Table 2.6 with the relevant Sections describing their implementation and use where appropriate, in addition to further details on these functions in Section 3.5.

Table 2.4: R installations used during thesis

		Viao Laptop	Lab Machine	Biochem Server	NeSI Pan Cluster
	OS	Elementary OS Freya 0.3.2	Elementary OS Loki 0.4	Red Hat Enterprise Maipo 7.2	Cent OS Final 6.4
Programming	R	3.3.2	3.3.2	3.3.1	3.3.0-intel (module)
Development	RStudio	1.0.136	1.0.136	1.0.136 (server)	

Table 2.5: R Packages used during thesis

Package	Version Used	Built	Repository
colorspace	1.3-2	3.3.1	CRAN
curl	2.3	3.3.1	CRAN
data.table	1.9.6	3.3.1	CRAN
dendextend	1.4.0	3.3.2	CRAN
DBI	0.5-1	3.3.1	CRAN
devtools	1.12.0	3.3.1	CRAN
dplyr	0.5.0	3.3.1	CRAN
ggplot2	2.2.1	3.3.1	CRAN
git2r	0.18.0	3.3.1	CRAN
gplots	3.0.1	3.3.1	CRAN
gtools	3.5.0	3.3.1	CRAN
igraph	1.0.1	3.3.1	CRAN
matrixcalc	1.0-3	3.3.1	CRAN
mclust	5.2.2	3.3.1	CRAN
mvtnorm	1.0-6	3.3.1	CRAN
org.Hs.eg.db	3.1.2	3.1.2	Bioconductor
openssl	0.9.6	3.3.1	CRAN
plyr	1.8.4	3.3.1	CRAN
purrr	0.2.2	3.3.1	CRAN

reactome.db	1.52.1	3.2.1	Bioconductor
RColorBrewer	1.1-2	3.3.1	CRAN
Rcpp	0.12.9	3.3.1	CRAN
ROCR	1.0-7	3.3.1	CRAN
roxygen2	6.0.1	3.3.2	CRAN
shiny	1.0.0	3.3.1	CRAN
snow	0.4-2	3.3.1	CRAN
testthat	1.0.2	3.3.2	CRAN
tidyverse	1.1.1	3.3.2	GitHub (hadley)
sm	2.2-5.4	3.3.1	CRAN
Unicode	9.0.0-1	3.3.2	CRAN
vioplot	0.2	3.3.1	CRAN
viridis	0.3.4	3.3.2	CRAN
xml2	1.1.1	3.3.2	CRAN
xtable	1.8-2	3.3.1	CRAN
zoo	1.7-14	3.3.1	CRAN
graphics	3.3.2	3.3.2	base
grDevices	3.3.2	3.3.2	base
cluster	2.0.5	3.3.1	base
graphics	3.3.2	3.3.2	base
grDevices	3.3.2	3.3.2	base
Matrix	1.2-8	3.3.1	base
stats	3.3.2	3.3.2	base

Table 2.6: R packages developed during thesis

Package Name	Description and GitHub Repository	Section
<code>slipt</code>	Synthetic lethal detection by SLIPT (to accompany publication) https://github.com/TomKellyGenetics/slipt	3.1
visualisation	<code>vioplotx</code> Customised violin plots (based on <code>vioplot</code>) https://github.com/TomKellyGenetics/vioplotx	3.4
	<code>heatmap.2x</code> Customised heatmaps (based on <code>gplots</code>) https://github.com/TomKellyGenetics/heatmap.2x	
igraph.extensions	<code>igraph.extensions</code> Meta-package to install the follow iGraph functions https://github.com/TomKellyGenetics/igraph.extensions	3.5.3
	<code>plot.igraph</code> Custom plotting of directed graphs https://github.com/TomKellyGenetics/plot.igraph	2.4.4
	<code>info.centrality</code> Computing information centrality from network efficiency https://github.com/TomKellyGenetics/info.centrality	3.4.2
	<code>pathway.structure.permutation</code> Testing pathway structure with resampling analysis https://github.com/TomKellyGenetics/pathway.structure.permutation	3.4.1.1
	<code>graphsim</code> Generating simulated expression from graph structures https://github.com/TomKellyGenetics/graphsim	3.4.2

2.5.3 High Performance and Parallel Computing

Another enabling technology for [bioinformatics](#) is parallel computing, performing independent operations using separate [central processing unit \(CPU\)](#) cores: this “multithreading” is widely used to increase the time to compute results. [Bioinformatics](#) is particularly amenable to this since performing multiple iterations of a simulation or testing separate genes is often “embarrassingly parallel”, as [CPUs](#) completely independent of each other.

The New Zealand eScience Infrastructure ([NeSI](#)) is a [High Performance Computing \(HPC\)](#) organisation providing the Intel Pan cluster or “supercomputer”, hosted by the University of Auckland ([NeSI, 2017](#)). The Pan cluster used throughout this thesis project to optimise and perform computations which would have otherwise been infeasible in the timeframe of thesis. Such technological developments and infrastructure initiatives have enabled [bioinformatics](#) research including this project. High performance computing on the Pan cluster was used extensively in this project including for resampling analysis (in Sections 2.3.6 and 3.4.1.1), calculating [information centrality](#) (in Section 2.4.4), and in simulations (in Sections 2.3.5, 3.2, and 3.4.2)

Scripts and data were transferred between the Pan cluster and University of Otago computing resources by `rsync` or the Globus file transfer service ([Globus, 2017](#)). R scripts ([R Core Team, 2016](#)) were run in parallel with the “simple network of workstations” `snow` R package [Tierney *et al.* \(2015\)](#). This utilised the “message passing interface” ([Yu, 2002](#)) when it was feasible with memory requirements to run in parallel across multiple compute nodes, otherwise [Socket Secure \(SOCKS\)](#) was used to access

multiple cores within an instance of R and pass input data to them. R jobs were submitted to queue for available resources and run on the Pan cluster via the [Simple Linux Utility for Resource Management \(Slurm\)](#) workload manager ([Slurm, 2017](#)). Slurm array job submission and independent running of different parameters (with arguments passed to R from the shell) were used to run memory-intensive job or scripts across many parameters simultaneously. In some cases, this submission was automated across a range of parameters with [Bash](#) scripts.

Chapter 3

Methods Developed During Thesis

In this Chapter, I outline the rationale and development of various methods used throughout this thesis to examine [synthetic lethality](#) in gene expression data, graph structures, models and simulations. Firstly, the [Synthetic Lethal Interaction Prediction Tool \(SLIPT\)](#), a [bioinformatics](#) approach to triage [synthetic lethal](#) candidate genes, will be described. This is one of the main research outputs of this thesis project and is supported by comparisons to an experimental screen from a related project and evaluation of performance on simulated data. These supporting findings will be covered in further chapters but simulation data is included to support the use and design of [SLIPT](#). This includes the construction of a statistical model of [synthetic lethality](#) in (continuous multivariate Gaussian) [gene expression](#) data, which enables testing [SLIPT](#) upon simulated data with known [synthetic lethal](#) partners. Another key component of this simulation pipeline is the generation of simulated data from a known [graph](#) structure or simulated biological pathway (as applied in Chapter 6). The development of this simulation procedure and other statistical treatment of graph and [network](#) structures will also be covered. Various R packages have been developed to support this project, including the `slipt` package to implement the [SLIPT](#) methodology. Additional R packages for handling [graph](#) structures, simulations, and custom plotting features will be described as research outputs of this thesis, methods applied throughout, and contributions of open-source software.

3.1 A Synthetic Lethal Detection Methodology

The [SLIPT](#) methodology identifies [gene expression](#) patterns consistent with [synthetic lethal](#) interactions, between a query gene and a panel of candidate interacting partners. Gene expression is scored “low”, “medium”, or “high”, sorting samples by tertiles (1/3-

quantiles) for each gene. Genes with insufficient expression across all samples are excluded by requiring that the first tertile of raw counts is above zero. A χ^2 test is then performed between the query gene and each candidate partner. The p-values for the χ^2 test are corrected for multiple testing using False discovery rate (FDR) error control to reduce false positives (Benjamini and Hochberg, 1995). Significance is called for FDR adjusted $p < 0.05$. A synthetic lethal interaction is predicted (as shown in Figure 3.1) when (i) the χ^2 test is significant; (ii) observed low-query, low-candidate samples are less frequent than expected; and (iii) observed low-query, high-candidate and high-query, low-candidate samples are more frequent than expected.

The synthetic lethal prediction procedure has also been performed with somatic mutation data for the query gene. This is intended for a query gene known which is recurrently mutated, with the majority of mutations disrupting gene function (e.g., null or frameshift mutations). A synthetic lethal interaction is predicted (as shown in Figure 3.2) when (i) the χ^2 test is significant; (ii) observed mutant-query, low-candidate samples are less frequent than expected; and (iii) observed mutant-query,

		Candidate Gene		
		Low	Medium	High
Query Gene (e.g. CDH1)	Low	Observed less than expected		Observed more than expected
	Medium			
	High	Observed more than expected		

Figure 3.1: **Framework for synthetic lethal prediction.** SLIPT was designed to identify candidate interacting genes from gene expression data using the χ^2 test against a query gene. Samples are sorted into low, medium, and high expression quantiles for each gene to test for a directional shift. A sample being low in both genes of a synthetic lethal pair is unlikely, since loss of both genes will be deleterious, and is expected to be statistically under-represented in a gene expression dataset. We expect a corresponding (symmetric) increase in frequency of sample with low-high gene pairs. Synthetic lethal candidate partners of a gene were identified by running this procedure on all possible partner genes, selecting those with an FDR-adjusted χ^2 -derived $p < 0.05$, and meeting the directional criteria. Since synthetic lethal genes are partners of each other, commutatively, the symmetric direction criteria were defined such that detected synthetic lethal genes are partners of each other.

		Candidate Gene		
		Low	Medium	High
Query Gene (e.g. <i>CDH1</i>)	Mutation	Observed less than expected		→ Observed more than expected
	Wild-type	↓ Observed more than expected		

Figure 3.2: **Synthetic lethal prediction adapted for mutation.** SLIPT was also adapted to identify candidate interacting genes using (somatic) **mutation** data of the query gene in the χ^2 test. Samples are sorted into low, medium, and high **expression** quantiles for each candidate gene and tested for a directional shift against **mutation** status of the query gene. A sample having low **expression** or **mutation** for the **synthetic lethal** pair is expected to be unlikely with a corresponding increase in frequency of sample with **mutant-high** or **wild-type-low** gene pairs. **Synthetic lethal** (mtSL) candidate partners of a gene were identified from running this procedure on all possible partner genes, selecting those with an **FDR**-adjusted χ^2 -derived $p < 0.05$, and meeting the directional criteria.

high-candidate and **wild-type-query**, low-candidate samples are more frequent than expected.

The **SLIPT** methodology can be performed on **expression** data, including pathway **metagenes** (as generated in Section 2.2.3). The application of the **SLIPT** methodology on public **gene expression** data will be supported with simulation results (in Section 3.3 and Chapter 6), including comparison to other statistical methods. **SLIPT** results for *CDH1* were compared experimental screen results in a breast cell line (Telford *et al.*, 2015). Primary screen results are discussed in Section 4.2 and secondary screen results are presented in Section 4.2.4.

3.2 Synthetic Lethal Simulation and Modelling

A statistical model of **synthetic lethality** was developed to generate simulated data and to evaluate the **SLIPT** procedure. This Section describes the **synthetic lethal** model and the simulation procedure for generating **gene expression** data with known **synthetic lethal** partners. Simulation results, to support usage of the **SLIPT** methodology throughout this thesis, will be presented in Section 3.3. The simulation procedure will

also be applied in Chapter 6, including in combination with simulations from graph structures (as described in Section 3.4.2).

3.2.1 A Model of Synthetic Lethality in Expression Data

A conceptual model of synthetic lethality was devised (as shown in Figure 3.3), which will be used to build a statistical model of synthetic lethal gene expression and to simulate expression data for assessing various potential synthetic lethal prediction methods, including SLIPT. In the model, synthetic lethality occurs between genes with related functions, as a cell death phenotype, when these functions are inactive.

This model suggests that synthetic lethality is detectable in measures of gene inactivation across a sample population, namely mutation, DNA copy number, DNA methylation, and expression levels. While any of these mechanisms of gene inactivation could lead to synthetic lethality, expression data is readily available and changes in other mechanisms are likely to impact on the amount of expressed RNA that is detectable. Functional relationships between genes could manifest in expression data in several ways, including coexpression, mutual exclusivity and directional shifts. Co-expression is overly simplistic (Lu *et al.*, 2015) and has previously performed poorly as a predictor of synthetic lethality (Jerby-Arnon *et al.*, 2014), although this will still be tested with correlation measures in later simulations. The alternative hypothesis is that synthetic lethality will result in a detectable shift in the number of samples which exhibit low or high expression of either gene. This model does not preclude mutual exclusivity, compensating expression, or co-loss under-representation which may occur between synthetic lethal genes (Lu *et al.*, 2015; Wappett *et al.*, 2016).

The first condition of the synthetic lethal model is that if there are only two synthetic lethal genes (e.g., *CDH1* and one SL partner), then they will not both be non-functional in the same sample (in an ideal model). Gene function is thus determined for each sample in a model of synthetic lethality with the proportion of samples which are functional or non-functional for a gene being arbitrary. Whether a gene is functional can similarly be modelled by an arbitrary threshold of continuous and normally distributed gene expression data to define gene function (as shown in Figure 3.4). For the purposes of modelling synthetic lethality in cancer expression data, a threshold of the 30th percentile of the expression levels was used because approximately 30% of samples analysed had *CDH1* inactivation (mutations) in breast cancer (Koboldt *et al.*, 2012). This was generalised for a model of the proportion of samples inactivated for each gene. The threshold of the 0.3 quantile was used in simulations derived from this

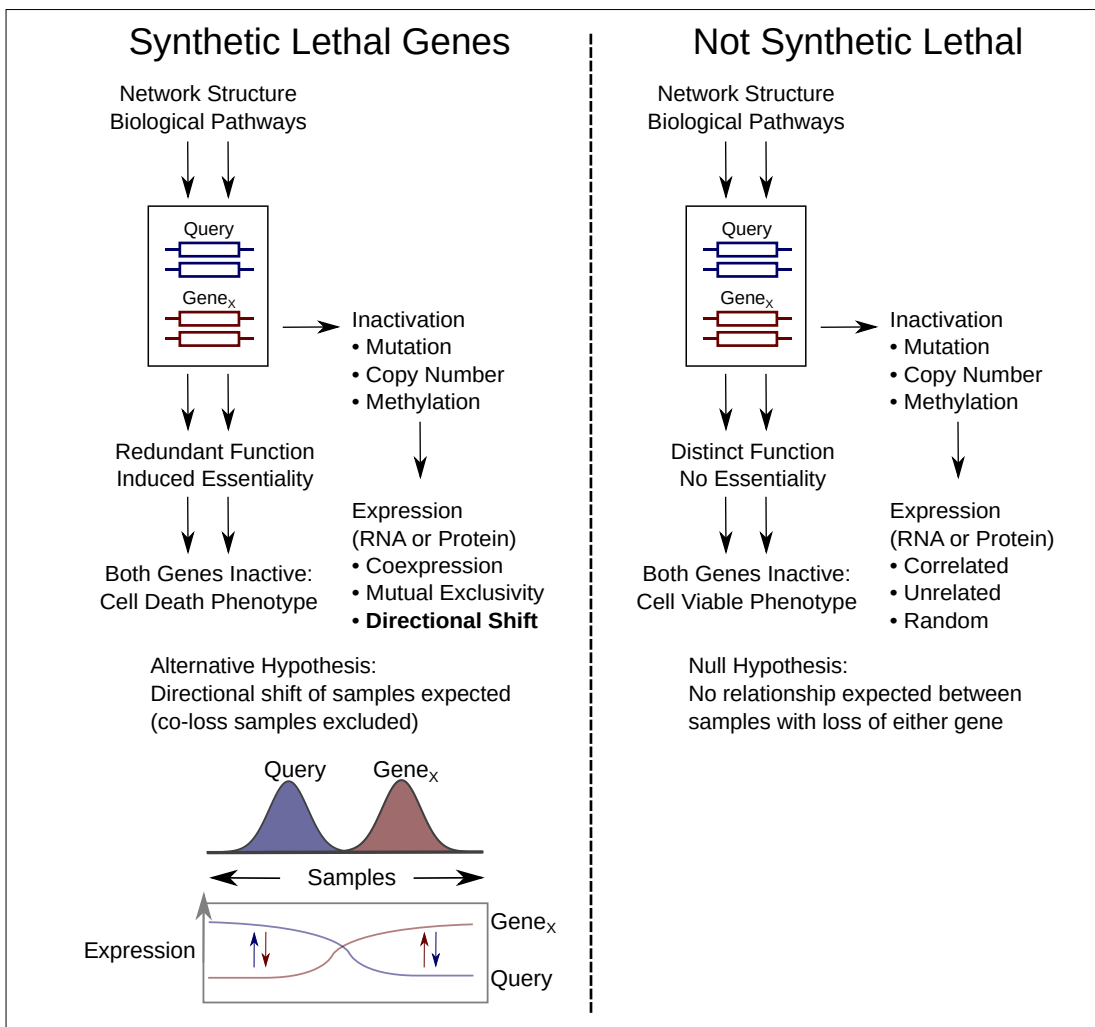


Figure 3.3: **A model of synthetic lethal gene expression.** A conceptual model of synthetic lethal interactions between a Query gene and partner gene (G_X). Genes that are synthetic lethal may not both be non-functional in the same sample without another gene compensating for the loss of function. This is most likely to be detectable as low gene expression, whether they are lost by mutation, deletion, DNA methylation, or suppressing regulatory signals. This could manifest as coexpression, mutual exclusivity, or directional shifts in sample frequency. Thus the alternative hypothesis (H_A) is that synthetic lethal genes will have a reduced frequency of co-loss samples while the null hypothesis (H_0) is that non synthetic lethal gene pairs would show no such relationship, even if they may be correlated for other means such as pathway relationships. In this model synthetic lethal genes may compensate for the loss of each other but this is not assumed, only that loss of both is unfavourable to cell viability and probability of detecting samples with combined gene loss.

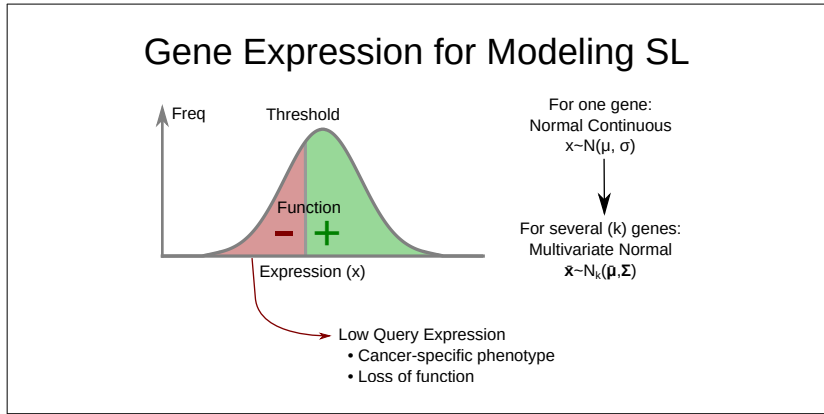


Figure 3.4: **Modelling synthetic lethal gene expression.** When modelling [synthetic lethal](#) interactions between a Query gene and partner genes (G_X and G_Y) above, cellular viability requires that at least one of genes is not inactivated. As a model of loss of function, genes are regarded as non-functional with expression below a threshold for the purposes of modelling [synthetic lethality](#). Tumour suppressor genes with loss of function also have cancer specific phenotypes (although these thresholds are not assumed to be the same). Expression is modelled by normally (Gaussian) distributed continuous data, such as (log-scale) data from RNA (microarray or [RNA-Seq](#)), protein, or pathway [metagenes](#). This rationale generalises to several genes on a multivariate normal distribution.

model throughout this thesis. In this ideal case, no samples lowly expressing both of these genes are expected to be observed. While this was not the case, that is to be expected as it is unlikely that only two genes will have an exclusive [synthetic lethal](#) partnership.

A [synthetic lethal](#) pair of genes is unlikely to act in isolation, therefore higher-order [synthetic lethal](#) interactions (i.e., 3 or more genes) must be considered in the model as shown in Figure 3.5. Even when testing pairwise interactions, it is important to model higher level interactions that may interfere. If there are additional [synthetic lethal](#) partners, there are two possibilities for adding these: 1) that they are independent partners of the query genes interacting pairwise (and not with each other) or 2) that an additional partner gene interacts with both of the [synthetic lethal](#) genes already in the system and any of the three (or more) are required to be functional for the cell to survive.

The signal (in terms of [gene expression](#) data) will be weaker for this latter case and this model has the more stringent assumption that all [synthetic lethal](#) partner genes interact with each other: that only one of these must be expressed to satisfy

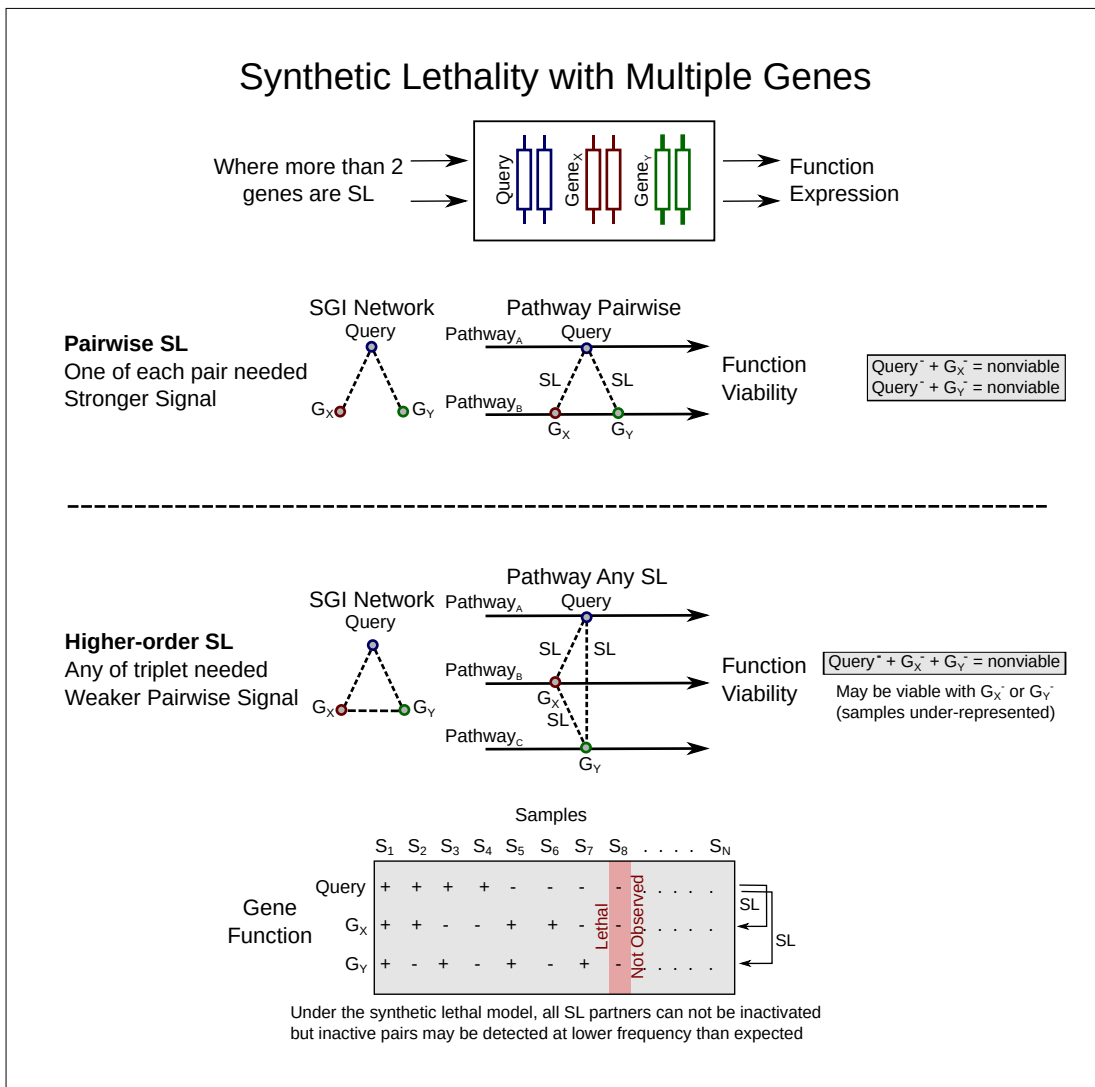


Figure 3.5: **Synthetic lethality with multiple genes.** Higher order synthetic lethal interactions may occur between 3 or more genes, affecting the simulated expression (or synthetic lethal predictions) even if undetected when observed pairwise. Consider interactions between a Query gene and two partner genes (G_x and G_y). They may interact with the Query pairwise (inviolate when either gene pair is lost) or form a higher-order interaction such as the “synthetic lethal triplet” if any of the genes provide an essential function (inviolate only when all are lost). Either is plausible with the potential pathway structures. A synthetic lethal triple has 8 potential combinations of gene function but one is not expected to be observed (due to inviability), however pairwise inactivation may be observed if additional partner genes are functional. The proportion of these combinations varies depending on the functional threshold.

the model of synthetic lethality. In this model, any of the synthetic lethal genes in a higher-order interaction are able to perform the essential function of the others, allowing for higher-level synthetic lethal partners to compensate for loss a synthetic lethal gene pair. While samples that express low levels of the synthetic lethal gene pairs will be under-represented, they may not be completely absent from the dataset, due to these higher-level interactions. In the example of three synthetic lethal genes (shown in Figure 3.5), only one of the genes involved in the higher-order synthetic lethal interaction is required for cell viability. For synthetic lethal pairs, only a subset of these samples will be inviable (i.e., removed from simulated data), leading to an under-representation.

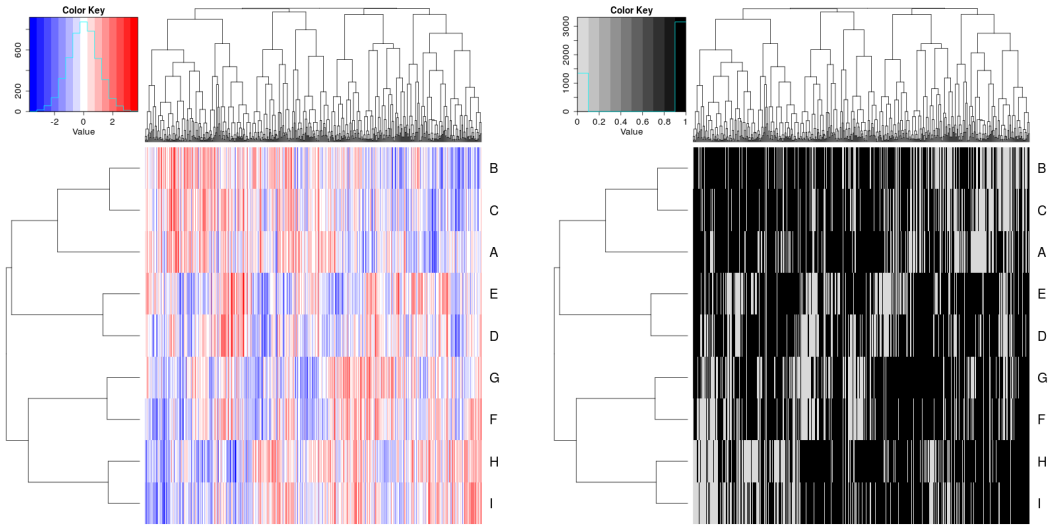
Samples were not actually removed from a simulated dataset, rather the expression and function of the query gene is generated across samples separately from the pool of potential partner genes. The query gene data was matched to simulated samples (as shown in Figure 3.7) satisfying the synthetic lethal condition with the procedure described in Section 3.2.2. This was performed to maintain a comparable samples size across simulations and the preserve the (multivariate) normal distribution of the data.

3.2.2 Simulation Procedure

Simulations were developed to generate normal distributions of expression data and define gene function with a threshold cut-off. While gene function was used as an intermediary step in modelling synthetic lethal genes in expression data, the normal distribution was sampled for simulated data to represent normalised empirical gene expression data for which SLIPT (and other methods) will be applicable.

Sampling a distribution for expression profiles has the advantage of enabling simulating correlation structures with the multivariate normal distribution, using the `mvtnorm` R package (Genz and Bretz, 2009; Genz *et al.*, 2016). The parameter Σ , the covariance matrix, defines the correlation structure between the simulated genes being sampled. With a diagonal of one, this Σ matrix simulates genes with a standard deviation of one and the covariance parameters between them are the correlations between each gene. In Figure 3.6, an example of such a simulated multivariate normal dataset is shown with the functional threshold applied.

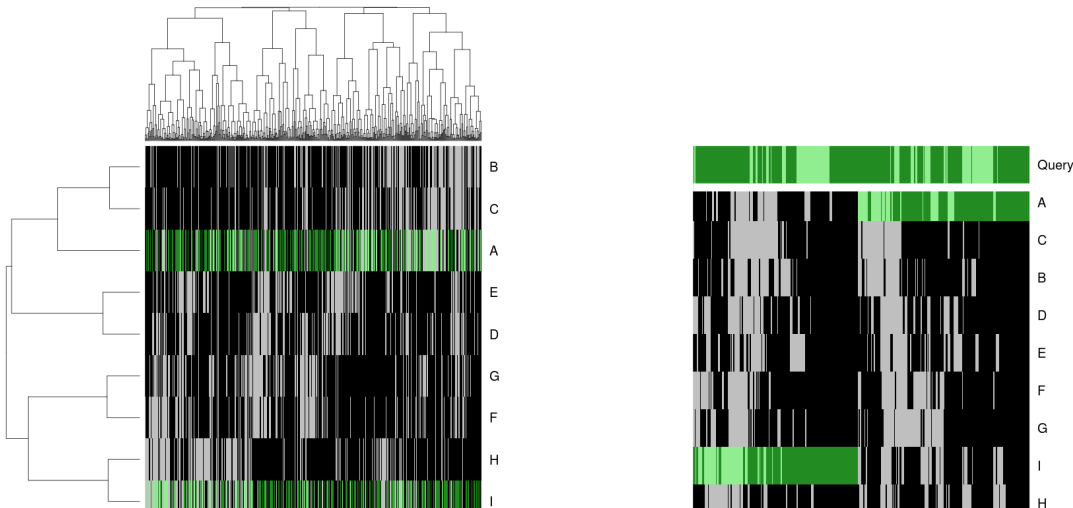
Once a simulated dataset has been generated, the samples were compared by gene function (as derived from a functional threshold). The known underlying synthetic lethal partners were selected within the dataset and a query gene was generated by sampling from the normal distribution. These were matched (as shown for two synthetic



(a) Simulated expression matrix

(b) Corresponding gene function calls

Figure 3.6: **Simulating gene function.** A simulated dataset with samples (columns) and genes A–I (rows) was transformed from a continuous (coloured blue–red) scale to a discrete matrix of gene function (black for functional levels and grey for non-functional).



(a) Simulated gene function with SL genes (b) Query gene added with SL condition

Figure 3.7: **Simulating synthetic lethal gene function.** In a discrete simulated gene function dataset (shaded for functional levels and pale otherwise) with samples (columns) and genes (rows), genes A and I are SL partners of a “Query” gene. A partner was selected (highlighted in green) randomly in each sample for simulating synthetic lethality, then ordered such that the query gene or an SL partner were functional in each sample.

lethal partners in Figure 3.7) such that the synthetic lethal condition was met: at least one of the synthetic lethal partner genes and the query gene are functional in any particular cell. The samples are ordered by functional data (without assuming correlation of underlying expression values) with the query gene in one direction and the remaining dataset ordered by the selected synthetic lethal partner.

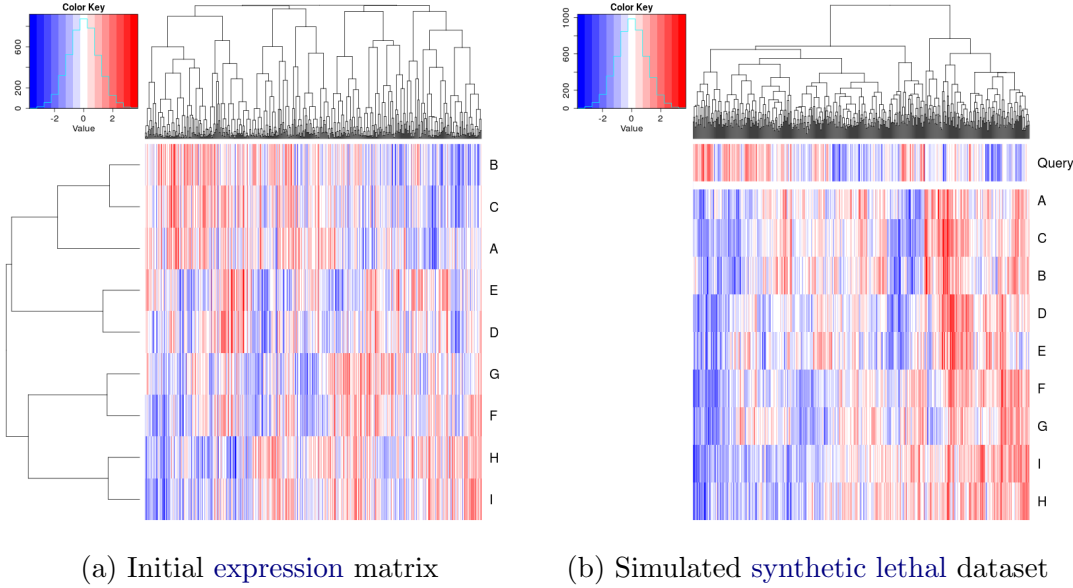


Figure 3.8: **Simulating synthetic lethal gene expression.** A simulated continuous expression dataset (blue–red scale) with samples (columns) and genes A–I (rows) was matched to a query gene such that at least one synthetic lethal partner was above a functional threshold when the query gene was below it which satisfied the synthetic lethal model.

This procedure produces a simulated dataset where samples with a non-functional query gene have at least one functional partner gene. Similarly, the query gene is functional in all samples where all of the synthetic lethal partner genes are non-functional. In this procedure, a dataset has been generated with known synthetic lethal partners (as shown in Figure 3.8) with few assumptions about the relationships between the each synthetic lethal pair (allowing compensating functions from higher-order interactions). This procedure has been designed to have the most stringent (least detectable) synthetic lethal relationships, where higher-order interactions are possible for the purposes of testing pairwise detection procedures such as SLIPT.

3.3 Detecting Simulated Synthetic Lethal Partners

The [synthetic lethal](#) detection methodology ([SLIPT](#)), as described in Section 3.1, was evaluated with simulated data containing known [synthetic lethal](#) partners, generated using the procedure described in Section 3.2.2. Simulations were performed to demonstrate the methodology and support its use throughout this thesis. These simulations were performed by sampling from statistical distributions, including the multivariate normal distribution with correlated blocks of genes, generated by Σ matrices such as those shown. A more complex multivariate normal sampling procedure based on pathway [graph](#) structures, as described in Section 3.4.2, was used for further investigations in Chapter 6.

3.3.1 Binomial Simulation of Synthetic Lethality

The [synthetic lethal](#) simulation procedure (described in Section 3.2.2) initially used gene function, sampled directly from a binomial distribution using the binomial probability of observing functional gene levels ($p = 0.3$) in one observation ($n = 1$) for each samples:

$$X \sim \text{Bin}(n, p)$$

Once a query gene with [synthetic lethal](#) partners has been added, these functional levels were passed directly into [SLIPT](#) as “low” and “high” samples.

The simulation procedure was performed with 20,000 total genes (as occurs in [expression](#) datasets) with a variable number of true [synthetic lethal](#) partners and 500, 1000, 2000, or 5000 samples. Each [ROC](#) curve was derived from the results of 10,000 replicate simulations. The statistical performance (as shown in Figure 3.9) of the χ^2 -derived p-value declined towards random predictions (an [AUROC](#) of 0.5) with an more underlying [synthetic lethal](#) partners to detect. However, increased sample size somewhat mitigated this decline, as expected with a statistical predictor, particularly for moderate numbers of [synthetic lethal](#) partners.

Simulations using this binomial model of [synthetic lethality](#) were simplistic but informed the development of more complex simulations including [expression](#) and correlation structures. It did not represent the data that [SLIPT](#) will be applied to but the binomial simulations demonstrated that [SLIPT](#) is able to distinguish small numbers of [synthetic lethal](#) partners in a simulated system with behaviours expected with respect to sample size. This supported further development of the [synthetic lethal](#) model

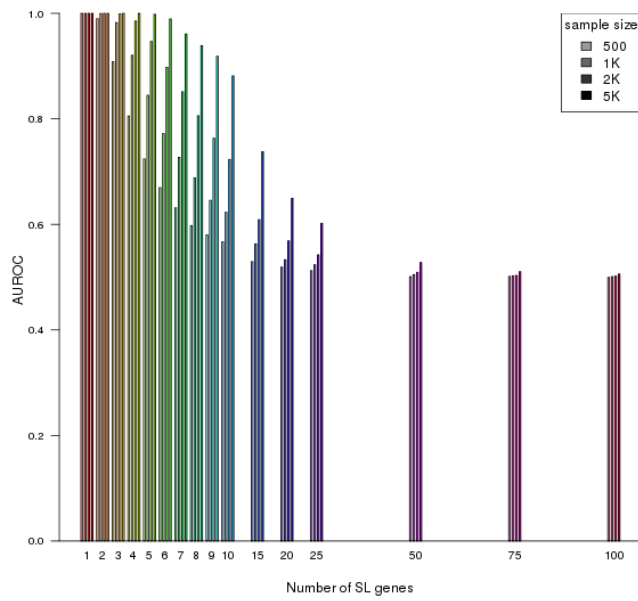


Figure 3.9: **Performance of binomial simulations.** Gene function was simulated by binomial sampling and tested for synthetic lethality by [SLIPT](#). Statistical performance declined with additional synthetic lethal partners but this was mitigated by increased sample sizes.

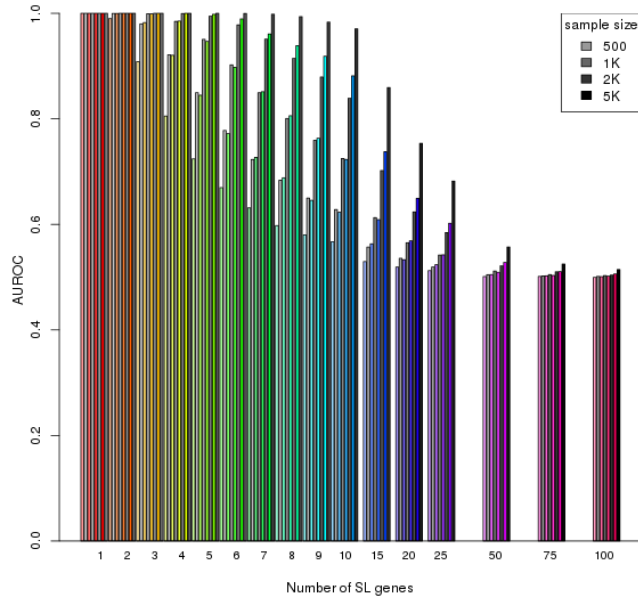


Figure 3.10: **Comparison of statistical performance.** Binomial simulation of synthetic lethality (in colour) in comparison to multivariate normal simulations (in greyscale), in which [SLIPT](#) consistently had higher performance across parameters.

and simulation pipeline (as described in Section 3.2) using the multivariate normal distribution.

The multivariate normal simulation procedure more closely recapitulates the (normalised) `expression` data that **SLIPT** was intended for and enables the methodology procedure to be tested without requiring modifications (in Section 3.3.2). Sampling continuous `expression` values from a normal distribution enabled the `expression` threshold for gene function to differ from the categorical “low” and “high” `expression` binning performed by **SLIPT** (as discussed in Section 3.2.1). The **SLIPT** procedure does not assume a known threshold for `expression` and instead uses `expression` as an estimate of gene function which does not compromise the statistical performance of the **SLIPT** in the multivariate normal simulation. The performance was an improvement over the binomial simulation procedure (shown in Figure 3.10) across simulation parameters in an equivalent simulation (without correlation structure). This multivariate normal model is also more refined since it defines the `synthetic lethal` condition, to ensure that at least one `synthetic lethal` partner was active in query-deficient samples, without disrupting the proportion of samples with each gene being functional.

3.3.2 Multivariate Normal Simulation of Synthetic Lethality

The multivariate normal simulation procedure was initially performed using the `mvttnorm` R package (Genz and Bretz, 2009; Genz *et al.*, 2016) (as described in Section 3.2) without correlation structure. Expression was sampled from multivariate normal distribution with a mean ($\mu = 0$), standard deviation ($\sigma = 1$), and no correlation between genes ($r = 0$):

$$X \sim N(\bar{\mu}, \Sigma).$$

Once a query gene with synthetic lethal partners has been added, the simulated `expression` values were tested by **SLIPT**, as described in Section 3.1.

The statistical accuracy of **SLIPT** as a binary classifier was high across simulations of a full dataset of 20,000 genes (shown in Figure 3.11a). Using the χ^2 -derived p-value as a threshold for prediction, this was largely due to high specificity: the majority of non synthetic lethal genes were distinguished from the underlying `synthetic lethal` genes. Thus the **SLIPT** methodology performed better with larger datasets with more expected negatives and the results of simulations of smaller numbers of genes (e.g., the `graph` structures analysed in Section 6.2.1) can be applied to larger datasets, where they are expected to perform comparably or better with a lower false negative rate

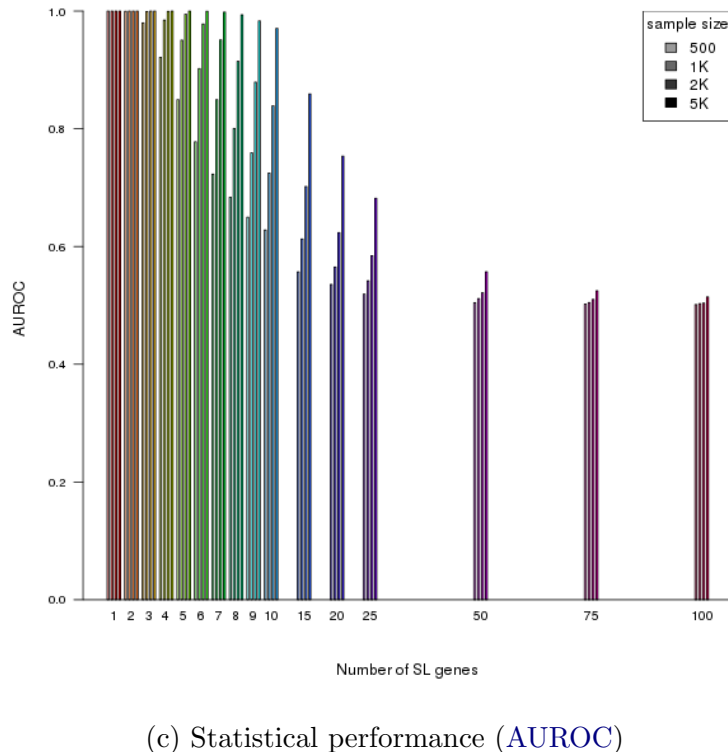
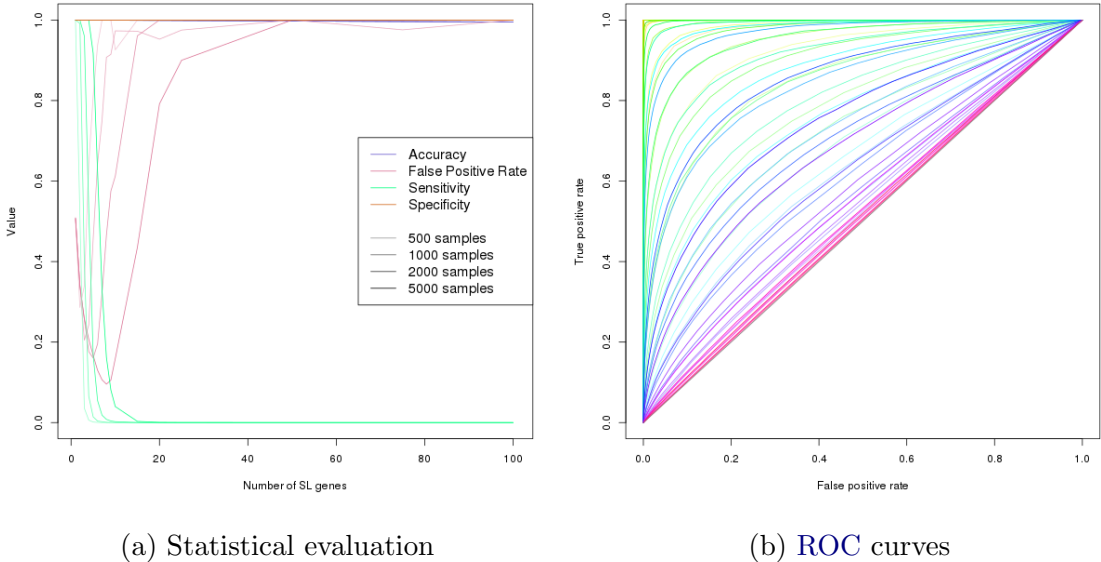


Figure 3.11: Performance of multivariate normal simulations. Simulation of synthetic lethality was performed by sampling from a multivariate normal distribution (without correlation structure). Performance of **SLIPT** declined with increasing numbers of synthetic lethal partners but this was mitigated by increased sample sizes (in darker colours). This occurred as the sensitivity decreased with a greater number of true positives to detect, which lead to a trade-off in accuracy as seen in a trough for false positive rate and the **ROC** curves.

(as shown in Sections 6.2.4 and 6.3.2). Accordingly, key results will be supported by replication with larger numbers of non synthetic lethal genes added to the simulations.

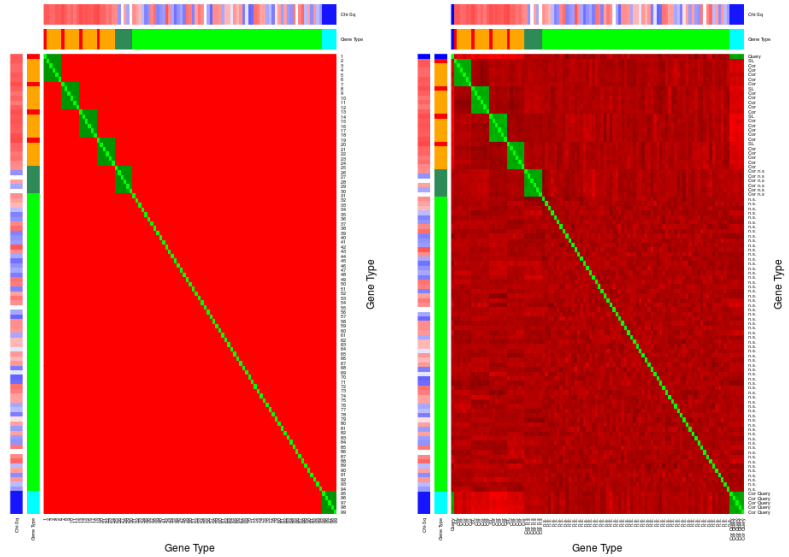
The sensitivity of **SLIPT** as a binary classifier of **synthetic lethality** (as shown in Figure 3.11a) declined with higher numbers of **synthetic lethal** genes to detect, although this is somewhat mitigated by higher sample sizes. The minority of true **synthetic lethal** partners are more difficult to distinguish when there are more of them (with a weaker **expression** signal from each). While a reduction of the false positive rate could be achieved for moderate numbers of underlying **synthetic lethal** partners, the number of partners to be detected in analyses of **expression** data is unknown. However, this simulation procedure is amenable to assessing the performance of **SLIPT** across simulation parameters, **graph** structures, and comparisons to other approaches (as presented in Chapter 6).

Not all of the genes detected by **SLIPT** were true **synthetic lethal** genes but they were among the strongest candidates and **SLIPT** had higher performance with fewer underlying **synthetic lethal** genes to detect. These results support a focus on pathway analyses, in particular, the selection of pathways for further investigation. Pathway over-representation analysis was performed to detect functional groups recurrently detected by **SLIPT** since individually detected gene candidates were not necessarily **synthetic lethal**. The detection of functionally related genes (in Chapter 4) supports the role of a pathway in **synthetic lethal** relationships. The use of pathway **metagenes** can reduce the number of potential pathways, compared to genes, to help identify **synthetic lethality**. These approaches were both applied in Chapter 4 to identify the synthetic lethal pathways of *CDH1*. Pathways are also more likely to replicate across experimental models, as demonstrated by Dixon *et al.* (2008).

The **ROC** curves showed that **SLIPT** is subject to a near equal trade-off between sensitivity and specificity across threshold values (as shown in Figure 3.11b). The lower sensitivity and higher specificity with a binary classification (as shown in Figure 3.11a) results from stringent testing by **SLIPT** with **FDR** adjusted p-values. The area under these curves (**AUROC**) was used to compare statistical performance (as shown in Figure 3.11c), which had lower performance for more underlying **synthetic lethal** partners, and higher performance for larger sample size in multivariate normal simulations.

3.3.2.1 Multivariate Normal Simulation with Correlated Genes

Correlation structures were added to the simulation procedure (with the Σ matrix, as discussed in Section 3.2), using correlated blocks of genes (as shown in Figure 3.12a). These correlated blocks represent genes with correlated **expression**, such as co-regulation



(a) Input Σ matrix parameter (b) Simulated correlation matrix

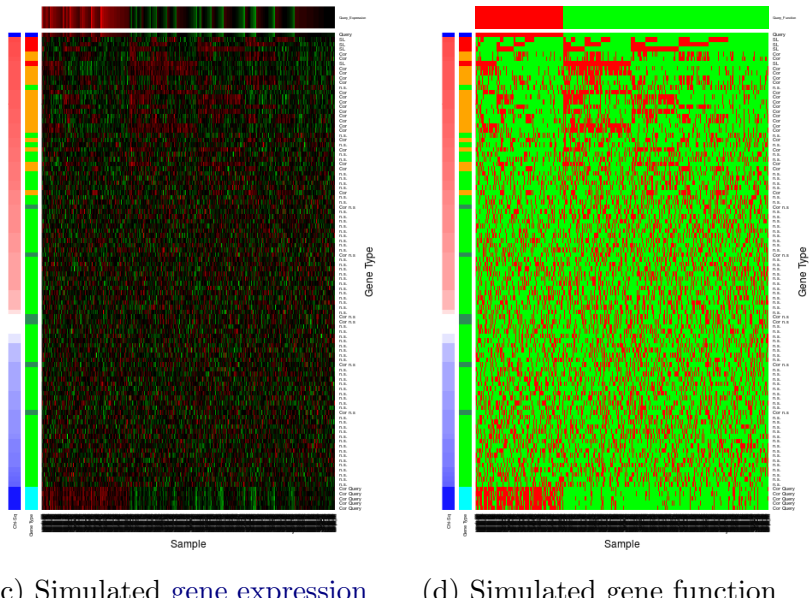


Figure 3.12: Simulating expression with correlated gene blocks. A Σ matrix (a) was used to generate 100 genes with a multivariate normal distribution, including correlated blocks of genes ($r = 0.8$) with correlation (b) similar to Σ , on a red-to-green scale. The annotation for genes gives the χ^2 (in blue for in the direction of SLIPT or red otherwise) and the gene category (blue for query, cyan for query-correlated, red for SL, orange for SL-correlated, forest green for non synthetic lethal-correlated, and green for non synthetic lethal). The simulated gene expression (c) and function (d) generated were ordered by χ^2 showing the functional structure of synthetic lethal genes and that they were among the strongest SLIPT results.

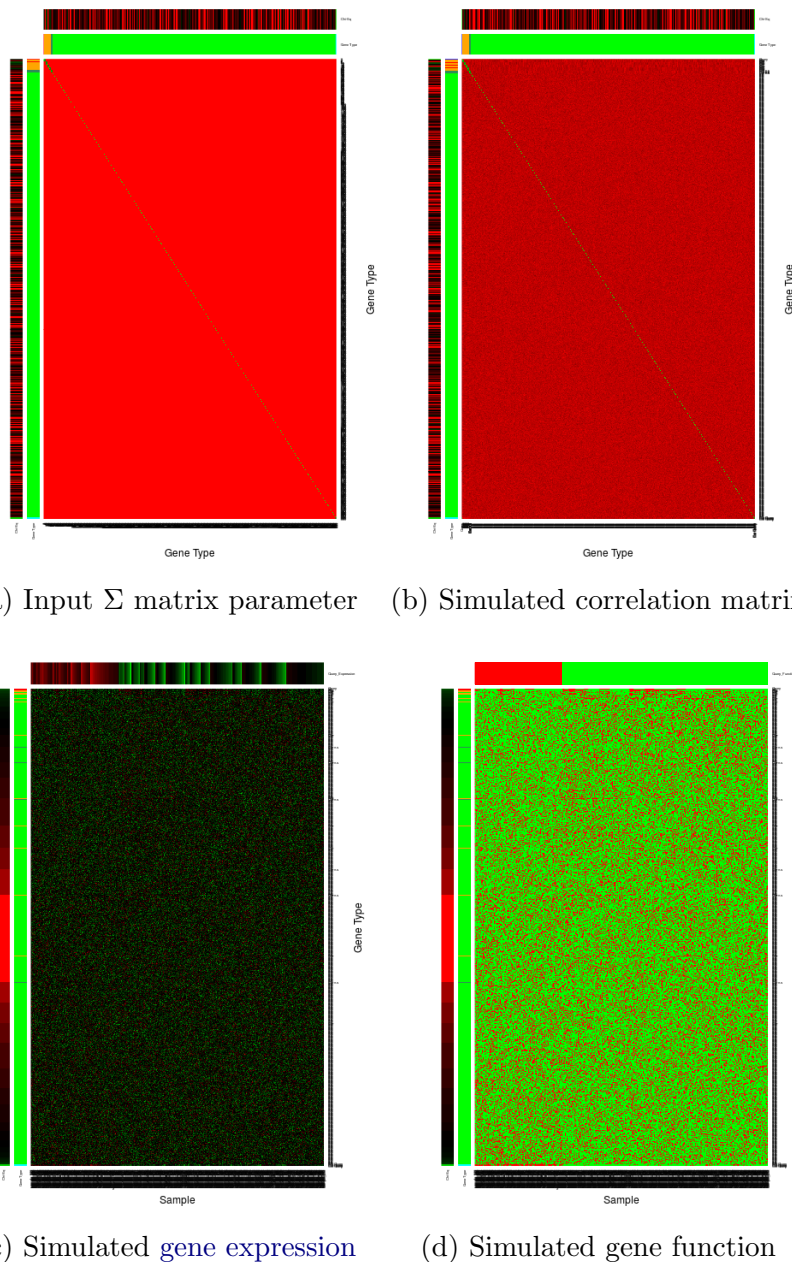


Figure 3.13: **Simulating expression with correlated gene blocks.** Using the Σ matrix (a), sampling 1000 genes from a multivariate normal distribution produced (b) correlated blocks of genes (correlated by 0.8) on a red-to-green scale. The simulated gene expression (c) and function (d) generated were ordered by χ^2 and SLIPT direction show that synthetic lethal genes are among the strongest SLIPT results with high specificity against many potential false positives. These are annotated for $\log\chi^2$ (on a red-to-green scale) and category (blue for query, cyan for query-correlated, red for SL, orange for SL-correlated, forest green for non synthetic lethal-correlated, and green for non synthetic lethal) for each gene.

or shared membership of biological pathways. The example (as shown in Figure 3.12) shows four **synthetic lethal** genes (out of 100), each with five correlated genes that are not themselves **synthetic lethal** partners of the query gene. These simulations address whether **synthetic lethal** genes are distinguishable from correlated partners. The Σ matrix produced a similar correlation structure (Figure 3.12b) and **expression** profiles (Figure 3.12c). Apart from correlated blocks of genes ($r = 0.8$), the remaining genes had small variations due to random sampling. The structure of the dataset, particularly between **synthetic lethal** genes and the query, was evident in the simulated **gene expression** (Figure 3.12c) and function (Figure 3.12d). When these genes were ordered by the **SLIPT** results, the **synthetic lethal** genes were highly ranked, a the majority of them were distinguishable from highly correlated genes.

The use of correlation structure was applied to larger datasets, such as the 1000 genes shown in Figure 3.13. **Synthetic lethal** genes were highly ranked by **SLIPT** and were often distinguishable from correlated genes. As previously discussed in Section 3.3.2, these **synthetic lethal** genes were still detectable among a larger number of non synthetic lethal genes, and the **SLIPT** methodology performed better on large datasets.

These plots (Figures 3.12 and 3.13) used similar correlated blocks with a non synthetic lethal gene (true negative) and the query gene (which is not **synthetic lethal** with itself). Neither of these were **synthetic lethal** but they could potentially affect performance methodology, particularly the specificity, as correlated non synthetic lethal genes may be distinguishable from **synthetic lethal** genes. The non synthetic lethal correlated block of genes had no impact on **synthetic lethal** detection but the query correlated genes were important (as shown in Sections 3.3.2.2 and and 6.1.1.1).

The simulations of **gene expression** data (with 100 genes) with correlations structure were used to examine the variation between detection in different samples and varying the number of underlying **synthetic lethal** partners. A small number of simulations (10 for each) are shown to demonstrate the variation between replicate simulations from iterative sampling from the same multivariate normal distribution (as shown in Figure 3.14). These simulations showed that **synthetic lethal** genes were highly ranked by **SLIPT** when there are few of them and these were relatively consistent across replicate simulations. However, they were less consistent for higher numbers of **synthetic lethal** partners to detect and were more difficult to distinguish from other genes, particularly those correlated with them. Similarly, the χ^2 values showed clear

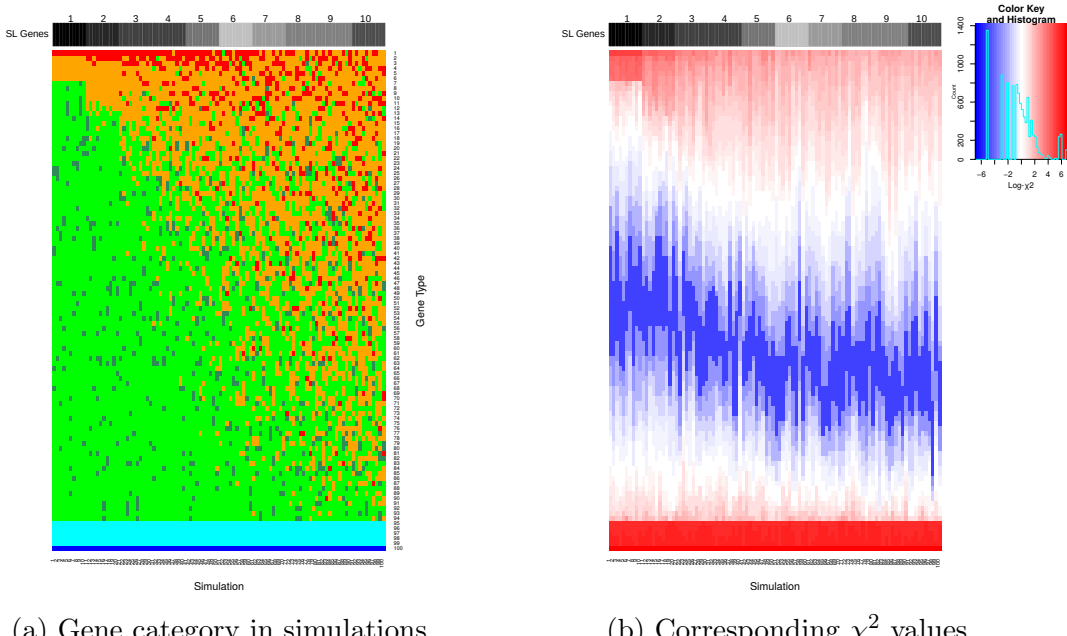
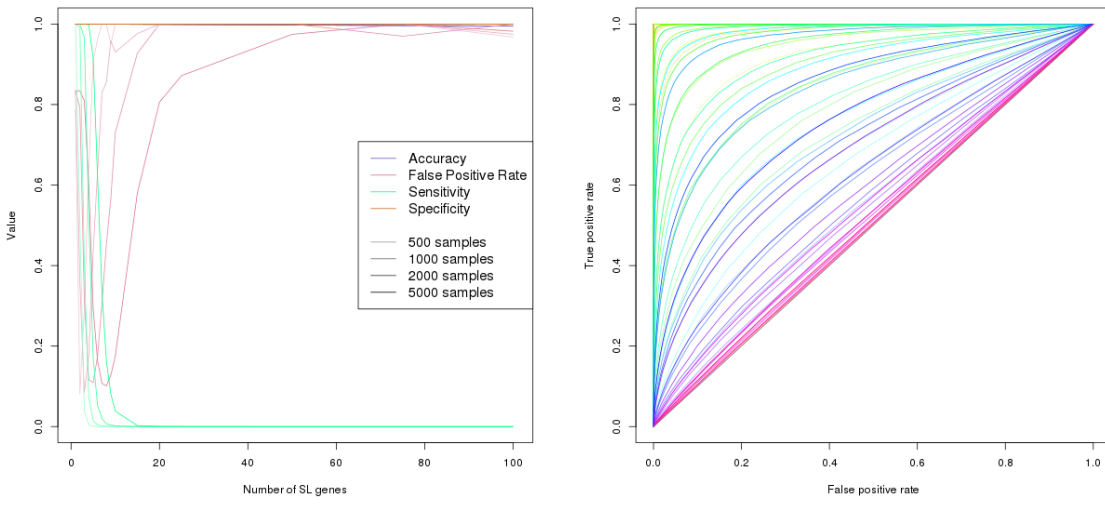


Figure 3.14: **Synthetic lethal prediction across simulations.** The gene category (a) ordered by χ^2 and the **SLIPT** directional condition is shown across simulations (blue for query, cyan for query-correlated, red for SL, orange for SL-correlated, forest green for non synthetic lethal-correlated, and green for non synthetic lethal). For each number (1–10) of **synthetic lethal** partners, 10 simulations show that the increasing numbers of **synthetic lethal** partners became harder detect (i.e., red cells become interspersed in the columns of (a)). The log- χ^2 values (b) showed a threshold for **synthetic lethal** and correlated genes when there are fewer of them, distinguishable from correlated genes in this case.

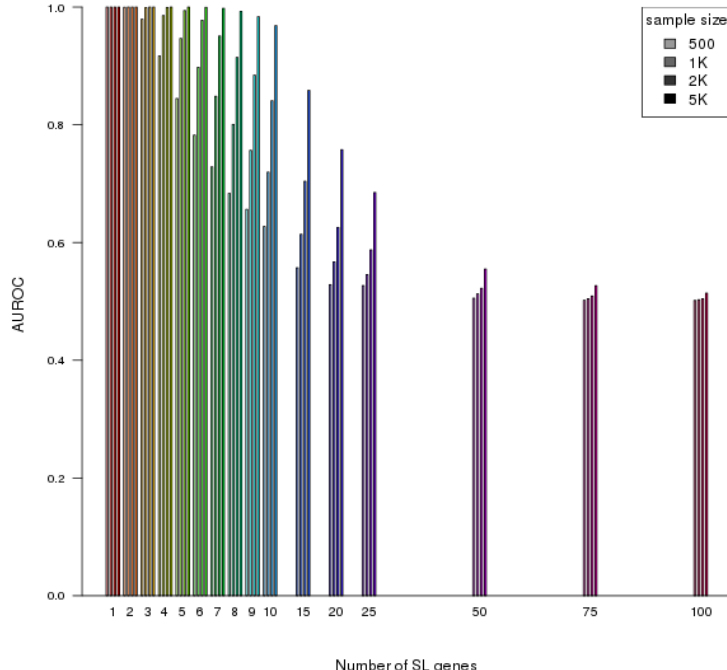
thresholds for synthetic lethal and correlated genes in simple simulations but these were more gradual for higher numbers of synthetic lethal partners.

While the **synthetic lethal** genes were detected in simple simulations (as shown in Figure 3.14), ROC analysis was performed to determine whether they were robustly detectable and to make further comparisons. These results (as shown in Figure 3.15) were similar to simulations without correlation structure. As a binary classifier, **SLIPT** had low sensitivity for higher numbers of **synthetic lethal** partners to detect and high specificity with the vast majority of non synthetic lethal genes (for 20,000 genes). This was reflected in a similar reduction in statistical performance for higher numbers of **synthetic lethal** partners and a higher performance with higher sample size. Overall, the statistical performance was no different to simulations without correlation structure (as shown in Figure 3.16).



(a) Statistical evaluation

(b) ROC curves



(c) Statistical performance (AUROC)

Figure 3.15: **Performance with correlations.** Simulation of synthetic lethality was performed by sampling from a multivariate normal distribution (with correlation structure). Performance of SLIPT declines for more synthetic lethal partners but this is mitigated by increased sample sizes (darker colours). This generally occurs as the sensitivity decreases for a greater number of true positives to detect, leading to a trade-off in accuracy as seen in a trough for false positive rate and the ROC curves.

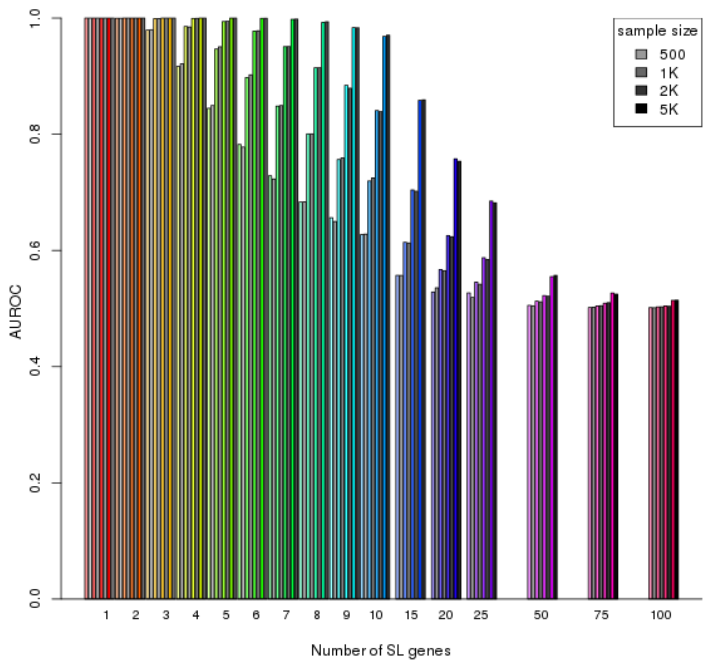


Figure 3.16: Comparison of statistical performance with correlation structure. Multivariate simulation of synthetic lethality with correlation structure (in colour) has comparable performance to simulation without correlations (in greyscale) with known synthetic lethal partners across parameters.

SLIPT was robust across correlation structures and is applicable to gene expression data, with pathway structures and correlations. These correlation structures were not intended to model specific biological pathways or represent them but showed potential impact of correlation structure on the performance of SLIPT using highly correlated ($r = 0.8$) gene blocks. More complex correlation structures, such as genes positively correlated with the query gene and derived from pathway graph structures (as described in 3.4.2) were examined further in Sections 3.3.2.2 and 6.2.1 respectively.

In particular, genes correlated with true synthetic lethal genes had little impact on the performance of SLIPT detection: synthetic lethal genes were as distinguishable from correlated genes as they are from true negative genes. Genes correlated with synthetic lethal partners did not interfere with the detection of true synthetic lethal genes, although they were often ranked next below them and may support synthetic lethal pathways by having related gene functions.

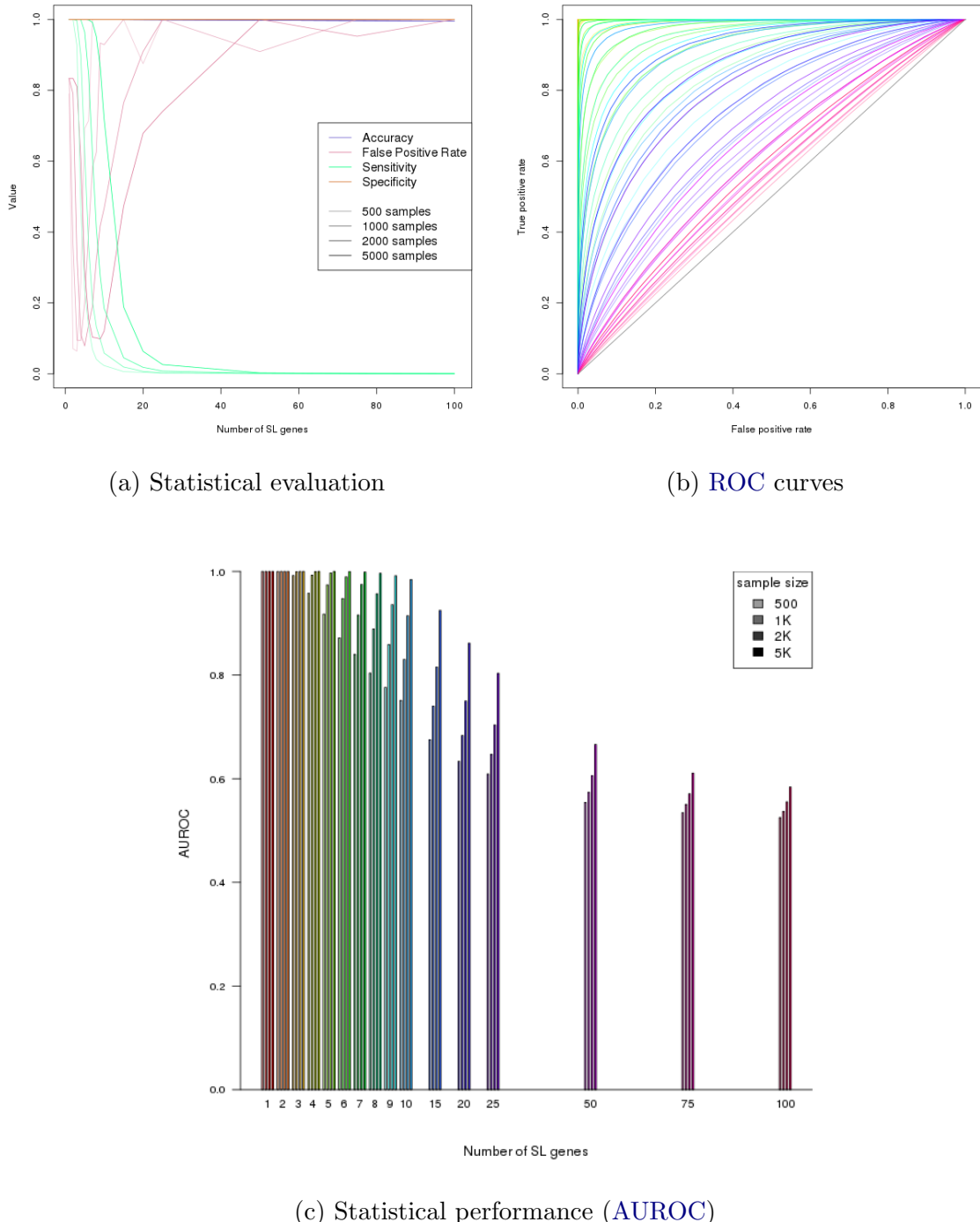


Figure 3.17: Performance with query correlations. Simulation of synthetic lethality was performed by sampling from a multivariate normal distribution (with correlation structure including correlated genes with non synthetic lethal and query genes). Performance of SLIPT declined for more synthetic lethal partners and is mitigated by increased sample sizes (darker colours) but the sensitivity remains higher for a greater number of true positives with corresponding improvements in ROC curves.

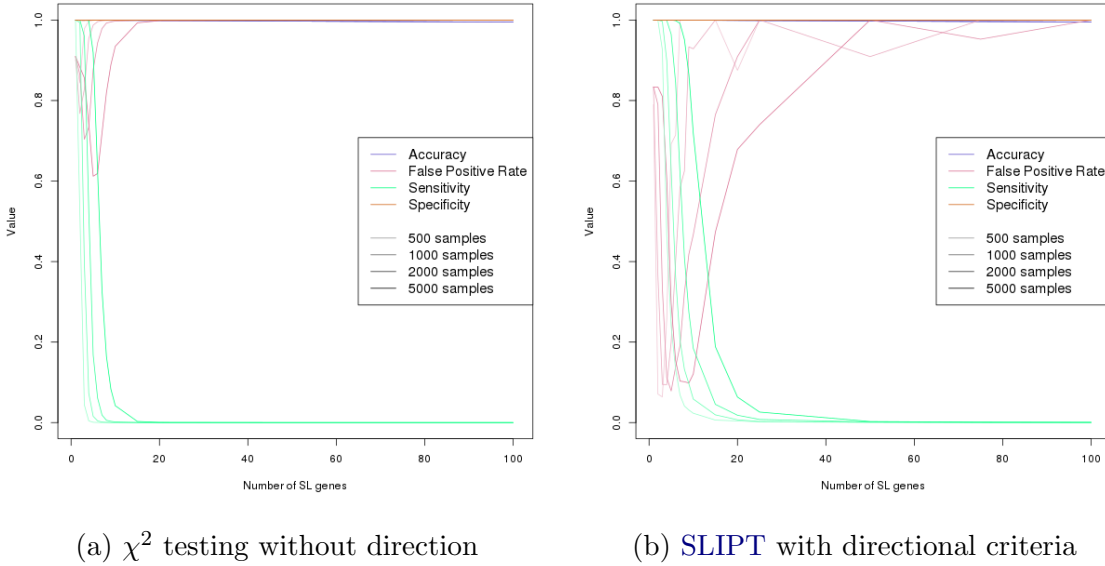
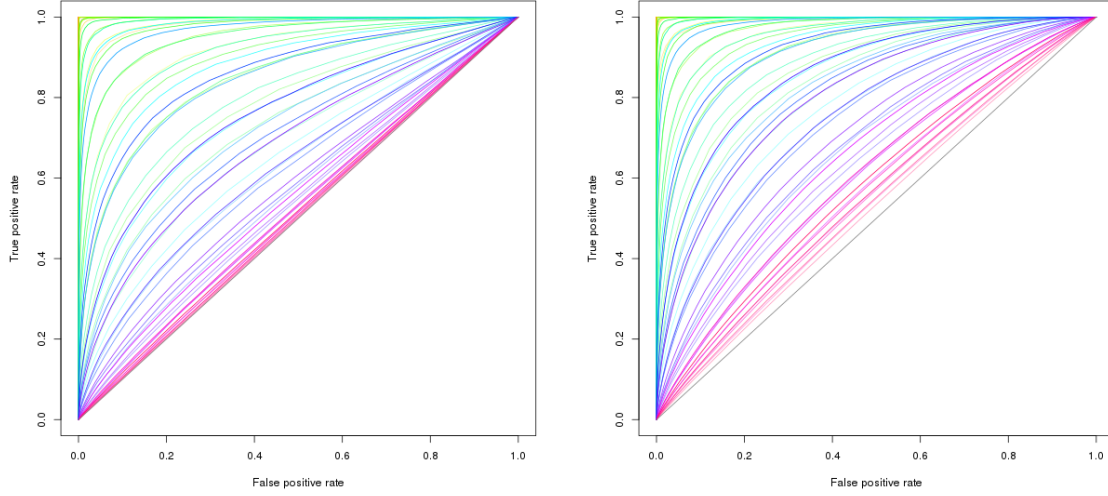


Figure 3.18: Statistical evaluation of directional criteria. A simulated multivariate normal dataset of 20,000 genes with correlation structures was tested by **SLIPT** with the directional condition and the χ^2 test. **SLIPT** exhibited a consistently higher sensitivity and lower false positive rate.

3.3.2.2 Specificity with Query-Correlated Pathways

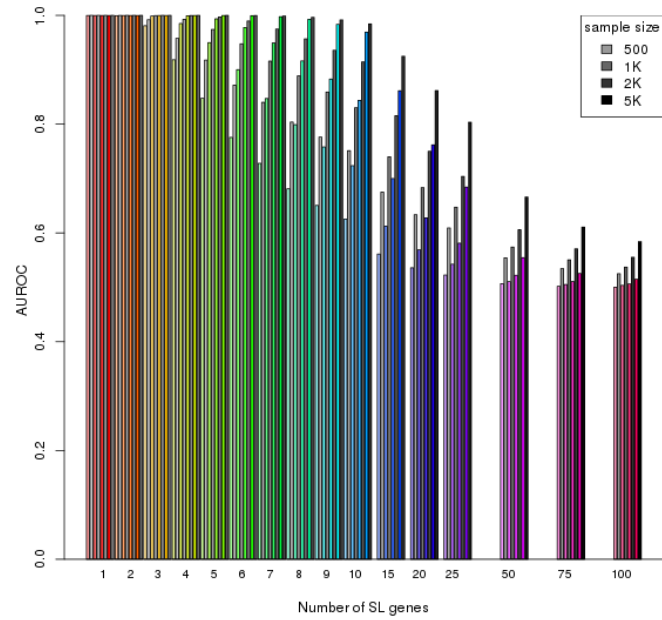
Correlation structures were also considered for non synthetic lethal genes that were (positively) correlated genes with the query gene. Specifically, five highly correlated ($r = 0.8$) with the query gene were added (as described in Section 3.3.2.1). These simulations had similar performance (as shown in Figure 3.17) to those without these correlations with a higher specificity and a lower false positive rate (shown in Figure 3.17a).

The directional criteria of the **SLIPT** procedure was important in this case, enhancing its performance, particularly in distinguishing positively correlated non synthetic lethal genes. The multivariate normal simulations were performed, with 20,000 genes, including all of the correlation structures discussed (with synthetic lethal, non synthetic lethal, and query correlated genes). These simulations were compared for the direction **SLIPT** and the χ^2 testing. There was a considerably higher statistical performance with **SLIPT**, particularly increased sensitivity and lower false positive rate (as shown in Figure 3.18).



(a) χ^2 testing without direction

(b) **SLIPT** with directional criteria



(c) Statistical performance (AUROC)

Figure 3.19: **Performance with directional criteria.** A simulated multivariate normal dataset of 20,000 genes with correlation structures was tested by **SLIPT** and χ^2 test. **SLIPT** had higher performance across simulation parameters, clearly differing from random (grey diagonal) in ROC curves up to 100 SL genes (b). The performance (c) of **SLIPT** (in greyscale) was consistently higher than the χ^2 test (in color).

These results show that the performance of **SLIPT** is appropriate for the analysis of **expression** datasets, where positively correlated genes commonly occur, with the directional condition robustly improving the performance of **SLIPT** across simulation parameters (compared to the χ^2 test). Without assuming the underlying number of **synthetic lethal** genes, **SLIPT** will performed than the χ^2 test alone, irrespective of the significance threshold as shown by **ROC** analysis (as shown in Figure 3.19). The directional **SLIPT** methodology outperformed the χ^2 test at detecting **synthetic lethal** partners with even up to 100 **synthetic lethal** genes.

Together these simulation results support the application of the **SLIPT** methodology as it has been performed throughout Chapters 4 and 5. The methodology and simulation procedure were explored further in Chapter 6, with comparison to other **synthetic lethal** detection approaches and the inclusion of **graph** structures.

3.4 Graph Structure Methods

Graph structures have been used in several ways in this project, including novel approaches to analysis and simulations. Procedures were developed for statistical and network analysis of gene states in **pathway** structures. Specifically, the relationships between **siRNA** and **SLIPT** genes were tested within biological pathways in Chapter 5. These **graph** structures were also used in Chapter 6 to derive correlation structure between simulated **gene expression** profiles to represent biological pathways.

3.4.1 Upstream and Downstream Gene Detection

Comparison of experimental and computational candidate **synthetic lethal** partner genes within **pathway** structures was performed to determine whether these sets of genes were related by **pathway** structure. Considering the differences in how these candidates were generated, it was unsurprising that they did not detect some identical genes within the candidate biological pathways. However, they could still be related by being upstream or downstream of each other.

Using the Reactome version 52 (Croft *et al.*, 2014), as described in Section 2.4.2, genes detected by each **synthetic lethal** discovery approach were mapped to the **graph** structure for each candidate pathway identified in Chapter 4 (with graphs defined as described in Section 2.4.3). To test whether **siRNA** candidate genes were upstream of **SLIPT** candidate genes, **shortest paths** were traced between each pair of these genes in a directed network. The paths where the **siRNA** candidate was upstream (“up”) and downstream (“down”) of a **SLIPT** candidate were scored. This procedure yielded

the total number of [shortest paths](#) which indicated that [siRNA](#) genes were upstream or downstream of the [SLIPT](#) genes and measured the difference between these to determine if there was an imbalance in a particular direction. While this difference was indicative of the number of paths between the gene candidate groups in either direction, it was not sufficient to statistically verify structure or relationships between [siRNA](#) and [SLIPT](#) genes. It was combined with a permutation resampling procedure (as described in Section 3.4.1.1) to test for directional relationships in either direction.

Initially, this procedure excluded genes that were detected by both approaches since they would count in both directions. Upon further consideration, these genes were restored to account for since they may contribute unequally to each gene set if there are unequal numbers of genes above or below them in the [pathway](#) structure.

3.4.1.1 Permutation Analysis for Statistical Significance

A permutation procedure was developed to randomly assign members of the pathway to [siRNA](#) and/or [SLIPT](#) groups, with the same number of each candidate partner gene set as observed in the pathway. These permuted genes were measured for [pathway](#) structure between the permuted gene groups as performed for the observed candidates (as performed in Section 3.4.1). A distribution of [pathway](#) structure relationships expected by chance was generated by permuting iteratively over these pathways. The resulting null distribution was compared to the observed counts of relationships (in either direction). This procedure yielded a permutation p-value as the proportion of permutations in which had a value greater than the observed value. The null hypothesis was that there was no relationship between these gene groups compared to genes that had been selected at random. Thus both the alternate hypotheses that the [siRNA](#) genes were either upstream of the [SLIPT](#) genes or that they are downstream of them were testable.

The permutation procedure does not assume the underlying distribution of the data under the null hypothesis and accounts for the total number of [nodes](#), [edges](#), [siRNA](#), and [SLIPT](#) genes in each [graph](#) or [network](#) pathway structure. The number of genes detected by both [siRNA](#) and [SLIPT](#) was not accounted for under the initial [shortest path](#) counts procedure that excluded them. Once they were included, it was ensured that the number of intersecting genes was equal to the number observed to test for [pathway](#) structure without changing the intersection size, the subject of prior analyses.

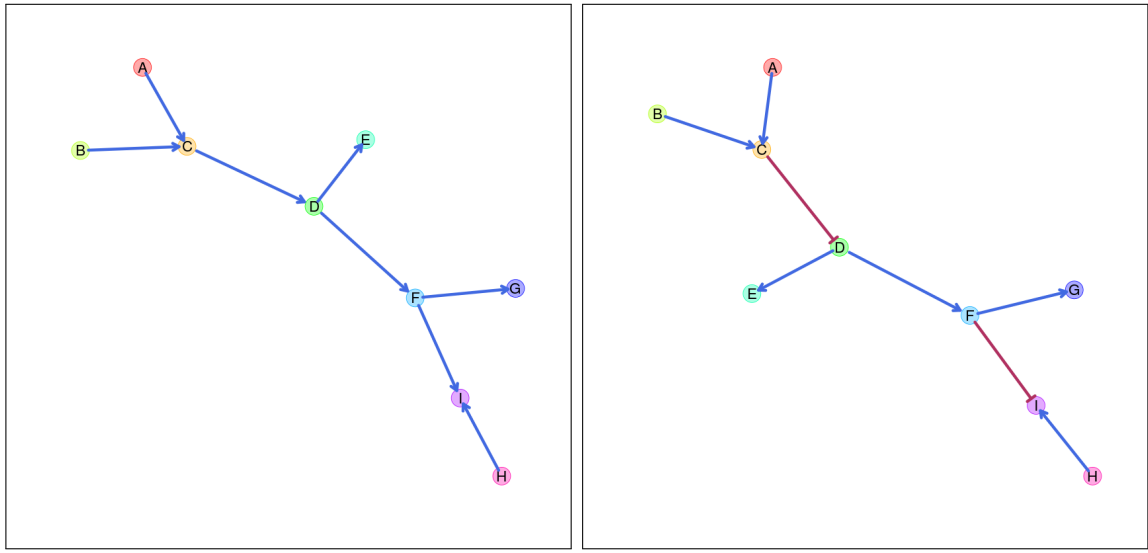
3.4.2 Simulating Gene Expression from Graph Structures

The simulation procedure was refined to generate `expression` data with correlation structure from a known `graph` structure. This enabled modelling of `synthetic` lethal partners within a biological pathway and the investigation of the impact of `pathway` structure on `synthetic lethal` prediction. Firstly, a simulated pathway was constructed as a `graph` structure, with the `igraph` R package [Csardi and Nepusz \(2006\)](#), with the state of the `edges` (i.e, whether they activate or inhibit downstream pathway members). This simulation procedure was intended for biological pathway members with correlated `gene expression` (higher than the background of genes in other pathways) but it may also be applicable to modelling protein levels (e.g, in a kinase regulation cascade) or substrates and products (e.g., in a metabolic pathway).

The `graph` structure was constructed from which simulated data will be generated from, sampling a multivariate normal distribution using the `mvtnorm` R package ([Genz and Bretz, 2009; Genz et al., 2016](#)). Throughout this Section, the simulation procedure will be demonstrated with the relatively simple constructed `graph` structure shown in Figure 3.20. This `graph` structure visualisation was specifically developed for (directed) iGraph objects in R and has been released in the `plot.igraph` package and `igraph.extensions` library (in Table 2.6 and Section 3.5.3). The `plot_directed` function enabled customisation of plot parameters for each `node` or `edge` and mixed (directed) `edge` types for indicating activation or inhibition. These inhibition `links` (which occur frequently in biological pathways) were demonstrated in Figure 3.20b.

The simulation procedure was designed to use such `graph` structures to inform development of a “Sigma” variance-covariance matrix (Σ) for sampling from a multivariate normal distribution (using the `mvtnorm` R package). Given a `graph` structure (or adjacency matrix), such as Figure 3.21a, a relation matrix was calculated based on distance such that nearer `nodes` are given higher weight than farther `nodes`. Throughout this thesis, a geometrically decreasing (relative) distance weighting was used, with each more distant `node` being related by $1/2$ compared to the next nearest, as shown in Figure 3.21b. An arithmetically decreasing (absolute) distance weighting is also supported in the `graphsim` R package release of this procedure.

A Σ matrix can be derived from this distance weighting matrix, creating a matrix (with a diagonal of 1) where each `node` has a variance and standard deviation of 1. Thus covariances between adjacent `nodes` were assigned by a correlation parameter and the remaining matrix based on weighting these correlations by the geometrically weighted distance matrix (or the nearest “positive definite” matrix for Σ weighted for

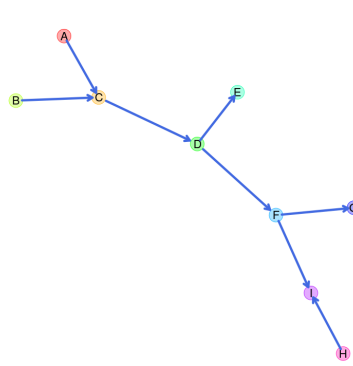


(a) Activating [pathway](#) structure (b) Pathway structure with inhibitions

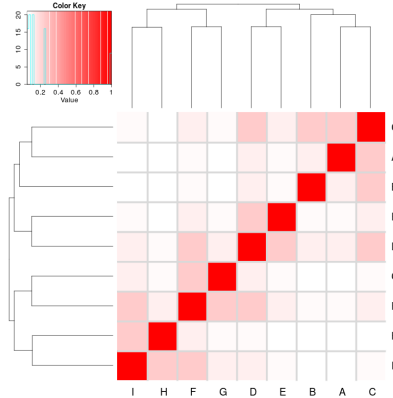
Figure 3.20: **Simulated graph structures.** A constructed [graph](#) structure used as an example to demonstrate the simulation procedure. Activating [links](#) are denoted by blue arrows and inhibiting [links](#) by red edges.

negatively correlated inhibitions). Throughout this thesis, the correlation parameter was 0.8, unless otherwise specified (as used for the example in Figure 3.21c). This Σ matrix was then used to sample from a multivariate normal distribution such that each gene had a mean of 0, standard deviation 1, and covariance within the range [0, 1] such that they are correlations. This procedure generated a simulated (continuous normally distributed) [expression](#) profile for each [node](#) (as shown in Figure 3.21e) with corresponding correlation structure (Figure 3.21d). The simulated correlation structure closely resembled the expected correlation structure (Sigma in 3.21c) even for the relatively modest sample size ($N = 100$) illustrated in 3.21. Once a simulated [gene expression](#) dataset has been generated (as in Figure 3.21e), then a discrete matrix of gene function was constructed with a functional threshold quantile to simulate functional relationships of [synthetic lethality](#) (as shown in Figure 3.4). Throughout this thesis, this threshold is the 0.3 quantile (as discussed in Section 3.2.1) which generates functional discrete matrices such as those used for [synthetic lethal](#) simulation in Section 3.2.2 (as shown Figure 3.21f).

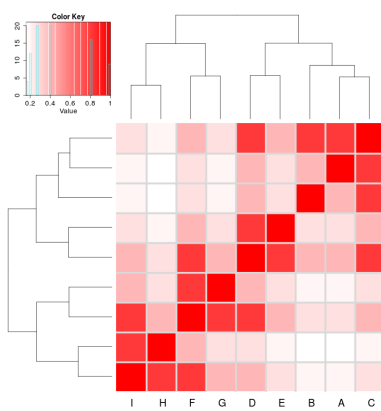
The simulation procedure (depicted in Figure 3.21) can be used for pathways containing inhibition [links](#) (as shown in Figure 3.22) with several refinements. With the inhibition [links](#) (as shown in Figure 3.22a), distances were calculated in the same manner



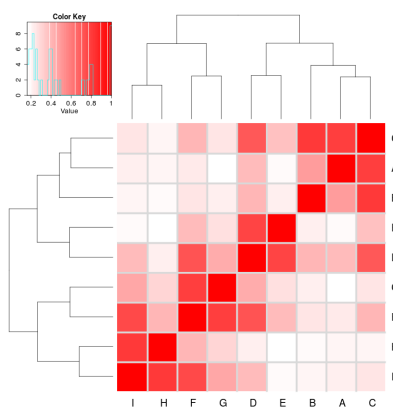
(a) Activating pathway structure



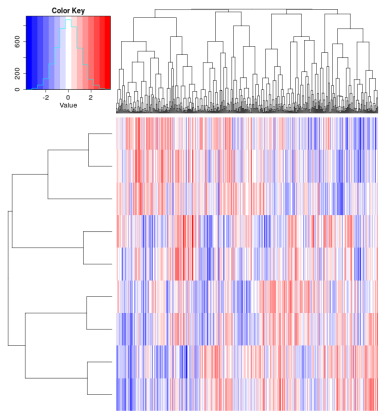
(b) Distance matrix



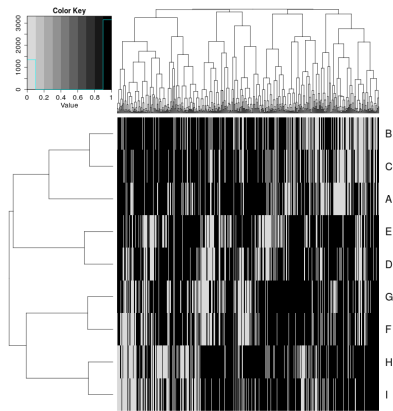
(c) Σ (expected correlation)



(d) Simulated correlation



(e) Simulated expression data



(f) Simulated gene function calls

Figure 3.21: **Simulating expression from a graph structure.** An example graph structure that was used to derive a correlation structure from the relative distances between nodes and simulate continuous gene expression with sampling from the multivariate normal distribution.

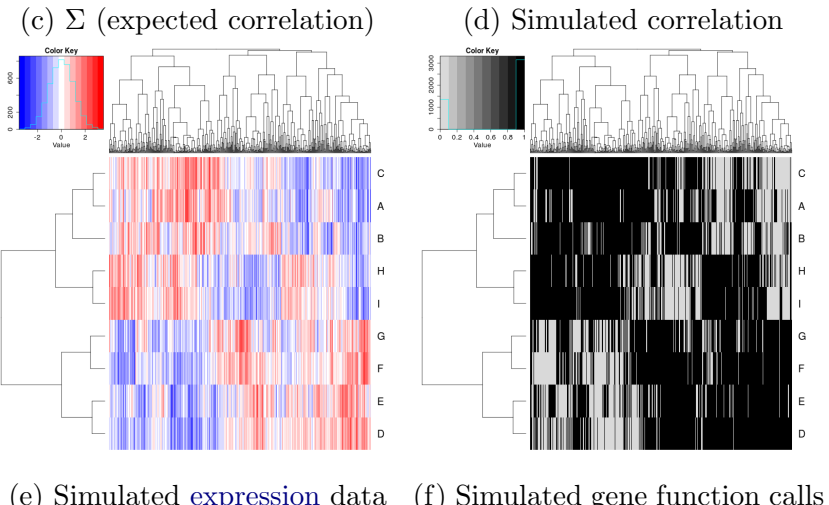
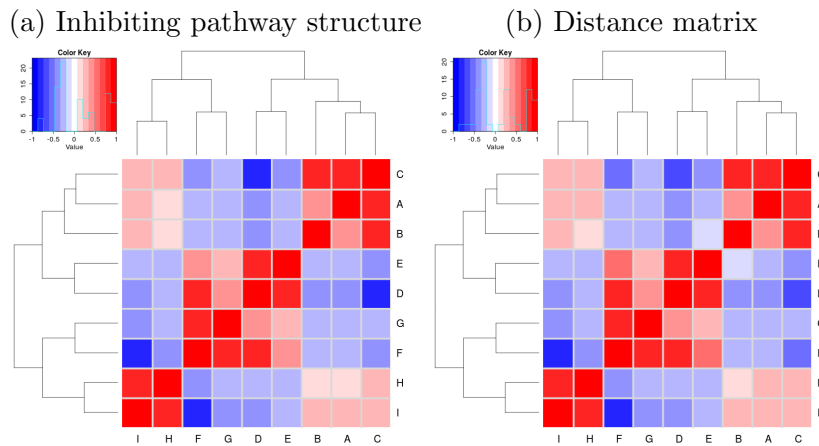
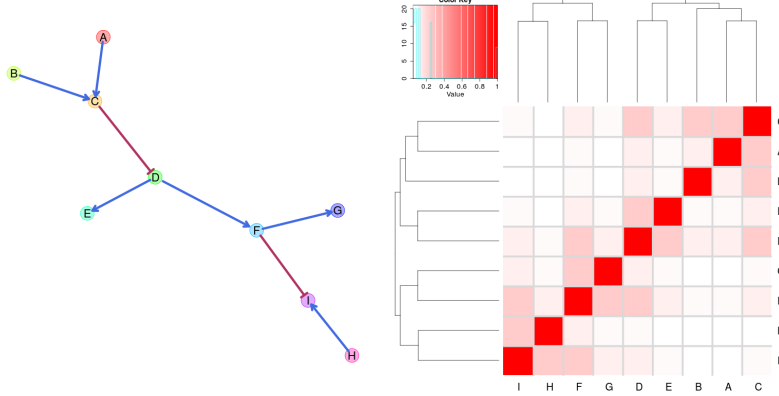


Figure 3.22: **Simulating expression from graph structure with inhibitions.** An example graph structure that was used to derive a correlation structure from the relative distances between nodes and simulate continuous gene expression with sampling from the multivariate normal distribution.

as before (Figure 3.22b) with inhibitions accounted for by iteratively multiplying downstream `nodes` by -1 to form blocks of negative correlations (as shown in Figures 3.22c and 3.22d). A multivariate normal distribution with these negative correlations can be sampled to generate simulated data (as shown in Figures 3.22e and 3.22f).

These simulated datasets could then be used for simulating synthetic lethal partners of a query gene within a graph network. The query gene was assumed to be separate from the graph network pathway and was added to the dataset using the procedure in Section 3.2.2. Thus we can simulate known synthetic lethal partner genes within a synthetic lethal partner pathway structure.

3.5 Customised Functions and Packages Developed

Various R packages (R Core Team, 2016) have been developed throughout this thesis using `devtools` (Wickham and Chang, 2016) and `roxygen` (Wickham *et al.*, 2017) to enable reproducibility of customised analysis and visualisation. Many of these have been documented, demonstrated in vignettes, and released on GitHub (<https://github.com/TomKellyGenetics>) to enable the research community to utilise them in their own analysis. These are summarised in Table 2.6, with the corresponding urls for their GitHub repository which contains instructions for installation with the `devtools` R package (Wickham and Chang, 2016) and links the relevant vignette(s).

3.5.1 Synthetic Lethal Interaction Prediction Tool

The statistical methodology for detection of synthetic lethality in gene expression data (**SLIPT**) is one of the main novel procedures developed in this thesis, as described in Section 3.1. The `slipt` R package has been prepared for release to accompany a publication demonstrating the applications of the methodology for identifying candidate interacting genes and pathways with *CDH1* in breast cancer (Koboldt *et al.*, 2012).

SLIPT can be used amenable to analysis of any effectively continuous measure of gene activity (e.g., microarray, RNA-Seq, protein abundance, or pathway metagenes). Executing `slipt` is straightforward: the `prep_data_for_SL` function scores samples as “low”, “medium”, or “high” for each gene, then the `detect_SL` function tests a given query gene against all potential partners by performing the chi-squared test and directional conditions. This function returns a table summarising the observed and expected sample numbers used for the directional criteria, the χ^2 values, and corresponding p-values including adjusting for multiple comparisons. The `count_of_SL`

and `table_of_SL` functions serve to facilitate summary and extraction of the positive `SLIPT` hits, respectively, from the table of predictions of synthetic lethal partners.

The `SLIPT` methodology in this package release was used in later analyses rather than the corresponding source R code, including use on remote machines and upon simulated data. In particular, the functions in the package facilitate alterations to parameters, such as the proportion of samples called as exhibiting low or high gene activity (as shown in Section 6.1.1). This release supports reproducible research and enables wider use of `SLIPT` in future investigations into other disease genes.

3.5.2 Data Visualisation

Customised data visualisations in R (R Core Team, 2016) were developed to present data throughout this thesis. The `vioplotx` and `heatmap.2x` packages are enhancements of the `vioplot` package (Adler, 2005) and `heatmap.2` provided by the `gplots` package (Warnes *et al.*, 2015).

The `vioplotx` package provides an alternative visualisation (of continuous variables against categories) to the more familiar boxplot, showing variability of the data by the width of the plots. As demonstrated in Figure 3.23, this version enables separate plotting parameters for each violin with vector inputs for colour, shape, and size of various elements of the median point, central boxplot, borders, and fill colour for the violin. Scaling violin width to adjust violin area and splitting data by a second categorical variable is also enabled. This function is intended to be backwards compatible with the inputs of `vioplot` (applying scalar inputs across all violins) and `boxplot` (by enabling formula inputs as an S3 method). Each of these features has been demonstrated with examples in respective vignettes on the package GitHub repository (<https://github.com/TomKellyGenetics/vioplotx>).

The `heatmap.2x` function provides extensions for annotation colour bars for both the rows and columns (as shown in Figure 3.24). Multiple bars are enabled on both axes with matrix inputs (rather than single vector for `heatmap.2`) which facilitates additional plotting of gene and sample characteristics for comparison with correlation matrices, `expression` profiles, or pathway `metagenes`. The annotation bar inputs correspond to their orientation on the plot, each colour bar is provided as a column for the row annotation on the left of the heatmap and as a row for the column annotation on top of the heatmap. Row and column annotation bars are labelled with the column or row names respectively. Additional parameters enable resizing of these annotation bar labels and control of reordering columns for when samples have been ordered in

advance (e.g., ranked by a `metagene` or split into groups clustered separately). These features were used through this thesis and have been provided in a package [GitHub repository \(`https://github.com/TomKellyGenetics/heatmap.2x`\)](#).

3.5.3 Extensions to the iGraph Package

The following features were developed during this thesis using “iGraph” data objects, building upon the `igraph` package (Csardi and Nepusz, 2006). These have been released as separate packages for each respective procedure and can be installed together as a collection of extensions to the `igraph` package ([https://github.com/TomKellyGenetics/igraph.extensions](#)).

3.5.3.1 Sampling Simulated Data from Graph Structures

The `graphsim` package implements the procedure for simulating gene expression from `graph` structures (as described in Section 3.4.2). By default, this derives a matrix with a geometrically decreasing weighting by distance (by `shortest paths`) between each pair of `nodes` with. An absolute decreasing weighting is also available with the option of to derive correlation structures from adjacency matrices or the number of `links` common partners (i.e., size of the shared “neighbourhood” (Hell, 1976)) between each pair of `nodes`. Functions to compute these are called directly by passing parameters to them when running the `generate_expression` or `make_sigma_mat` commands. This package enables simulating `expression` data directly from a `graph` structure (with the intermediate steps automated) or generating Σ parameters for `mvtnorm` from `graph` structures or matrices derived from them. These functions support assignment of activating or inhibiting relationships to each `edge` (with a `state` parameter).

3.5.3.2 Plotting Directed Graph Structures

The `plot.igraph` package provides the `plot_directed` function, specifically developed for directed `graph` structures, to plot activating or inhibiting for each `edge` (as described in Section 3.4.2). As shown in Figure 3.25, this function supports separate plotting parameters for each `node`, `node` label, and `edge`. This includes colours of `node` fill, border, label text, and `edges` and size of `nodes`, `edge` widths, arrowhead lengths, and font size of labels. The `state` parameter for assigning activating or inhibiting to each `edge` determines whether `edges` were depicted with 30° or 90° arrowheads. Colours are assigned separately so they may be customised. Vectorised parameters are applied across each `node` or `edge`, whereas scalar parameters apply the same plotting parameters across them. The default layout function is `layout.fruchterman.reingold` but any

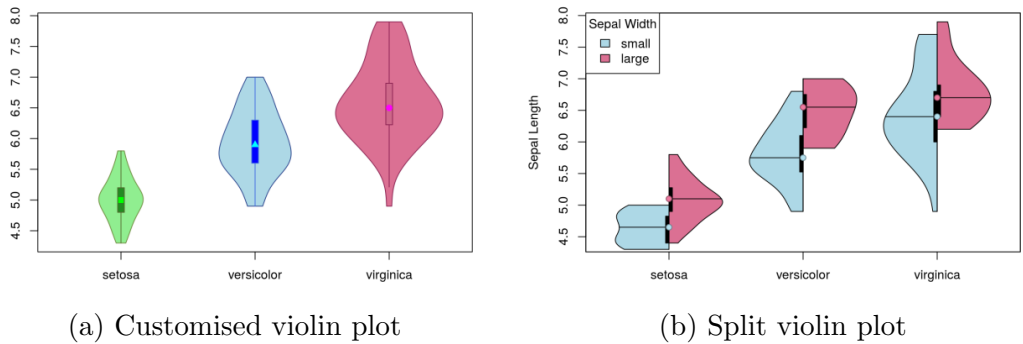


Figure 3.23: **Demonstration of violin plots with custom features.** An example of the *iris* dataset is plotted to show the custom features of the `vioplotx` package including (a) individual colour, shape and size parameters of each violin, scaling violin widths by area, and (b) splitting violins to compare subsets of data.

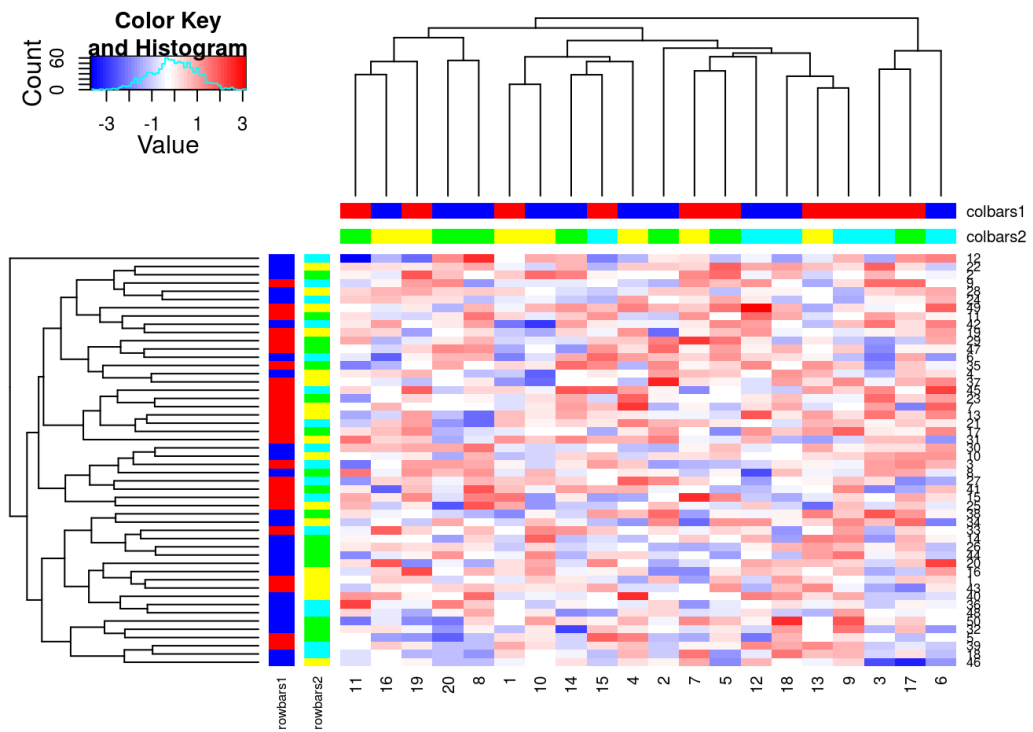


Figure 3.24: **Demonstration of annotated heatmap.** The example heatmap depicts the additional row and column annotation bars enabled by `heatmap.2x`, extending the features of `gplots` with backwards compatible inputs.

layout function supported by `plot` function in `igraph` (Csardi and Nepusz, 2006) was compatible, such as `layout.kamada.kawai` used to implement the Kamada–Kawai algorithm (Kamada and Kawai, 1989) for graph plots throughout this thesis.

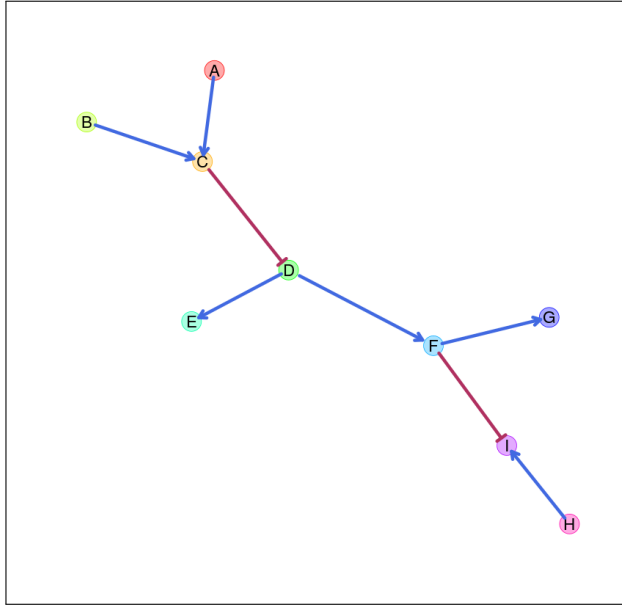


Figure 3.25: **Simulating graph structures.** An example `graph` structure which has been used throughout demonstrating the simulation procedure from `graph` structures. Activating links are denoted by blue arrows and inhibiting links by red edges.

3.5.3.3 Computing Information Centrality

The `shortest paths` of a network were computed by the `igraph` package (Csardi and Nepusz, 2006) which can be extended to calculate the network efficiency but was not provided by the package itself (as described in Section 2.4.4). The “information centrality” of a `vertex` is computed as the relative change in the network efficiency when the `vertex` is removed. `Information centrality` is calculated iteratively for each node and the sum of `information centrality` for each `vertex` is the `information centrality` for the network. These metrics were released in the `info.centrality` package (<https://github.com/TomKellyGenetics/info.centrality>).

3.5.3.4 Testing Pathway Structure with Permutation Testing

A network-based procedure developed was used to compare of `siRNA` and `SLIPT` candidate genes in a `pathway` structure. Such `pathway` structure relationships were tested by computing the number of `shortest paths` between two different groups of `nodes` in either direction within a graph . This pathway relationship metric was im-

plemented in the `pathway.structure.permutation` package (<https://github.com/TomKellyGenetics/pathway.structure.permutation>) with permutation testing (as described in Sections 3.4.1 and 3.4.1.1).

3.5.3.5 Metapackage to Install iGraph Functions

These features may be installed together with `igraph.extensions`, which can be accessed from a GitHub repository (<https://github.com/TomKellyGenetics/igraph.extensions>). This meta-package installs `igraph` (Csardi and Nepusz, 2006) and the packages described in Section 3.5.3 including their dependencies for matrix operations and statistical procedures: `Matrix`, `matrixcalc`, and `mvtnorm` (Bates and Maechler, 2016; Genz and Bretz, 2009; Genz *et al.*, 2016; Novomestky, 2012).

Bibliography

- Aarts, M., Bajrami, I., Herrera-Abreu, M.T., Elliott, R., Brough, R., Ashworth, A., Lord, C.J., and Turner, N.C. (2015) Functional genetic screen identifies increased sensitivity to wee1 inhibition in cells with defects in fanconi anemia and hr pathways. *Mol Cancer Ther*, **14**(4): 865–76.
- Abeshouse, A., Ahn, J., Akbani, R., Ally, A., Amin, S., Andry, C.D., Annala, M., Aprikian, A., Armenia, J., Arora, A., *et al.* (2015) The Molecular Taxonomy of Primary Prostate Cancer. *Cell*, **163**(4): 1011–1025.
- Adler, D. (2005) *vioplot: Violin plot*. R package version 0.2.
- Akbani, R., Akdemir, K.C., Aksoy, B.A., Albert, M., Ally, A., Amin, S.B., Arachchi, H., Arora, A., Auman, J.T., Ayala, B., *et al.* (2015) Genomic Classification of Cutaneous Melanoma. *Cell*, **161**(7): 1681–1696.
- Akobeng, A.K. (2007) Understanding diagnostic tests 3: receiver operating characteristic curves. *Acta Pdiatrica*, **96**(5): 644–647.
- American Cancer Society (2017) Genetics and cancer. <https://www.cancer.org/cancer/cancer-causes/genetics.html>. Accessed: 22/03/2017.
- Anjomshoaa, A., Lin, Y.H., Black, M.A., McCall, J.L., Humar, B., Song, S., Fukuzawa, R., Yoon, H.S., Holzmann, B., Friederichs, J., *et al.* (2008) Reduced expression of a gene proliferation signature is associated with enhanced malignancy in colon cancer. *Br J Cancer*, **99**(6): 966–973.
- Araki, H., Knapp, C., Tsai, P., and Print, C. (2012) GeneSetDB: A comprehensive meta-database, statistical and visualisation framework for gene set analysis. *FEBS Open Bio*, **2**: 76–82.

- Ashburner, M., Ball, C.A., Blake, J.A., Botstein, D., Butler, H., Cherry, J.M., Davis, A.P., Dolinski, K., Dwight, S.S., Eppig, J.T., *et al.* (2000) Gene ontology: tool for the unification of biology. The Gene Ontology Consortium. *Nat Genet*, **25**(1): 25–29.
- Ashworth, A. (2008) A synthetic lethal therapeutic approach: poly(adp) ribose polymerase inhibitors for the treatment of cancers deficient in dna double-strand break repair. *J Clin Oncol*, **26**(22): 3785–90.
- Ashworth, A., Lord, C.J., and Reis-Filho, J.S. (2011) Genetic interactions in cancer progression and treatment. *Cell*, **145**(1): 30–38.
- Audeh, M.W., Carmichael, J., Penson, R.T., Friedlander, M., Powell, B., Bell-McGuinn, K.M., Scott, C., Weitzel, J.N., Oaknin, A., Loman, N., *et al.* (2010) Oral poly(adp-ribose) polymerase inhibitor olaparib in patients with *BRCA1* or *BRCA2* mutations and recurrent ovarian cancer: a proof-of-concept trial. *Lancet*, **376**(9737): 245–51.
- Babyak, M.A. (2004) What you see may not be what you get: a brief, nontechnical introduction to overfitting in regression-type models. *Psychosom Med*, **66**(3): 411–21.
- Bamford, S., Dawson, E., Forbes, S., Clements, J., Pettett, R., Dogan, A., Flanagan, A., Teague, J., Futreal, P.A., Stratton, M.R., *et al.* (2004) The COSMIC (Catalogue of Somatic Mutations in Cancer) database and website. *Br J Cancer*, **91**(2): 355–358.
- Barabási, A.L. and Albert, R. (1999) Emergence of scaling in random networks. *Science*, **286**(5439): 509–12.
- Barabási, A.L., Gulbahce, N., and Loscalzo, J. (2011) Network medicine: a network-based approach to human disease. *Nat Rev Genet*, **12**(1): 56–68.
- Barabási, A.L. and Oltvai, Z.N. (2004) Network biology: understanding the cell's functional organization. *Nat Rev Genet*, **5**(2): 101–13.
- Barrat, A. and Weigt, M. (2000) On the properties of small-world network models. *The European Physical Journal B - Condensed Matter and Complex Systems*, **13**(3): 547–560.

- Barretina, J., Caponigro, G., Stransky, N., Venkatesan, K., Margolin, A.A., Kim, S., Wilson, C.J., Lehar, J., Kryukov, G.V., Sonkin, D., *et al.* (2012) The Cancer Cell Line Encyclopedia enables predictive modelling of anticancer drug sensitivity. *Nature*, **483**(7391): 603–607.
- Barry, W.T. (2016) *safe: Significance Analysis of Function and Expression*. R package version 3.14.0.
- Baryshnikova, A., Costanzo, M., Dixon, S., Vizeacoumar, F.J., Myers, C.L., Andrews, B., and Boone, C. (2010a) Synthetic genetic array (sga) analysis in *saccharomyces cerevisiae* and *schizosaccharomyces pombe*. *Methods Enzymol*, **470**: 145–79.
- Baryshnikova, A., Costanzo, M., Kim, Y., Ding, H., Koh, J., Toufighi, K., Youn, J.Y., Ou, J., San Luis, B.J., Bandyopadhyay, S., *et al.* (2010b) Quantitative analysis of fitness and genetic interactions in yeast on a genome scale. *Nat Meth*, **7**(12): 1017–1024.
- Bass, A.J., Thorsson, V., Shmulevich, I., Reynolds, S.M., Miller, M., Bernard, B., Hinoue, T., Laird, P.W., Curtis, C., Shen, H., *et al.* (2014) Comprehensive molecular characterization of gastric adenocarcinoma. *Nature*, **513**(7517): 202–209.
- Bates, D. and Maechler, M. (2016) *Matrix: Sparse and Dense Matrix Classes and Methods*. R package version 1.2-7.1.
- Bateson, W. and Mendel, G. (1909) *Mendel's principles of heredity, by W. Bateson*. University Press, Cambridge [Eng.].
- Becker, K.F., Atkinson, M.J., Reich, U., Becker, I., Nekarda, H., Siewert, J.R., and Hfler, H. (1994) E-cadherin gene mutations provide clues to diffuse type gastric carcinomas. *Cancer Research*, **54**(14): 3845–3852.
- Bell, D., Berchuck, A., Birrer, M., Chien, J., Cramer, D., Dao, F., Dhir, R., DiSaia, P., Gabra, H., Glenn, P., *et al.* (2011) Integrated genomic analyses of ovarian carcinoma. *Nature*, **474**(7353): 609–615.
- Benjamini, Y. and Hochberg, Y. (1995) Controlling the false discovery rate: A practical and powerful approach to multiple testing. *Journal of the Royal Statistical Society Series B (Methodological)*, **57**(1): 289–300.

- Berx, G., Cleton-Jansen, A.M., Nollet, F., de Leeuw, W.J., van de Vijver, M., Cornelisse, C., and van Roy, F. (1995) E-cadherin is a tumour/invasion suppressor gene mutated in human lobular breast cancers. *EMBO J*, **14**(24): 6107–15.
- Berx, G., Cleton-Jansen, A.M., Strumane, K., de Leeuw, W.J., Nollet, F., van Roy, F., and Cornelisse, C. (1996) E-cadherin is inactivated in a majority of invasive human lobular breast cancers by truncation mutations throughout its extracellular domain. *Oncogene*, **13**(9): 1919–25.
- Berx, G. and van Roy, F. (2009) Involvement of members of the cadherin superfamily in cancer. *Cold Spring Harb Perspect Biol*, **1**: a003129.
- Bitler, B.G., Aird, K.M., Garipov, A., Li, H., Amatangelo, M., Kossenkov, A.V., Schultz, D.C., Liu, Q., Shih Ie, M., Conejo-Garcia, J.R., et al. (2015) Synthetic lethality by targeting ezh2 methyltransferase activity in arid1a-mutated cancers. *Nat Med*, **21**(3): 231–8.
- Blake, J.A., Christie, K.R., Dolan, M.E., Drabkin, H.J., Hill, D.P., Ni, L., Sitnikov, D., Burgess, S., Buza, T., Gresham, C., et al. (2015) Gene Ontology Consortium: going forward. *Nucleic Acids Res*, **43**(Database issue): D1049–1056.
- Boettcher, M., Lawson, A., Ladenburger, V., Fredebohm, J., Wolf, J., Hoheisel, J.D., Frezza, C., and Shlomi, T. (2014) High throughput synthetic lethality screen reveals a tumorigenic role of adenylate cyclase in fumarate hydratase-deficient cancer cells. *BMC Genomics*, **15**: 158.
- Boone, C., Bussey, H., and Andrews, B.J. (2007) Exploring genetic interactions and networks with yeast. *Nat Rev Genet*, **8**(6): 437–49.
- Borgatti, S.P. (2005) Centrality and network flow. *Social Networks*, **27**(1): 55 – 71.
- Boucher, B. and Jenna, S. (2013) Genetic interaction networks: better understand to better predict. *Front Genet*, **4**: 290.
- Bozovic-Spasojevic, I., Azambuja, E., McCaskill-Stevens, W., Dinh, P., and Cardoso, F. (2012) Chemoprevention for breast cancer. *Cancer treatment reviews*, **38**(5): 329–339.
- Breiman, L. (2001) Random forests. *Machine Learning*, **45**(1): 5–32.

- Brin, S. and Page, L. (1998) The anatomy of a large-scale hypertextual web search engine. *Computer Networks and ISDN Systems*, **30**(1): 107 – 117.
- Brouxhon, S.M., Kyrkanides, S., Teng, X., Athar, M., Ghazizadeh, S., Simon, M., O'Banion, M.K., and Ma, L. (2014) Soluble E-cadherin: a critical oncogene modulating receptor tyrosine kinases, MAPK and PI3K/Akt/mTOR signaling. *Oncogene*, **33**(2): 225–235.
- Brückner, A., Polge, C., Lentze, N., Auerbach, D., and Schlattner, U. (2009) Yeast two-hybrid, a powerful tool for systems biology. *Int J Mol Sci*, **10**(6): 2763–2788.
- Bryant, H.E., Schultz, N., Thomas, H.D., Parker, K.M., Flower, D., Lopez, E., Kyle, S., Meuth, M., Curtin, N.J., and Helleday, T. (2005) Specific killing of *BRCA2*-deficient tumours with inhibitors of polyadribose polymerase. *Nature*, **434**(7035): 913–7.
- Bussey, H., Andrews, B., and Boone, C. (2006) From worm genetic networks to complex human diseases. *Nat Genet*, **38**(8): 862–3.
- Butland, G., Babu, M., Diaz-Mejia, J.J., Bohdana, F., Phanse, S., Gold, B., Yang, W., Li, J., Gagarinova, A.G., Pogoutse, O., et al. (2008) esga: *E. coli* synthetic genetic array analysis. *Nat Methods*, **5**(9): 789–95.
- Cardiff, R.D., Couto, S., and Bolon, B. (2011) Three interrelated themes in current breast cancer research: gene addiction, phenotypic plasticity, and cancer stem cells. *Breast Cancer Res*, **13**(5): 216.
- cBioPortal for Cancer Genomics (cBioPortal) (2017) cBioPortal for Cancer Genomics. <http://www.cbioportal.org/>. Accessed: 26/03/2017.
- Cerami, E.G., Gross, B.E., Demir, E., Rodchenkov, I., Babur, O., Anwar, N., Schultz, N., Bader, G.D., and Sander, C. (2011) Pathway Commons, a web resource for biological pathway data. *Nucleic Acids Res*, **39**(Database issue): D685–690.
- Chen, A., Beetham, H., Black, M.A., Priya, R., Telford, B.J., Guest, J., Wiggins, G.A.R., Godwin, T.D., Yap, A.S., and Guilford, P.J. (2014) E-cadherin loss alters cytoskeletal organization and adhesion in non-malignant breast cells but is insufficient to induce an epithelial-mesenchymal transition. *BMC Cancer*, **14**(1): 552.
- Chen, S. and Parmigiani, G. (2007) Meta-analysis of BRCA1 and BRCA2 penetrance. *J Clin Oncol*, **25**(11): 1329–1333.

- Chipman, K. and Singh, A. (2009) Predicting genetic interactions with random walks on biological networks. *BMC Bioinformatics*, **10**(1): 17.
- Christofori, G. and Semb, H. (1999) The role of the cell-adhesion molecule E-cadherin as a tumour-suppressor gene. *Trends in Biochemical Sciences*, **24**(2): 73 – 76.
- Ciriello, G., Gatzka, M.L., Beck, A.H., Wilkerson, M.D., Rhie, S.K., Pastore, A., Zhang, H., McLellan, M., Yau, C., Kandoth, C., *et al.* (2015) Comprehensive Molecular Portraits of Invasive Lobular Breast Cancer. *Cell*, **163**(2): 506–519.
- Clark, M.J. (2004) Endogenous Regulator of G Protein Signaling Proteins Suppress G_o-Dependent -Opioid Agonist-Mediated Adenylyl Cyclase Supersensitization. *Journal of Pharmacology and Experimental Therapeutics*, **310**(1): 215–222.
- Collingridge, D.S. (2013) A primer on quantitized data analysis and permutation testing. *Journal of Mixed Methods Research*, **7**(1): 81–97.
- Collins, F.S. and Barker, A.D. (2007) Mapping the cancer genome. Pinpointing the genes involved in cancer will help chart a new course across the complex landscape of human malignancies. *Sci Am*, **296**(3): 50–57.
- Collisson, E., Campbell, J., Brooks, A., Berger, A., Lee, W., Chmielecki, J., Beer, D., Cope, L., Creighton, C., Danilova, L., *et al.* (2014) Comprehensive molecular profiling of lung adenocarcinoma. *Nature*, **511**(7511): 543–550.
- Costanzo, M., Baryshnikova, A., Bellay, J., Kim, Y., Spear, E.D., Sevier, C.S., Ding, H., Koh, J.L., Toufighi, K., Mostafavi, S., *et al.* (2010) The genetic landscape of a cell. *Science*, **327**(5964): 425–31.
- Costanzo, M., Baryshnikova, A., Myers, C.L., Andrews, B., and Boone, C. (2011) Charting the genetic interaction map of a cell. *Curr Opin Biotechnol*, **22**(1): 66–74.
- Courtney, K.D., Corcoran, R.B., and Engelman, J.A. (2010) The PI3K pathway as drug target in human cancer. *J Clin Oncol*, **28**(6): 1075–1083.
- Creighton, C.J., Morgan, M., Gunaratne, P.H., Wheeler, D.A., Gibbs, R.A., Robertson, A., Chu, A., Beroukhim, R., Cibulskis, K., Signoretti, S., *et al.* (2013) Comprehensive molecular characterization of clear cell renal cell carcinoma. *Nature*, **499**(7456): 43–49.

- Croft, D., Mundo, A.F., Haw, R., Milacic, M., Weiser, J., Wu, G., Caudy, M., Garapati, P., Gillespie, M., Kamdar, M.R., *et al.* (2014) The Reactome pathway knowledge-base. *Nucleic Acids Res*, **42**(database issue): D472D477.
- Crunkhorn, S. (2014) Cancer: Predicting synthetic lethal interactions. *Nat Rev Drug Discov*, **13**(11): 812.
- Csardi, G. and Nepusz, T. (2006) The igraph software package for complex network research. *InterJournal, Complex Systems*: 1695.
- Dai, X., Li, T., Bai, Z., Yang, Y., Liu, X., Zhan, J., and Shi, B. (2015) Breast cancer intrinsic subtype classification, clinical use and future trends. *Am J Cancer Res*, **5**(10): 2929–2943.
- Davierwala, A.P., Haynes, J., Li, Z., Brost, R.L., Robinson, M.D., Yu, L., Mnaimneh, S., Ding, H., Zhu, H., Chen, Y., *et al.* (2005) The synthetic genetic interaction spectrum of essential genes. *Nat Genet*, **37**(10): 1147–1152.
- De Leeuw, W.J., Berx, G., Vos, C.B., Peterse, J.L., Van de Vijver, M.J., Litvinov, S., Van Roy, F., Cornelisse, C.J., and Cleton-Jansen, A.M. (1997) Simultaneous loss of E-cadherin and catenins in invasive lobular breast cancer and lobular carcinoma in situ. *J Pathol*, **183**(4): 404–11.
- De Santis, G., Miotti, S., Mazzi, M., Canevari, S., and Tomassetti, A. (2009) E-cadherin directly contributes to PI3K/AKT activation by engaging the PI3K-p85 regulatory subunit to adherens junctions of ovarian carcinoma cells. *Oncogene*, **28**(9): 1206–1217.
- Demir, E., Babur, O., Rodchenkov, I., Aksoy, B.A., Fukuda, K.I., Gross, B., Sumer, O.S., Bader, G.D., and Sander, C. (2013) Using biological pathway data with Paxtools. *PLoS Comput Biol*, **9**(9): e1003194.
- Deshpande, R., Asiedu, M.K., Klebig, M., Sutor, S., Kuzmin, E., Nelson, J., Piotrowski, J., Shin, S.H., Yoshida, M., Costanzo, M., *et al.* (2013) A comparative genomic approach for identifying synthetic lethal interactions in human cancer. *Cancer Res*, **73**(20): 6128–36.
- Dickson, D. (1999) Wellcome funds cancer database. *Nature*, **401**(6755): 729.
- Dijkstra, E.W. (1959) A note on two problems in connexion with graphs. *Numerische Mathematik*, **1**(1): 269–271.

- Dixon, S.J., Andrews, B.J., and Boone, C. (2009) Exploring the conservation of synthetic lethal genetic interaction networks. *Commun Integr Biol*, **2**(2): 78–81.
- Dixon, S.J., Fedyshyn, Y., Koh, J.L., Prasad, T.S., Chahwan, C., Chua, G., Toufighi, K., Baryshnikova, A., Hayles, J., Hoe, K.L., et al. (2008) Significant conservation of synthetic lethal genetic interaction networks between distantly related eukaryotes. *Proc Natl Acad Sci U S A*, **105**(43): 16653–8.
- Dong, L.L., Liu, L., Ma, C.H., Li, J.S., Du, C., Xu, S., Han, L.H., Li, L., and Wang, X.W. (2012) E-cadherin promotes proliferation of human ovarian cancer cells in vitro via activating MEK/ERK pathway. *Acta Pharmacol Sin*, **33**(6): 817–822.
- Dorsam, R.T. and Gutkind, J.S. (2007) G-protein-coupled receptors and cancer. *Nat Rev Cancer*, **7**(2): 79–94.
- Erdős, P. and Rényi, A. (1959) On random graphs I. *Publ Math Debrecen*, **6**: 290–297.
- Erdős, P. and Rényi, A. (1960) On the evolution of random graphs. In *Publ. Math. Inst. Hung. Acad. Sci*, volume 5, 17–61.
- Eroles, P., Bosch, A., Perez-Fidalgo, J.A., and Lluch, A. (2012) Molecular biology in breast cancer: intrinsic subtypes and signaling pathways. *Cancer Treat Rev*, **38**(6): 698–707.
- Farmer, H., McCabe, N., Lord, C.J., Tutt, A.N., Johnson, D.A., Richardson, T.B., Santarosa, M., Dillon, K.J., Hickson, I., Knights, C., et al. (2005) Targeting the dna repair defect in BRCA mutant cells as a therapeutic strategy. *Nature*, **434**(7035): 917–21.
- Fawcett, T. (2006) An introduction to ROC analysis. *Pattern Recognition Letters*, **27**(8): 861 – 874. {ROC} Analysis in Pattern Recognition.
- Fece de la Cruz, F., Gapp, B.V., and Nijman, S.M. (2015) Synthetic lethal vulnerabilities of cancer. *Annu Rev Pharmacol Toxicol*, **55**: 513–531.
- Ferlay, J., Soerjomataram, I., Dikshit, R., Eser, S., Mathers, C., Rebelo, M., Parkin, D.M., Forman, D., and Bray, F. (2015) Cancer incidence and mortality worldwide: sources, methods and major patterns in GLOBOCAN 2012. *Int J Cancer*, **136**(5): E359–386.

- Fisher, R.A. (1919) Xv.the correlation between relatives on the supposition of mendelian inheritance. *Earth and Environmental Science Transactions of the Royal Society of Edinburgh*, **52**(02): 399–433.
- Fong, P.C., Boss, D.S., Yap, T.A., Tutt, A., Wu, P., Mergui-Roelvink, M., Mortimer, P., Swaisland, H., Lau, A., O'Connor, M.J., *et al.* (2009) Inhibition of poly(adp-ribose) polymerase in tumors from BRCA mutation carriers. *N Engl J Med*, **361**(2): 123–34.
- Fong, P.C., Yap, T.A., Boss, D.S., Carden, C.P., Mergui-Roelvink, M., Gourley, C., De Greve, J., Lubinski, J., Shanley, S., Messiou, C., *et al.* (2010) Poly(adp)-ribose polymerase inhibition: frequent durable responses in BRCA carrier ovarian cancer correlating with platinum-free interval. *J Clin Oncol*, **28**(15): 2512–9.
- Forbes, S.A., Beare, D., Gunasekaran, P., Leung, K., Bindal, N., Boutselakis, H., Ding, M., Bamford, S., Cole, C., Ward, S., *et al.* (2015) COSMIC: exploring the world's knowledge of somatic mutations in human cancer. *Nucleic Acids Res*, **43**(Database issue): D805–811.
- Fraser, A. (2004) Towards full employment: using RNAi to find roles for the redundant. *Oncogene*, **23**(51): 8346–52.
- Friedman, N., Linial, M., Nachman, I., and Pe'er, D. (2000) Using Bayesian networks to analyze expression data. *J Comput Biol*, **7**(3-4): 601–620.
- Fromental-Ramain, C., Warot, X., Lakkaraju, S., Favier, B., Haack, H., Birling, C., Dierich, A., Doll e, P., and Chambon, P. (1996) Specific and redundant functions of the paralogous Hoxa-9 and Hoxd-9 genes in forelimb and axial skeleton patterning. *Development*, **122**(2): 461–472.
- Futreal, P.A., Coin, L., Marshall, M., Down, T., Hubbard, T., Wooster, R., Rahman, N., and Stratton, M.R. (2004) A census of human cancer genes. *Nat Rev Cancer*, **4**(3): 177–183.
- Futreal, P.A., Kasprzyk, A., Birney, E., Mullikin, J.C., Wooster, R., and Stratton, M.R. (2001) Cancer and genomics. *Nature*, **409**(6822): 850–852.
- Gao, B. and Roux, P.P. (2015) Translational control by oncogenic signaling pathways. *Biochimica et Biophysica Acta*, **1849**(7): 753–65.

- Gatza, M.L., Kung, H.N., Blackwell, K.L., Dewhirst, M.W., Marks, J.R., and Chi, J.T. (2011) Analysis of tumor environmental response and oncogenic pathway activation identifies distinct basal and luminal features in HER2-related breast tumor subtypes. *Breast Cancer Res*, **13**(3): R62.
- Gatza, M.L., Lucas, J.E., Barry, W.T., Kim, J.W., Wang, Q., Crawford, M.D., Datto, M.B., Kelley, M., Mathey-Prevot, B., Potti, A., *et al.* (2010) A pathway-based classification of human breast cancer. *Proc Natl Acad Sci USA*, **107**(15): 6994–6999.
- Gatza, M.L., Silva, G.O., Parker, J.S., Fan, C., and Perou, C.M. (2014) An integrated genomics approach identifies drivers of proliferation in luminal-subtype human breast cancer. *Nat Genet*, **46**(10): 1051–1059.
- Gentleman, R.C., Carey, V.J., Bates, D.M., Bolstad, B., Dettling, M., Dudoit, S., Ellis, B., Gautier, L., Ge, Y., Gentry, J., *et al.* (2004) Bioconductor: open software development for computational biology and bioinformatics. *Genome Biol*, **5**(10): R80.
- Genz, A. and Bretz, F. (2009) Computation of multivariate normal and t probabilities. In *Lecture Notes in Statistics*, volume 195. Springer-Verlag, Heidelberg.
- Genz, A., Bretz, F., Miwa, T., Mi, X., Leisch, F., Scheipl, F., and Hothorn, T. (2016) *mvtnorm: Multivariate Normal and t Distributions*. R package version 1.0-5. URL.
- Glaire, M.A., Brown, M., Church, D.N., and Tomlinson, I. (2017) Cancer predisposition syndromes: lessons for truly precision medicine. *J Pathol*, **241**(2): 226–235.
- Globus (Globus) (2017) Research data management simplified. <https://www.globus.org/>. Accessed: 25/03/2017.
- Goodwin, S., McPherson, J.D., and McCombie, W.R. (2016) Coming of age: ten years of next-generation sequencing technologies. *Nat Rev Genet*, **17**(6): 333–351.
- Grady, W.M., Willis, J., Guilford, P.J., Dunbier, A.K., Toro, T.T., Lynch, H., Wiesner, G., Ferguson, K., Eng, C., Park, J.G., *et al.* (2000) Methylation of the CDH1 promoter as the second genetic hit in hereditary diffuse gastric cancer. *Nat Genet*, **26**(1): 16–17.
- Graziano, F., Humar, B., and Guilford, P. (2003) The role of the E-cadherin gene (*CDH1*) in diffuse gastric cancer susceptibility: from the laboratory to clinical practice. *Annals of Oncology*, **14**(12): 1705–1713.

- Guaragnella, N., Palermo, V., Galli, A., Moro, L., Mazzoni, C., and Giannattasio, S. (2014) The expanding role of yeast in cancer research and diagnosis: insights into the function of the oncosuppressors p53 and BRCA1/2. *FEMS Yeast Res*, **14**(1): 2–16.
- Güell, O., Sagus, F., and Serrano, M. (2014) Essential plasticity and redundancy of metabolism unveiled by synthetic lethality analysis. *PLoS Comput Biol*, **10**(5): e1003637.
- Guilford, P. (1999) E-cadherin downregulation in cancer: fuel on the fire? *Molecular Medicine Today*, **5**(4): 172 – 177.
- Guilford, P., Hopkins, J., Harraway, J., McLeod, M., McLeod, N., Harawira, P., Taite, H., Scouler, R., Miller, A., and Reeve, A.E. (1998) E-cadherin germline mutations in familial gastric cancer. *Nature*, **392**(6674): 402–5.
- Guilford, P., Humar, B., and Blair, V. (2010) Hereditary diffuse gastric cancer: translation of *CDH1* germline mutations into clinical practice. *Gastric Cancer*, **13**(1): 1–10.
- Guilford, P.J., Hopkins, J.B., Grady, W.M., Markowitz, S.D., Willis, J., Lynch, H., Rajput, A., Wiesner, G.L., Lindor, N.M., Burgart, L.J., *et al.* (1999) E-cadherin germline mutations define an inherited cancer syndrome dominated by diffuse gastric cancer. *Hum Mutat*, **14**(3): 249–55.
- Guo, J., Liu, H., and Zheng, J. (2016) SynLethDB: synthetic lethality database toward discovery of selective and sensitive anticancer drug targets. *Nucleic Acids Res*, **44**(D1): D1011–1017.
- Hajian-Tilaki, K. (2013) Receiver Operating Characteristic (ROC) Curve Analysis for Medical Diagnostic Test Evaluation. *Caspian J Intern Med*, **4**(2): 627–635.
- Hall, M., Frank, E., Holmes, G., Pfahringer, B., Reutemann, P., and Witten, I.H. (2009) The weka data mining software: an update. *SIGKDD Explor Newsl*, **11**(1): 10–18.
- Hamerman, P.S., Lawrence, M.S., Voet, D., Jing, R., Cibulskis, K., Sivachenko, A., Stojanov, P., McKenna, A., Lander, E.S., Gabriel, S., *et al.* (2012) Comprehensive genomic characterization of squamous cell lung cancers. *Nature*, **489**(7417): 519–525.

- Hanahan, D. and Weinberg, R.A. (2000) The hallmarks of cancer. *Cell*, **100**(1): 57–70.
- Hanahan, D. and Weinberg, R.A. (2011) Hallmarks of cancer: the next generation. *Cell*, **144**(5): 646–674.
- Hanna, S. (2003) Cancer incidence in new zealand (2003-2007). In D. Forman, D. Bray F Brewster, C. Gombe Mbalawa, B. Kohler, M. Piñeros, E. Steliarova-Foucher, R. Swaminathan, and J. Ferlay (editors), *Cancer Incidence in Five Continents*, volume X, 902–907. International Agency for Research on Cancer, Lyon, France. Electronic version <http://ci5.iarc.fr> Accessed 22/03/2017.
- Hansford, S., Kaurah, P., Li-Chang, H., Woo, M., Senz, J., Pinheiro, H., Schrader, K.A., Schaeffer, D.F., Shumansky, K., Zogopoulos, G., et al. (2015) Hereditary Diffuse Gastric Cancer Syndrome: CDH1 Mutations and Beyond. *JAMA Oncol*, **1**(1): 23–32.
- Heiskanen, M.A. and Aittokallio, T. (2012) Mining high-throughput screens for cancer drug targets-lessons from yeast chemical-genomic profiling and synthetic lethality. *Wiley Interdisciplinary Reviews: Data Mining and Knowledge Discovery*, **2**(3): 263–272.
- Hell, P. (1976) Graphs with given neighbourhoods i. problèmes combinatoires at theorie des graphes. *Proc Coll Int CNRS, Orsay*, **260**: 219–223.
- Higgins, M.E., Claremont, M., Major, J.E., Sander, C., and Lash, A.E. (2007) CancerGenes: a gene selection resource for cancer genome projects. *Nucleic Acids Res*, **35**(Database issue): D721–726.
- Hillenmeyer, M.E. (2008) The chemical genomic portrait of yeast: uncovering a phenotype for all genes. *Science*, **320**: 362–365.
- Hoadley, K.A., Yau, C., Wolf, D.M., Cherniack, A.D., Tamborero, D., Ng, S., Leiserson, M.D., Niu, B., McLellan, M.D., Uzunangelov, V., et al. (2014) Multiplatform analysis of 12 cancer types reveals molecular classification within and across tissues of origin. *Cell*, **158**(4): 929–944.
- Hoehndorf, R., Hardy, N.W., Osumi-Sutherland, D., Tweedie, S., Schofield, P.N., and Gkoutos, G.V. (2013) Systematic analysis of experimental phenotype data reveals gene functions. *PLoS ONE*, **8**(4): e60847.

- Holm, S. (1979) A simple sequentially rejective multiple test procedure. *Scandinavian Journal of Statistics*, **6**(2): 65–70.
- Hopkins, A.L. (2008) Network pharmacology: the next paradigm in drug discovery. *Nat Chem Biol*, **4**(11): 682–690.
- Hu, Z., Fan, C., Oh, D.S., Marron, J.S., He, X., Qaqish, B.F., Livasy, C., Carey, L.A., Reynolds, E., Dressler, L., *et al.* (2006) The molecular portraits of breast tumors are conserved across microarray platforms. *BMC Genomics*, **7**: 96.
- Huang, E., Cheng, S., Dressman, H., Pittman, J., Tsou, M., Horng, C., Bild, A., Iversen, E., Liao, M., Chen, C., *et al.* (2003) Gene expression predictors of breast cancer outcomes. *Lancet*, **361**: 1590–1596.
- Hutchison, C.A., Chuang, R.Y., Noskov, V.N., Assad-Garcia, N., Deerinck, T.J., Ellisman, M.H., Gill, J., Kannan, K., Karas, B.J., Ma, L., *et al.* (2016) Design and synthesis of a minimal bacterial genome. *Science*, **351**(6280): aad6253.
- Imoto, S., Higuchi, T., Goto, T., Tashiro, K., Kuhara, S., and Miyano, S. (2004) Combining microarrays and biological knowledge for estimating gene networks via bayesian networks. *J Bioinform Comput Biol*, **2**(1): 77–98.
- International HapMap 3 Consortium (HapMap) (2003) The International HapMap Project. *Nature*, **426**(6968): 789–796.
- Jansen, R., Yu, H., Greenbaum, D., Kluger, Y., Krogan, N.J., Chung, S., Emili, A., Snyder, M., Greenblatt, J.F., and Gerstein, M. (2003) A Bayesian networks approach for predicting protein-protein interactions from genomic data. *Science*, **302**(5644): 449–453.
- Jeanes, A., Gottardi, C.J., and Yap, A.S. (2008) Cadherins and cancer: how does cadherin dysfunction promote tumor progression? *Oncogene*, **27**(55): 6920–6929.
- Jerby-Arnon, L., Pfetzer, N., Waldman, Y., McGarry, L., James, D., Shanks, E., Seashore-Ludlow, B., Weinstock, A., Geiger, T., Clemons, P., *et al.* (2014) Predicting cancer-specific vulnerability via data-driven detection of synthetic lethality. *Cell*, **158**(5): 1199–1209.
- Joachims, T. (1999) Making large-scale support vector machine learning practical. In S. Bernhard, lkopf, J.C.B. Christopher, and J.S. Alexander (editors), *Advances in kernel methods*, 169–184. MIT Press.

- Kaelin, Jr, W. (2005) The concept of synthetic lethality in the context of anticancer therapy. *Nat Rev Cancer*, **5**(9): 689–98.
- Kaelin, Jr, W. (2009) Synthetic lethality: a framework for the development of wiser cancer therapeutics. *Genome Med*, **1**: 99.
- Kamada, T. and Kawai, S. (1989) An algorithm for drawing general undirected graphs. *Information Processing Letters*, **31**(1): 7–15.
- Kawai, J., Shinagawa, A., Shibata, K., Yoshino, M., Itoh, M., Ishii, Y., Arakawa, T., Hara, A., Fukunishi, Y., Konno, H., et al. (2001) Functional annotation of a full-length mouse cDNA collection. *Nature*, **409**(6821): 685–690.
- Kelley, R. and Ideker, T. (2005) Systematic interpretation of genetic interactions using protein networks. *Nat Biotech*, **23**(5): 561–566.
- Kelly, S.T. (2013) *Statistical Predictions of Synthetic Lethal Interactions in Cancer*. Dissertation, University of Otago.
- Keshava Prasad, T.S., Goel, R., Kandasamy, K., Keerthikumar, S., Kumar, S., Mathivanan, S., Telikicherla, D., Raju, R., Shafreen, B., Venugopal, A., et al. (2009) Human Protein Reference Database—2009 update. *Nucleic Acids Res*, **37**(Database issue): D767–772.
- Kim, N.G., Koh, E., Chen, X., and Gumbiner, B.M. (2011) E-cadherin mediates contact inhibition of proliferation through Hippo signaling-pathway components. *Proc Natl Acad Sci USA*, **108**(29): 11930–11935.
- Koboldt, D.C., Fulton, R.S., McLellan, M.D., Schmidt, H., Kalicki-Veizer, J., McMichael, J.F., Fulton, L.L., Dooling, D.J., Ding, L., Mardis, E.R., et al. (2012) Comprehensive molecular portraits of human breast tumours. *Nature*, **490**(7418): 61–70.
- Kockel, L., Zeitlinger, J., Staszewski, L.M., Mlodzik, M., and Bohmann, D. (1997) Jun in drosophila development: redundant and nonredundant functions and regulation by two mapk signal transduction pathways. *Genes & Development*, **11**(13): 1748–1758.
- Kozlov, K.N., Gursky, V.V., Kulakovskiy, I.V., and Samsonova, M.G. (2015) Sequence-based model of gap gene regulation network. *BMC Genomics*, **15**(Suppl 12): S6.

- Kranthi, S., Rao, S., and Manimaran, P. (2013) Identification of synthetic lethal pairs in biological systems through network information centrality. *Mol BioSyst*, **9**(8): 2163–2167.
- Kroepil, F., Fluegen, G., Totikov, Z., Baldus, S.E., Vay, C., Schauer, M., Topp, S.A., Esch, J.S., Knoefel, W.T., and Stoecklein, N.H. (2012) Down-regulation of CDH1 is associated with expression of SNAI1 in colorectal adenomas. *PLoS ONE*, **7**(9): e46665.
- Lander, E.S. (2011) Initial impact of the sequencing of the human genome. *Nature*, **470**(7333): 187–197.
- Lander, E.S., Linton, L.M., Birren, B., Nusbaum, C., Zody, M.C., Baldwin, J., Devon, K., Dewar, K., Doyle, M., FitzHugh, W., et al. (2001) Initial sequencing and analysis of the human genome. *Nature*, **409**(6822): 860–921.
- Langmead, B., Trapnell, C., Pop, M., and Salzberg, S.L. (2009) Ultrafast and memory-efficient alignment of short DNA sequences to the human genome. *Genome Biol*, **10**(3): R25.
- Latora, V. and Marchiori, M. (2001) Efficient behavior of small-world networks. *Phys Rev Lett*, **87**: 198701.
- Laufer, C., Fischer, B., Billmann, M., Huber, W., and Boutros, M. (2013) Mapping genetic interactions in human cancer cells with RNAi and multiparametric phenotyping. *Nat Methods*, **10**(5): 427–31.
- Law, C.W., Chen, Y., Shi, W., and Smyth, G.K. (2014) voom: precision weights unlock linear model analysis tools for RNA-seq read counts. *Genome Biol*, **15**(2): R29.
- Le Meur, N. and Gentleman, R. (2008) Modeling synthetic lethality. *Genome Biol*, **9**(9): R135.
- Le Meur, N., Jiang, Z., Liu, T., Mar, J., and Gentleman, R.C. (2014) Slgi: Synthetic lethal genetic interaction. r package version 1.26.0.
- Lee, A.Y., Perreault, R., Harel, S., Boulier, E.L., Suderman, M., Hallett, M., and Jenna, S. (2010a) Searching for signaling balance through the identification of genetic interactors of the rab guanine-nucleotide dissociation inhibitor gdi-1. *PLoS ONE*, **5**(5): e10624.

- Lee, I., Lehner, B., Vavouri, T., Shin, J., Fraser, A.G., and Marcotte, E.M. (2010b) Predicting genetic modifier loci using functional gene networks. *Genome Research*, **20**(8): 1143–1153.
- Lee, I. and Marcotte, E.M. (2009) Effects of functional bias on supervised learning of a gene network model. *Methods Mol Biol*, **541**: 463–75.
- Lee, M.J., Ye, A.S., Gardino, A.K., Heijink, A.M., Sorger, P.K., MacBeath, G., and Yaffe, M.B. (2012) Sequential application of anticancer drugs enhances cell death by rewiring apoptotic signaling networks. *Cell*, **149**(4): 780–94.
- Lehner, B., Crombie, C., Tischler, J., Fortunato, A., and Fraser, A.G. (2006) Systematic mapping of genetic interactions in *caenorhabditis elegans* identifies common modifiers of diverse signaling pathways. *Nat Genet*, **38**(8): 896–903.
- Li, B., Ruotti, V., Stewart, R.M., Thomson, J.A., and Dewey, C.N. (2010) RNA-Seq gene expression estimation with read mapping uncertainty. *Bioinformatics*, **26**(4): 493–500.
- Li, X.J., Mishra, S.K., Wu, M., Zhang, F., and Zheng, J. (2014) Syn-lethality: An integrative knowledge base of synthetic lethality towards discovery of selective anticancer therapies. *Biomed Res Int*, **2014**: 196034.
- Linehan, W.M., Spellman, P.T., Ricketts, C.J., Creighton, C.J., Fei, S.S., Davis, C., Wheeler, D.A., Murray, B.A., Schmidt, L., Vocke, C.D., *et al.* (2016) Comprehensive Molecular Characterization of Papillary Renal-Cell Carcinoma. *N Engl J Med*, **374**(2): 135–145.
- Lokody, I. (2014) Computational modelling: A computational crystal ball. *Nature Reviews Cancer*, **14**(10): 649–649.
- Lord, C.J., Tutt, A.N., and Ashworth, A. (2015) Synthetic lethality and cancer therapy: lessons learned from the development of PARP inhibitors. *Annu Rev Med*, **66**: 455–470.
- Lu, X., Kensche, P.R., Huynen, M.A., and Notebaart, R.A. (2013) Genome evolution predicts genetic interactions in protein complexes and reveals cancer drug targets. *Nat Commun*, **4**: 2124.

- Lu, X., Megchelenbrink, W., Notebaart, R.A., and Huynen, M.A. (2015) Predicting human genetic interactions from cancer genome evolution. *PLoS One*, **10**(5): e0125795.
- Lum, P.Y., Armour, C.D., Stepaniants, S.B., Cavet, G., Wolf, M.K., Butler, J.S., Hinchshaw, J.C., Garnier, P., Prestwich, G.D., Leonardson, A., *et al.* (2004) Discovering modes of action for therapeutic compounds using a genome-wide screen of yeast heterozygotes. *Cell*, **116**(1): 121–137.
- Luo, J., Solimini, N.L., and Elledge, S.J. (2009) Principles of Cancer Therapy: Oncogene and Non-oncogene Addiction. *Cell*, **136**(5): 823–837.
- Machado, J., Olivera, C., Carvalh, R., Soares, P., Berx, G., Caldas, C., Sercuca, R., Carneiro, F., and Sorbrinho-Simoes, M. (2001) E-cadherin gene (*CDH1*) promoter methylation as the second hit in sporadic diffuse gastric carcinoma. *Oncogene*, **20**: 1525–1528.
- Markowetz, F. (2017) All biology is computational biology. *PLoS Biol*, **15**(3): e2002050.
- Masciari, S., Larsson, N., Senz, J., Boyd, N., Kaurah, P., Kandel, M.J., Harris, L.N., Pinheiro, H.C., Troussard, A., Miron, P., *et al.* (2007) Germline E-cadherin mutations in familial lobular breast cancer. *J Med Genet*, **44**(11): 726–31.
- Mattison, J., van der Weyden, L., Hubbard, T., and Adams, D.J. (2009) Cancer gene discovery in mouse and man. *Biochim Biophys Acta*, **1796**(2): 140–161.
- McLachlan, J., George, A., and Banerjee, S. (2016) The current status of parp inhibitors in ovarian cancer. *Tumori*, **102**(5): 433–440.
- McLendon, R., Friedman, A., Bigner, D., Van Meir, E.G., Brat, D.J., Mastrogianakis, G.M., Olson, J.J., Mikkelsen, T., Lehman, N., Aldape, K., *et al.* (2008) Comprehensive genomic characterization defines human glioblastoma genes and core pathways. *Nature*, **455**(7216): 1061–1068.
- Miles, D.W. (2001) Update on HER-2 as a target for cancer therapy: herceptin in the clinical setting. *Breast Cancer Res*, **3**(6): 380–384.
- Muzny, D.M., Bainbridge, M.N., Chang, K., Dinh, H.H., Drummond, J.A., Fowler, G., Kovar, C.L., Lewis, L.R., Morgan, M.B., Newsham, I.F., *et al.* (2012) Comprehensive

molecular characterization of human colon and rectal cancer. *Nature*, **487**(7407): 330–337.

Nagalla, S., Chou, J.W., Willingham, M.C., Ruiz, J., Vaughn, J.P., Dubey, P., Lash, T.L., Hamilton-Dutoit, S.J., Bergh, J., Sotiriou, C., *et al.* (2013) Interactions between immunity, proliferation and molecular subtype in breast cancer prognosis. *Genome Biol*, **14**(4): R34.

Novomestky, F. (2012) *matrixcalc: Collection of functions for matrix calculations*. R package version 1.0-3.

Nowak, M.A., Boerlijst, M.C., Cooke, J., and Smith, J.M. (1997) Evolution of genetic redundancy. *Nature*, **388**(6638): 167–171.

Oliveira, C., Senz, J., Kaurah, P., Pinheiro, H., Sanges, R., Haegert, A., Corso, G., Schouten, J., Fitzgerald, R., Vogelsang, H., *et al.* (2009) Germline *CDH1* deletions in hereditary diffuse gastric cancer families. *Human Molecular Genetics*, **18**(9): 1545–1555.

Oliveira, C., Seruca, R., Hoogerbrugge, N., Ligtenberg, M., and Carneiro, F. (2013) Clinical utility gene card for: Hereditary diffuse gastric cancer (HDGC). *Eur J Hum Genet*, **21**(8).

Pandey, G., Zhang, B., Chang, A.N., Myers, C.L., Zhu, J., Kumar, V., and Schadt, E.E. (2010) An integrative multi-network and multi-classifier approach to predict genetic interactions. *PLoS Comput Biol*, **6**(9).

Parker, J., Mullins, M., Cheung, M., Leung, S., Voduc, D., Vickery, T., Davies, S., Fauron, C., He, X., Hu, Z., *et al.* (2009) Supervised risk predictor of breast cancer based on intrinsic subtypes. *Journal of Clinical Oncology*, **27**(8): 1160–1167.

Pereira, B., Chin, S.F., Rueda, O.M., Vollan, H.K., Provenzano, E., Bardwell, H.A., Pugh, M., Jones, L., Russell, R., Sammut, S.J., *et al.* (2016) Erratum: The somatic mutation profiles of 2,433 breast cancers refine their genomic and transcriptomic landscapes. *Nat Commun*, **7**: 11908.

Perou, C.M., Sørlie, T., Eisen, M.B., van de Rijn, M., Jeffrey, S.S., Rees, C.A., Pollack, J.R., Ross, D.T., Johnsen, H., Akslen, L.A., *et al.* (2000) Molecular portraits of human breast tumours. *Nature*, **406**(6797): 747–752.

- Polyak, K. and Weinberg, R.A. (2009) Transitions between epithelial and mesenchymal states: acquisition of malignant and stem cell traits. *Nat Rev Cancer*, **9**(4): 265–73.
- R Core Team (2016) *R: A Language and Environment for Statistical Computing*. R Foundation for Statistical Computing, Vienna, Austria. R version 3.3.2.
- Ritchie, M.E., Phipson, B., Wu, D., Hu, Y., Law, C.W., Shi, W., and Smyth, G.K. (2015) limma powers differential expression analyses for RNA-sequencing and microarray studies. *Nucleic Acids Research*, **43**(7): e47.
- Roguev, A., Bandyopadhyay, S., Zofall, M., Zhang, K., Fischer, T., Collins, S.R., Qu, H., Shales, M., Park, H.O., Hayles, J., *et al.* (2008) Conservation and rewiring of functional modules revealed by an epistasis map in fission yeast. *Science*, **322**(5900): 405–10.
- Roychowdhury, S. and Chinnaiyan, A.M. (2016) Translating cancer genomes and transcriptomes for precision oncology. *CA Cancer J Clin*, **66**(1): 75–88.
- Rung, J. and Brazma, A. (2013) Reuse of public genome-wide gene expression data. *Nat Rev Genet*, **14**(2): 89–99.
- Ryan, C., Lord, C., and Ashworth, A. (2014) Daisy: Picking synthetic lethals from cancer genomes. *Cancer Cell*, **26**(3): 306–308.
- Schena, M. (1996) Genome analysis with gene expression microarrays. *Bioessays*, **18**(5): 427–431.
- Scheuer, L., Kauff, N., Robson, M., Kelly, B., Barakat, R., Satagopan, J., Ellis, N., Hensley, M., Boyd, J., Borgen, P., *et al.* (2002) Outcome of preventive surgery and screening for breast and ovarian cancer in BRCA mutation carriers. *J Clin Oncol*, **20**(5): 1260–1268.
- Semb, H. and Christofori, G. (1998) The tumor-suppressor function of E-cadherin. *Am J Hum Genet*, **63**(6): 1588–93.
- Sing, T., Sander, O., Beerenwinkel, N., and Lengauer, T. (2005) Rocr: visualizing classifier performance in r. *Bioinformatics*, **21**(20): 7881.
- Slurm development team (Slurm) (2017) Slurm workload manager. <https://slurm.schedmd.com/>. Accessed: 25/03/2017.

- Sørlie, T., Perou, C.M., Tibshirani, R., Aas, T., Geisler, S., Johnsen, H., Hastie, T., Eisen, M.B., van de Rijn, M., Jeffrey, S.S., *et al.* (2001) Gene expression patterns of breast carcinomas distinguish tumor subclasses with clinical implications. *Proc Natl Acad Sci USA*, **98**(19): 10869–10874.
- Srihari, S., Singla, J., Wong, L., and Ragan, M.A. (2015) Inferring synthetic lethal interactions from mutual exclusivity of genetic events in cancer. *Biology Direct*, **10**(1): 57.
- Stajich, J.E. and Lapp, H. (2006) Open source tools and toolkits for bioinformatics: significance, and where are we? *Brief Bioinformatics*, **7**(3): 287–296.
- Stratton, M.R., Campbell, P.J., and Futreal, P.A. (2009) The cancer genome. *Nature*, **458**(7239): 719–724.
- Ström, C. and Helleday, T. (2012) Strategies for the use of poly(adenosine diphosphate ribose) polymerase (parp) inhibitors in cancer therapy. *Biomolecules*, **2**(4): 635–649.
- Tarazona, S., Garcia-Alcalde, F., Dopazo, J., Ferrer, A., and Conesa, A. (2011) Differential expression in RNA-seq: a matter of depth. *Genome Res*, **21**(12): 2213–2223.
- Telford, B.J., Chen, A., Beetham, H., Frick, J., Brew, T.P., Gould, C.M., Single, A., Godwin, T., Simpson, K.J., and Guilford, P. (2015) Synthetic lethal screens identify vulnerabilities in gpcr signalling and cytoskeletal organization in E-cadherin-deficient cells. *Mol Cancer Ther*, **14**(5): 1213–1223.
- The 1000 Genomes Project Consortium (1000 Genomes) (2010) A map of human genome variation from population-scale sequencing. *Nature*, **467**(7319): 1061–1073.
- The Cancer Genome Atlas Research Network (TCGA) (2017) The Cancer Genome Atlas Project. <https://cancergenome.nih.gov/>. Accessed: 26/03/2017.
- The Catalogue Of Somatic Mutations In Cancer (COSMIC) (2016) Cosmic: The catalogue of somatic mutations in cancer. <http://cancer.sanger.ac.uk/cosmic>. Release 79 (23/08/2016), Accessed: 05/02/2017.
- The Comprehensive R Archive Network (CRAN) (2017) Cran. <https://cran.r-project.org/>. Accessed: 24/03/2017.
- The ENCODE Project Consortium (ENCODE) (2004) The ENCODE (ENCyclopedia Of DNA Elements) Project. *Science*, **306**(5696): 636–640.

The National Cancer Institute (NCI) (2015) The genetics of cancer. <https://www.cancer.gov/about-cancer/causes-prevention/genetics>. Published: 22/04/2015, Accessed: 22/03/2017.

The New Zealand eScience Infrastructure (NeSI) (2017) NeSI. <https://www.nesi.org.nz/>. Accessed: 25/03/2017.

Tierney, L., Rossini, A.J., Li, N., and Sevcikova, H. (2015) *snow: Simple Network of Workstations*. R package version 0.4-2.

Tiong, K.L., Chang, K.C., Yeh, K.T., Liu, T.Y., Wu, J.H., Hsieh, P.H., Lin, S.H., Lai, W.Y., Hsu, Y.C., Chen, J.Y., *et al.* (2014) Csnk1e/ctnnb1 are synthetic lethal to tp53 in colorectal cancer and are markers for prognosis. *Neoplasia*, **16**(5): 441–50.

Tischler, J., Lehner, B., and Fraser, A.G. (2008) Evolutionary plasticity of genetic interaction networks. *Nat Genet*, **40**(4): 390–391.

Tomasetti, C. and Vogelstein, B. (2015) Cancer etiology. Variation in cancer risk among tissues can be explained by the number of stem cell divisions. *Science*, **347**(6217): 78–81.

Tong, A.H., Evangelista, M., Parsons, A.B., Xu, H., Bader, G.D., Page, N., Robinson, M., Raghibizadeh, S., Hogue, C.W., Bussey, H., *et al.* (2001) Systematic genetic analysis with ordered arrays of yeast deletion mutants. *Science*, **294**(5550): 2364–8.

Tong, A.H., Lesage, G., Bader, G.D., Ding, H., Xu, H., Xin, X., Young, J., Berriz, G.F., Brost, R.L., Chang, M., *et al.* (2004) Global mapping of the yeast genetic interaction network. *Science*, **303**(5659): 808–13.

Tran, B., Dancey, J.E., Kamel-Reid, S., McPherson, J.D., Bedard, P.L., Brown, A.M., Zhang, T., Shaw, P., Onetto, N., Stein, L., *et al.* (2012) Cancer genomics: technology, discovery, and translation. *J Clin Oncol*, **30**(6): 647–660.

Travers, J. and Milgram, S. (1969) An experimental study of the small world problem. *Sociometry*, **32**(4): 425–443.

Tunggal, J.A., Helfrich, I., Schmitz, A., Schwarz, H., Gunzel, D., Fromm, M., Kemler, R., Krieg, T., and Niessen, C.M. (2005) E-cadherin is essential for in vivo epidermal barrier function by regulating tight junctions. *EMBO J*, **24**(6): 1146–1156.

- Tutt, A., Robson, M., Garber, J.E., Domchek, S.M., Audeh, M.W., Weitzel, J.N., Friedlander, M., Arun, B., Loman, N., Schmutzler, R.K., *et al.* (2010) Oral poly(adenylic ribose) polymerase inhibitor olaparib in patients with *BRCA1* or *BRCA2* mutations and advanced breast cancer: a proof-of-concept trial. *Lancet*, **376**(9737): 235–44.
- University of California, Santa Cruz (UCSC) (2012) Ucsc cancer browser. Accessed 29/03/2012.
- van der Meer, R., Song, H.Y., Park, S.H., Abdulkadir, S.A., and Roh, M. (2014) RNAi screen identifies a synthetic lethal interaction between PIM1 overexpression and PLK1 inhibition. *Clinical Cancer Research*, **20**(12): 3211–3221.
- van der Post, R.S., Vogelaar, I.P., Carneiro, F., Guilford, P., Huntsman, D., Hoogerbrugge, N., Caldas, C., Schreiber, K.E., Hardwick, R.H., Ausems, M.G., *et al.* (2015) Hereditary diffuse gastric cancer: updated clinical guidelines with an emphasis on germline CDH1 mutation carriers. *J Med Genet*, **52**(6): 361–374.
- van Steen, K. (2012) Travelling the world of gene-gene interactions. *Briefings in Bioinformatics*, **13**(1): 1–19.
- van Steen, M. (2010) *Graph Theory and Complex Networks: An Introduction*. Maarten van Steen, VU Amsterdam.
- Vapnik, V.N. (1995) *The nature of statistical learning theory*. Springer-Verlag New York, Inc.
- Vizeacoumar, F.J., Arnold, R., Vizeacoumar, F.S., Chandrashekhar, M., Buzina, A., Young, J.T., Kwan, J.H., Sayad, A., Mero, P., Lawo, S., *et al.* (2013) A negative genetic interaction map in isogenic cancer cell lines reveals cancer cell vulnerabilities. *Mol Syst Biol*, **9**: 696.
- Vogelstein, B., Papadopoulos, N., Velculescu, V.E., Zhou, S., Diaz, L.A., and Kinzler, K.W. (2013) Cancer genome landscapes. *Science*, **339**(6127): 1546–1558.
- Vos, C.B., Cleton-Jansen, A.M., Berx, G., de Leeuw, W.J., ter Haar, N.T., van Roy, F., Cornelisse, C.J., Peterse, J.L., and van de Vijver, M.J. (1997) E-cadherin inactivation in lobular carcinoma in situ of the breast: an early event in tumorigenesis. *Br J Cancer*, **76**(9): 1131–3.
- Waldron, D. (2016) Cancer genomics: A multi-layer omics approach to cancer. *Nat Rev Genet*, **17**(8): 436–437.

- Wang, K., Singh, D., Zeng, Z., Coleman, S.J., Huang, Y., Savich, G.L., He, X., Mieczkowski, P., Grimm, S.A., Perou, C.M., *et al.* (2010) MapSplice: accurate mapping of RNA-seq reads for splice junction discovery. *Nucleic Acids Res*, **38**(18): e178.
- Wang, X. and Simon, R. (2013) Identification of potential synthetic lethal genes to p53 using a computational biology approach. *BMC Medical Genomics*, **6**(1): 30.
- Wappett, M. (2014) Bisep: Toolkit to identify candidate synthetic lethality. r package version 2.0.
- Wappett, M., Dulak, A., Yang, Z.R., Al-Watban, A., Bradford, J.R., and Dry, J.R. (2016) Multi-omic measurement of mutually exclusive loss-of-function enriches for candidate synthetic lethal gene pairs. *BMC Genomics*, **17**: 65.
- Warnes, G.R., Bolker, B., Bonebakker, L., Gentleman, R., Liaw, W.H.A., Lumley, T., Maechler, M., Magnusson, A., Moeller, S., Schwartz, M., *et al.* (2015) *gplots: Various R Programming Tools for Plotting Data*. R package version 2.17.0.
- Watts, D.J. and Strogatz, S.H. (1998) Collective dynamics of 'small-world' networks. *Nature*, **393**(6684): 440–2.
- Weinstein, I.B. (2000) Disorders in cell circuitry during multistage carcinogenesis: the role of homeostasis. *Carcinogenesis*, **21**(5): 857–864.
- Weinstein, J.N., Akbani, R., Broom, B.M., Wang, W., Verhaak, R.G., McConkey, D., Lerner, S., Morgan, M., Creighton, C.J., Smith, C., *et al.* (2014) Comprehensive molecular characterization of urothelial bladder carcinoma. *Nature*, **507**(7492): 315–322.
- Weinstein, J.N., Collisson, E.A., Mills, G.B., Shaw, K.R., Ozenberger, B.A., Ellrott, K., Shmulevich, I., Sander, C., Stuart, J.M., Chang, K., *et al.* (2013) The Cancer Genome Atlas Pan-Cancer analysis project. *Nat Genet*, **45**(10): 1113–1120.
- Wickham, H. and Chang, W. (2016) *devtools: Tools to Make Developing R Packages Easier*. R package version 1.12.0.
- Wickham, H., Danenberg, P., and Eugster, M. (2017) *roxygen2: In-Line Documentation for R*. R package version 6.0.1.

- Wojtukiewicz, M.Z., Hempel, D., Sierko, E., Tucker, S.C., and Honn, K.V. (2016) Thrombin-unique coagulation system protein with multifaceted impacts on cancer and metastasis. *Cancer Metastasis Rev*, **35**(2): 213–233.
- Wong, S.L., Zhang, L.V., Tong, A.H.Y., Li, Z., Goldberg, D.S., King, O.D., Lesage, G., Vidal, M., Andrews, B., Bussey, H., et al. (2004) Combining biological networks to predict genetic interactions. *Proceedings of the National Academy of Sciences of the United States of America*, **101**(44): 15682–15687.
- World Health Organization (WHO) (2017) Fact sheet: Cancer. <http://www.who.int/mediacentre/factsheets/fs297/en/>. Updated February 2017, Accessed: 22/03/2017.
- Wu, M., Li, X., Zhang, F., Li, X., Kwoh, C.K., and Zheng, J. (2014) In silico prediction of synthetic lethality by meta-analysis of genetic interactions, functions, and pathways in yeast and human cancer. *Cancer Inform*, **13**(Suppl 3): 71–80.
- Yu, H. (2002) Rmpi: Parallel statistical computing in r. *R News*, **2**(2): 10–14.
- Zhang, F., Wu, M., Li, X.J., Li, X.L., Kwoh, C.K., and Zheng, J. (2015) Predicting essential genes and synthetic lethality via influence propagation in signaling pathways of cancer cell fates. *J Bioinform Comput Biol*, **13**(3): 1541002.
- Zhang, J., Baran, J., Cros, A., Guberman, J.M., Haider, S., Hsu, J., Liang, Y., Rivkin, E., Wang, J., Whitty, B., et al. (2011) International cancer genome consortium data portal a one-stop shop for cancer genomics data. *Database: The Journal of Biological Databases and Curation*, **2011**: bar026.
- Zhong, W. and Sternberg, P.W. (2006) Genome-wide prediction of c. elegans genetic interactions. *Science*, **311**(5766): 1481–1484.
- Zweig, M.H. and Campbell, G. (1993) Receiver-operating characteristic (roc) plots: a fundamental evaluation tool in clinical medicine. *Clinical Chemistry*, **39**(4): 561–577.